AN ABSTRACT OF THE THESIS OF

Malcolm Coombs for degree of Master of Science in Forest Products Presented on February 2, 1988.

Title: Predicting the Machinability of Finger-Joints in Ponderosa Pine Cutting Stock

Signature redacted for privacy.

Abstract approved: _____
Charles Brunner

Cutting forces and the occurrence of chip-out were investigated in finger-joints machined into ponderosa pine (Pinus ponderosa) cutting stock. Finger-joints were orthogonally cut in sample blocks at four depths of cut (chip thicknesses) from 0.005 to 0.020 inch, twelve fiber angles from -30 to +40 degrees, and at specific gravities from 0.35 to 0.50. Cutting force measurements were made with reference to the machined surface in all three axes.

The results showed that cutting forces are directly related to specific gravity and chip thickness. Fiber angle was found to effect only the cutting forces perpendicular to the cut surface, but it was found to determine the occurrence of wood failure (chip-out) at a block's trailing edge. It was further established that there was no measurable interaction of forces between the finger-joint cutting bits. Observation also showed that a joint's surface quality was inversely related to chip thicknesses but directly related to fiber angle.

A cutting force model for the peripheral milling process used in production line finger-jointers was developed from the orthogonal cutting tests. It predicted that the cutting forces reach a maximum at the beginning of the cut when the full length of the finger-joint bits' sides are cutting wood. A peripheral milling model for predicting the probability of chip-out for a given chip thickness and fiber angle was also developed.

A theory to explain the relationship between fiber orientation and the occurrence of chip-out was developed. It postulates that chip-out is determined by how the cutting force is oriented with respect to the fibers and not by the magnitude of the cutting force. Chip-out occurs when the cutting force is approximately perpendicular to the fibers. This theory suggests that chip-out can be eliminated by orienting blocks so the cutting edge loads the fibers in tension parallel to the fiber direction.

Preliminary studies of growth ring patterns, knot parameters (including knot-wood density distribution), and fiber-flow models were conducted to determine the feasibility of using them for predicting the machinability of wood surrounding knots. Results indicate that a comprehensive model using these factors is possible following further verification studies. Portions of the preliminary study may also prove useful in defining sawing boundaries close to knots.

Predicting the Machinability of Finger-Joints in Ponderosa Pine Cutting Stock

by

Malcolm Coombs

A Thesis

submitted to

Oregon State University

in partial fulfillment of
the requirements for the
degree of

Master of Science

Completed February 2, 1988

Commencement June, 1988

APPROVED:

Signature redacted for privacy.

Professor of Forest Products in charge of major

Signature redacted for privacy.

Head of department of Forest Products

Signature redacted for privacy.

Dean of Graduate School

Date thesis presented: February 2, 1988

Typed for researcher by Malcolm Coombs

Acknowledgements

This thesis is dedicated to my wife, Ann Coombs, for her constant love and support.

I am also grateful to Charles Brunner, my major professor, for his guidance and assistance in this project.

Table of Contents

List of Figures

List of Tables

Predicting the Machinability of Finger-Joints in Ponderosa Pine Cutting Stock

INTRODUCTION

Finger-jointing is a special wood machining process that forms a strong end-glued joint. It is used both in decorative and structural lumber products. Woods commonly finger-jointed in the West are alders, Douglas-fir, hemlocks, pines and redwood.

Chip-out is the term used to describe the breaking of the corner or small chips from the trailing edge of a block as the finger-joints are being machined (Figure 1). The goal of this project was to discover the factors controlling the occurrence of chip-out. Implementation of this knowledge could reduce chip-out and subsequently the number of manufacturing defects and increase recovery by allowing finger-joints to be machined closer to knots than is presently practiced.

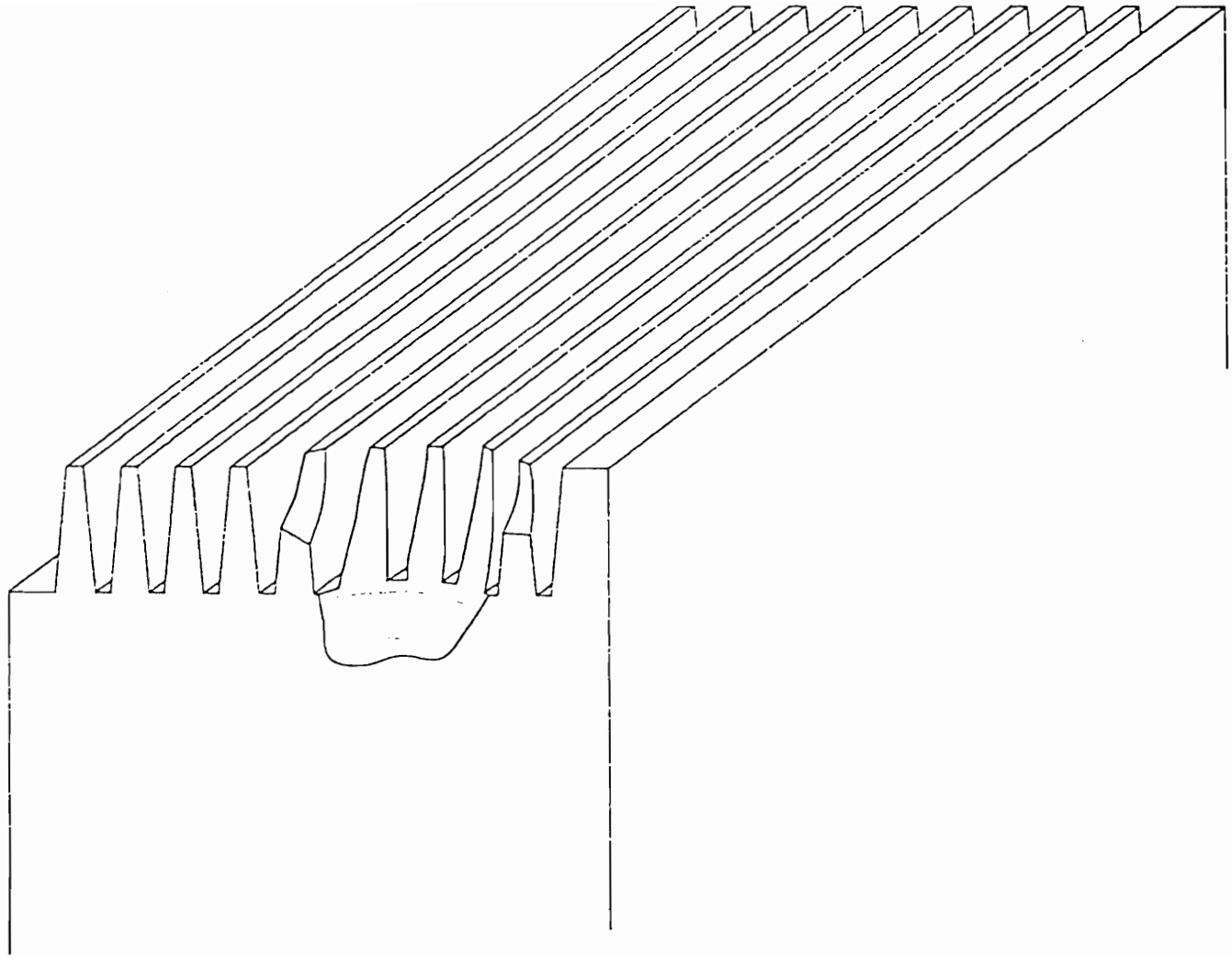

Figure 1. Finger-joint block with chip-out

Background on Manufacturing

Ponderosa pine (Pinus ponderosa) is one of the species especially suited for making moulding and door and window parts. Most of the clear cuttings to be made into these products are short and must be finger-jointed into usable lengths.

In a typical cut-stock plant (Figure 2), shop boards containing knots and other defects are processed through multiple rip saws followed by a cross-cut chop saw. The rip saw operator tries to maximize the number of long clear cuttings. The chop saw operators remove all of the defects and sort the cuttings into different grades. Most of the volume of material goes to the finger-jointers. These machines cut an interlocking pattern in both ends of each block (Figure 3). An inspector checks the fingers on each block for chip-out and recycles the defective ones back to the chop saws. An adhesive is applied to one end of the good blocks. They are joined into one continuous board which is cut to appropriate length by a flying cut-off saw. These boards then enter a long press and are longitudinally squeezed to ensure tight joints. After the glue cures, the new longer boards are then ready to be made into moulding or door and window parts.

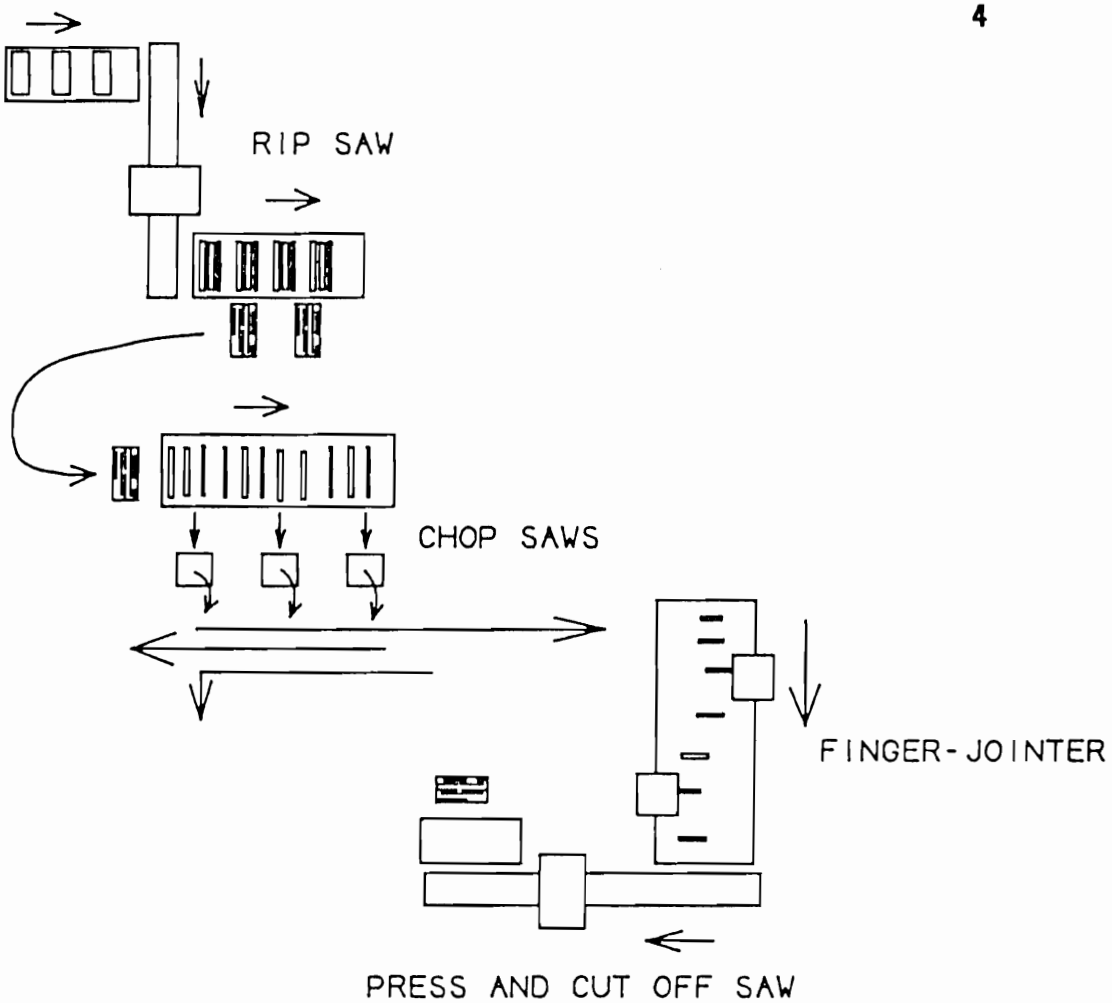

Figure 2. Typical cut-stock plant layout

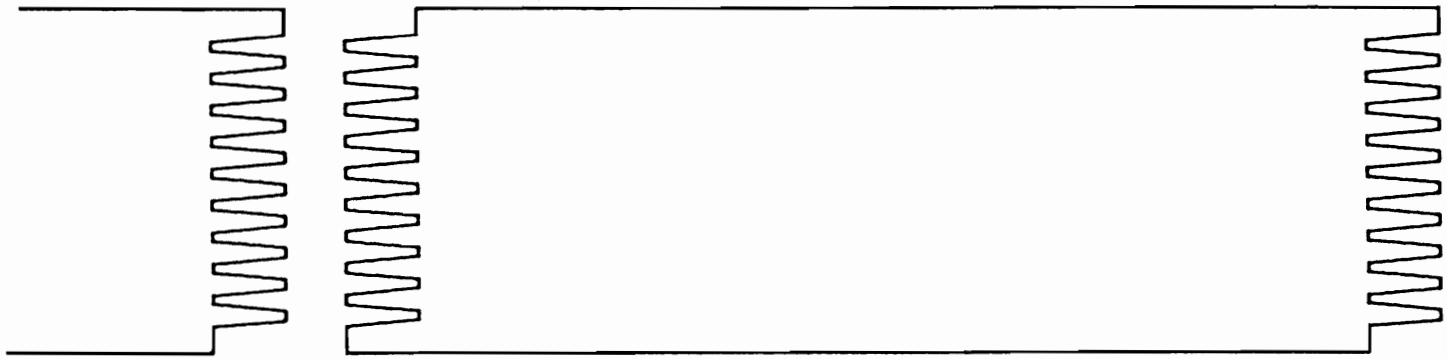

Figure 3. Interlocking finger-joint pattern

Problem Approach

In a preliminary investigation the occurrence of chip-out was determined to be closely related to the presence of cross grain. In a piece of wood, cross grain is an area where the fibers are not parallel to the edge of the board. An examination of the chipped area on several finger-jointed blocks revealed that the fibers were inclined into the knife at 20 degrees or more. Further it showed that the failure almost always exposed a radial surface since the wood rays were always visible.

Chip-out occurs when the stresses developed in the wood during cutting exceed the strength of the wood in tension across the grain or in cleavage, before the fibers are severed. To adequately address the problem of chip-out, a good understanding of wood machining as well as the strength and anatomical characteristics of wood are required. This thesis project is divided into two separate but related studies. The first involves the modeling of the machining of finger-joints in ponderosa pine by analyzing the finger-joint cutting parameters, measuring cutting forces and determining the causes of chip-out. The second study is on the anatomical properties near knots which influence wood machining, i.e. local specific gravity and fiber distortion.

STUDY I - MACHINING FINGER-JOINTS

Most studies on the machining of wood have measured the cutting forces and classified the different types of chip formation. Results from these studies have been used to develop the accepted theories on how wood cuts and models which predict the cutting forces.

This investigation into the machining of finger-joints first defined finger-joint machining parameters. Tests were then designed and conducted for measuring orthogonal finger-joint cutting forces and the occurrence of chip-out. From this, a model was developed which predicts the cutting forces and chip-out in peripheral milling of finger-joints.

LITERATURE REVIEW

Definitions

The terminology used to describe the geometry of a cutting edge first needs defining (Figure 4).

1. The rake angle (also hook or cutting angle) is the angle between the tool face and a plane perpendicular to the direction of tool travel.
2. The clearance angle is measured between the back of the tool and the surface of the material.
3. The chip thickness is the distance between the existing surface of the material and the new surface being formed by the cut.
4. The parallel and normal cutting forces are the components of the cutting force which are parallel and perpendicular to the direction of the tool motion.
5. The resultant cutting force is the total force applied on the chip and workpiece by the knife. It is the vector combination of the normal and parallel components.

Orthogonal Cutting

Orthogonal cutting is defined as cutting with a knife whose edge is perpendicular to the direction of motion resulting in a new surface

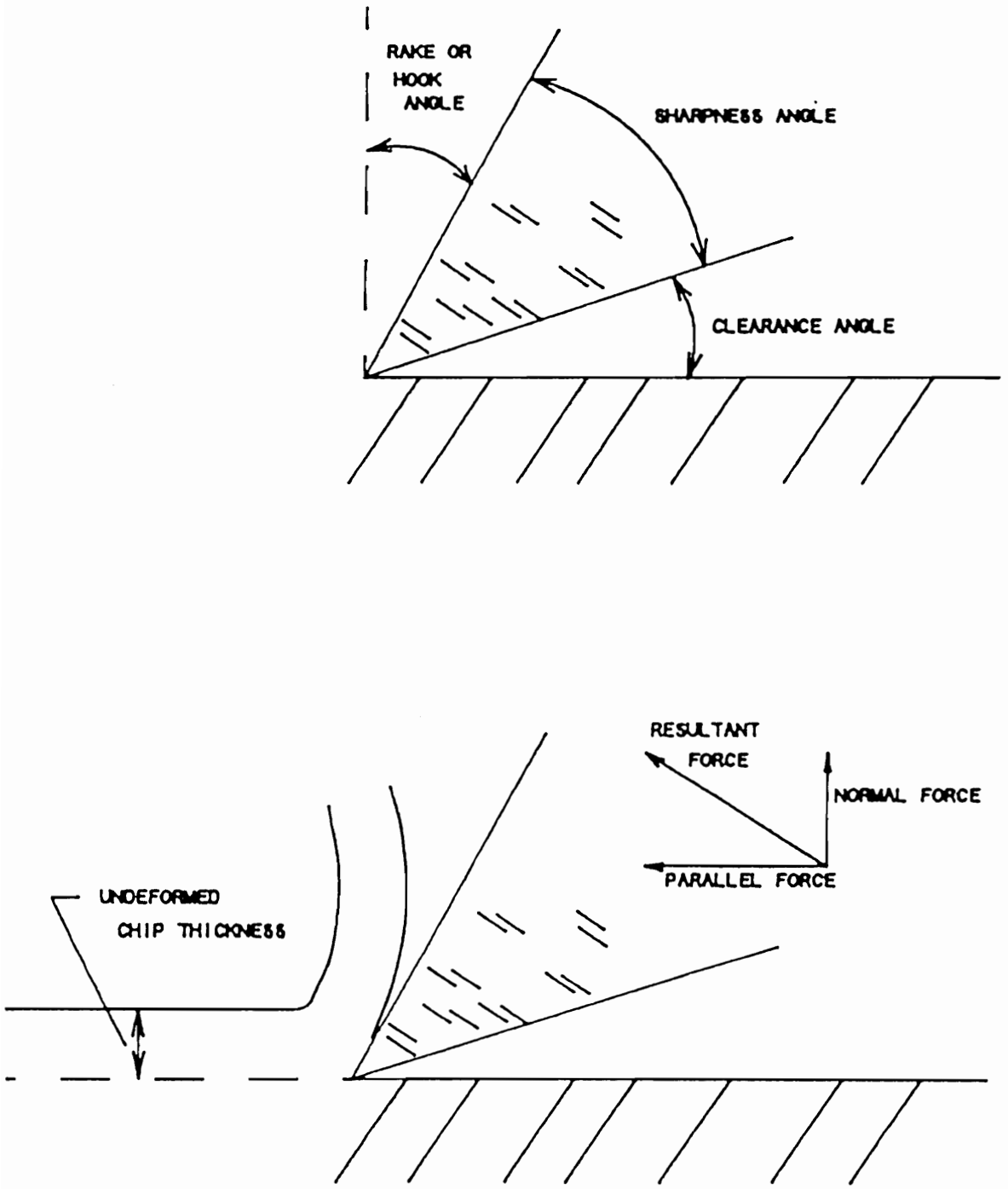

Figure 4. Basic nomenclature of cutting configuration

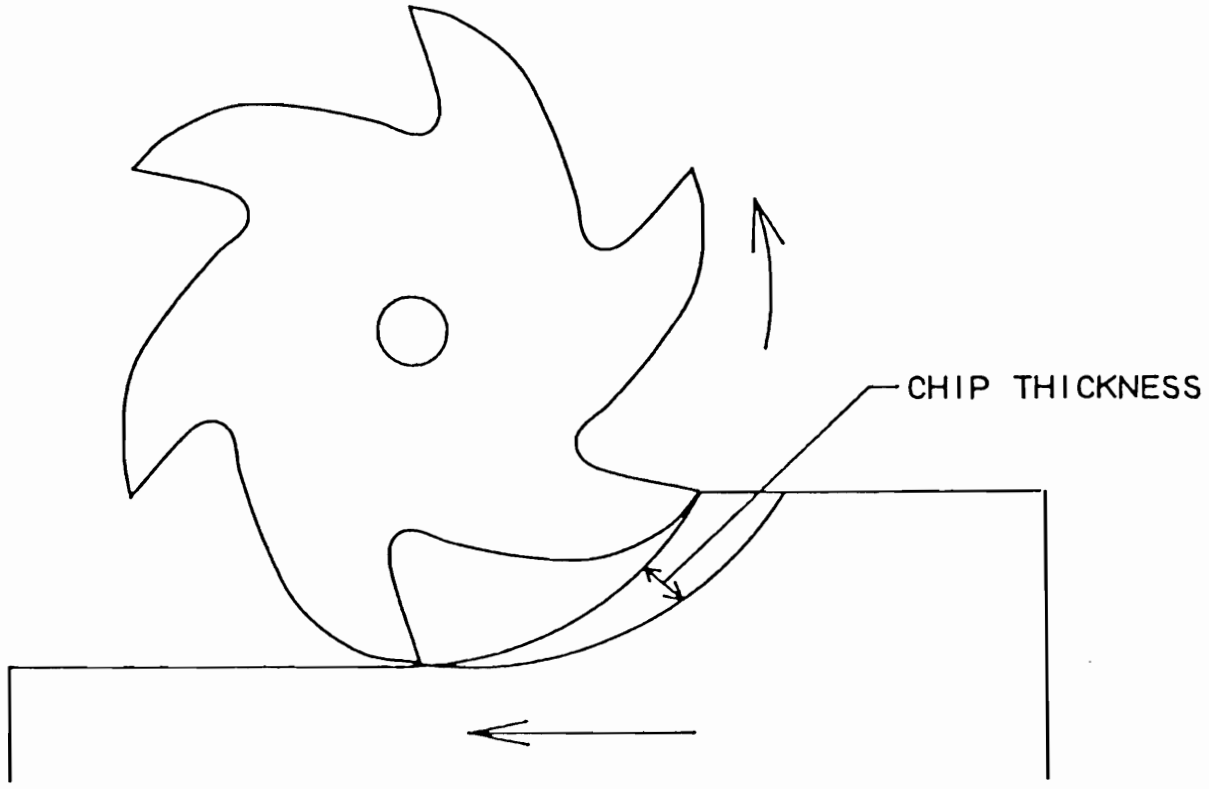

Figure 5. Chip formation in peripheral milling operation, chip thickness increases as knife progresses through the cut

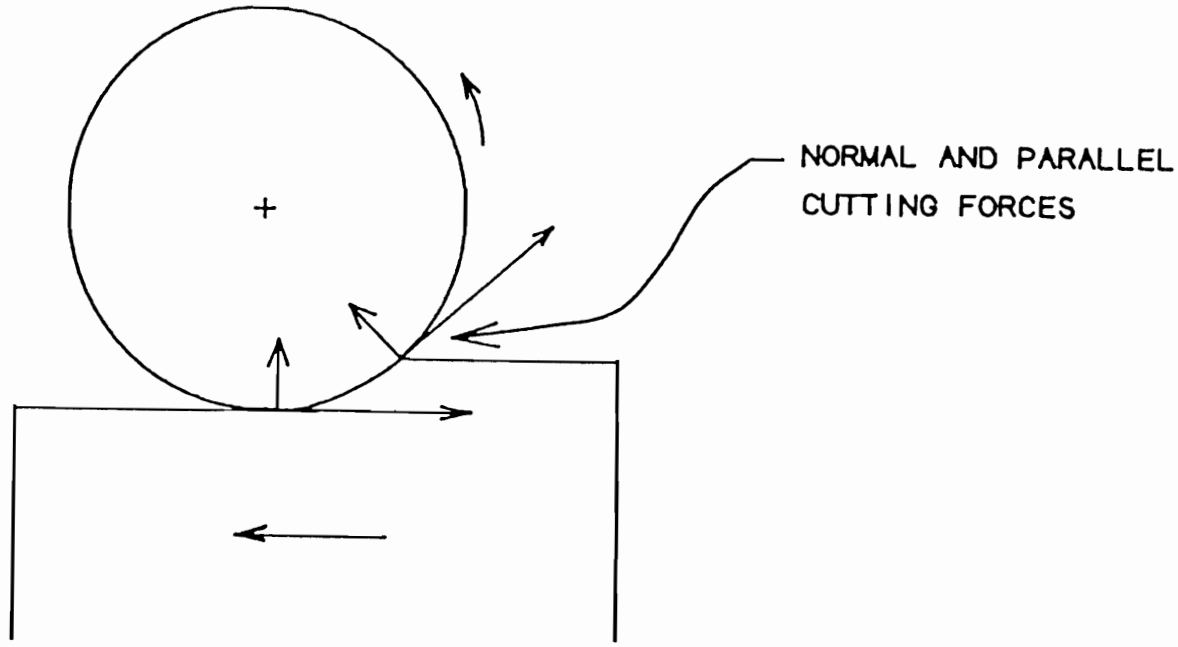

Figure 6. Peripheral up-milling cutting force vectors change direction with respect to the work piece as the knife progresses through cut

which is a plane parallel to the original surface. Simply put, it is slicing.

Most studies of machining wood, i.e. sawing and planing, have used orthogonal cutting. The advantages of this type of cutting test are that the cutting action and chip thickness are easier to control and forces are easier to measure.

Peripheral Milling

Peripheral milling is defined as cutting with a rotating cutterhead. Most industrial processes are peripheral milling because machining times are shorter and the quality of the finished product is good. Finger-jointing is a peripheral milling operation. Here the cutterhead rotates in an up-milling configuration (Figure 5). There are two important aspects of the geometry of peripheral milling. First, the chip formed by each individual tooth increases in thickness through the cut. Second, the direction of the applied cutting forces, parallel and normal, are radial and tangential to the cutting circle at the location of the tooth (Figure 6). These two factors taken together mean that the direction and magnitude of the forces with respect to the workpiece are constantly changing as the knife progresses through the cut.

The path of a knife edge in a rotating head is circular. Because the work piece is moving into the cutterhead, the path of the knife edge relative to the work piece is a prolate trochoid. As the spindle speed increases relative to the workpiece feed speed, the trochoid becomes more circular. At typical machining speeds the circular approximation gives results which are quite accurate (Armarego, 1969). The geometric parameters of peripheral milling can be found with the following equations.

The Feed per tooth (inches), F_t, can be found from

$$F_t = 12\ F\ /\ (T\ n)$$

where F is the Feed rate (feet/minute), T is the number of knives, and n is the spindle speed of the cutterhead (revolutions/minute).

The instantaneous curvature (inches), ρ, can be found from

$$\rho = \frac{\left[R^2 + \left(\frac{F_t T}{2\pi}\right) + \left(\frac{F_t T}{\pi}\right)(R-d) \right]^{3/2}}{\left(\frac{F_t T}{2\pi}\right)(R-d) + R^2}$$

where R is the radius of the cutterhead (inches) and d is the depth of cut (inches).

The length of knife path (inches), L, can be found from

$$L = R \arccos\left(1-\frac{d}{R}\right) + \left[\frac{F_t T}{\pi D}\left(Dd-d^2\right)^{1/2}\right]$$

where D is diameter of cutterhead (inches).

The average chip thickness, t ave, is found with

$$t\ ave = \frac{F_z d}{L} \quad .$$

The maximum chip thickness, t max, is found with

$$t\ max = 2\ F_t \sqrt{\frac{d}{D}\left(1 - \frac{d}{D}\right)} \quad .$$

Wood Orientation Terminology

The convention used to describe the knife/block orientation is the one developed by McKenzie (1961) in his study of wood cutting. Orthogonal cutting of end grain is 90-90 and cutting along the grain is 90-0. The first number is the angle between the cutting edge and the direction of the wood fibers. The second number is the angle between the cutting motion and the fiber orientation.

Effects of Velocity on Cutting Force

Cutting at slower speeds is easier to control and measure. The validity of the extrapolation of such tests to high speed cutting has been the subject of much discussion. Some effects of higher velocity increase cutting force while others decrease it (Koch, 1964). Chip acceleration and the fact that wood is stronger at higher strain rates

causes the cutting forces to increase. The reduced strength of wood at elevated temperatures and the reduced friction at higher velocities will tend to decrease the cutting forces. The net effect is that the cutting forces only increase about 5% over a very wide range of cutting speeds (McKenzie 1961). Tests by Kivimaa (1950 as cited in Kollman, 1968) show that cutting forces remain constant over a range of speeds from 5 to 50 meters per second.

It has also been argued that peripheral milling is a percussion operation with impact forces while orthogonal cutting is not (Kollman, 1968). In spite of this, orthogonal cutting has been used by many researchers to study wood cutting.

Force Measuring Dynamometers

In order to measure cutting forces, most researchers have used a force measuring dynamometer (Loewen, 1951; Clarke, 1963). There have been two types of dynamometers used in wood cutting studies (Figure 7). The first, a beam type, measures forces in two directions and the other, a plate on load-cells, measures forces in all three major axes. Both types use strain gauges with bridge circuits to measure deflections and loads.

A dynamometer can either measure forces on the knife or forces on the test material depending on which is held by the dynamometer. The

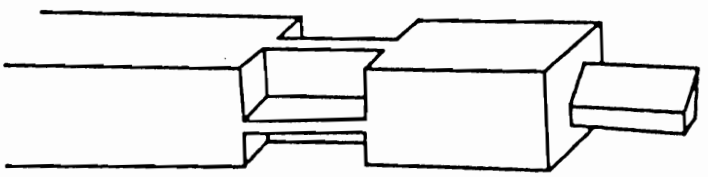

BEAM DYNAMOMETER

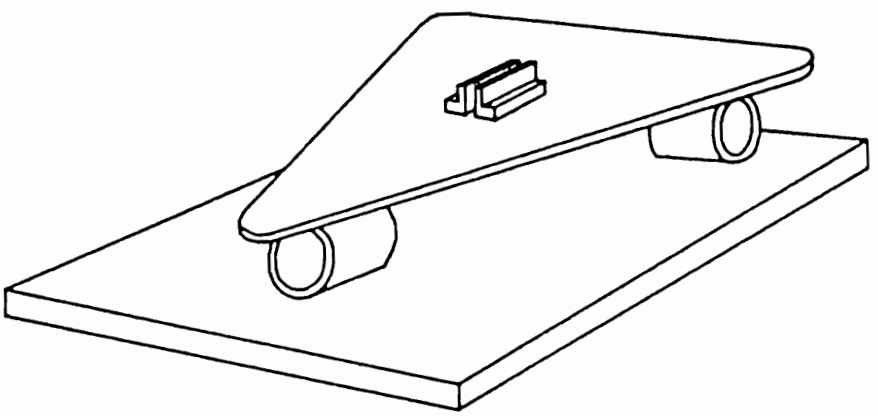

THREE LOAD CELL DYNAMOMETER

Figure 7. Two types of force measuring dynamometers

only difference is the chip acceleration force which is negligible at slow speeds.

The three ring dynamometer as designed and described by Clarke (1963) forms the basis for the design of the dynamometer used in the tests reported in this thesis. It consists of two steel plates separated by three steel load rings. The load is applied to an object attached to the center of the top plate. The bottom plate is securely anchored to prevent movement during testing. The three rings lay on their sides and are bolted to the plates so that their centerlines converge directly below the load point. Small deflections of the three load rings during cutting will be detected by the strain gauges. The top plate is reinforced with a web to prevent its deflection.

Each load ring has four strain gauges. Two are attached to the inside of the ring and two to the outside. They are wired into a Wheatstone bridge circuit. A force applied to a load cell will cause it to deflect which will in turn change its voltage output. Dynamometers are typically calibrated with dead weights by scaling the change in output voltage to the change in load.

Measuring and Predicting the Orthogonal Cutting Forces of Wood

Franz (1958) investigated the orthogonal cutting of wood along the grain, in the 90-0 orientation. He defined three types of chip

formation. A Franz Type I chip splits ahead of the tool's cutting edge and is generally caused by a rake angle which is too high. A Franz Type II chip forms when the wood fails along a plane extending from the cutting edge to the surface of the wood ahead of the knife. This is ideal cutting. A Franz Type III chip crushes the wood ahead of the cutting edge because the rake angle is too small. Franz then related the surface quality and cutting forces to the type of chip being formed, the geometry of the cutter, and the moisture content of the wood (Table 1). Franz Chip Type I results in chipped grain and Franz Type III in fuzzy grain. Type II results in a clean-cut surface free of defects.

Chip Thickness (inches)	Rake Angle 5	10	15	20	25
0.002	III	II	II	II	II
0.005	III	II	II	II	I
0.010	III	II	II	II	I
0.015	III	II	II	I	I
0.020	III	III	II	I	I
0.025	III	III	III	I	I

Table 1. Franz chip types for different chip thicknesses and rake angles for sugar pine at 8% moisture content (Franz, 1958)

Franz also found that the cutting forces increase with increasing specific gravity and depth of cut but decrease with higher moisture contents. Increasing the rake angle decreases the cutting forces. Results from a stress analysis by Franz led him to recommend using a

rake angle of 18 degrees for sugar pine at 8% moisture content in order to develop Franz Type II chips.

Lubkin (1957 as cited in Koch, 1964) found that parallel cutting forces could be modeled by a linear equation,

$$Fp = (A+Bt)w$$

where Fp is parallel cutting force, t is chip thickness, w is width of the chip, and A and B are the appropriate empirical constants for the species, moisture content and cutting configuration.

In a few situations this linear relationship does not hold for very thin chip thicknesses (0.003 inch and less). Instead the forces decrease rapidly and are better modeled by

$$Fp = K\ t^m\ w$$

where K is a constant and m is a constant between 0 and 1. In effect, for very thin chips, the cutting forces decrease exponentially below the linear model.

McKenzie (1960) carried out a study measuring cutting forces and chip formation across the end grain in the 90-90 orientation. He observed significant deflection of the fibers before they were severed. He attributed wood's unique cutting behavior to its cellular structure and the fact that the cutting radius of a sharp working knife ranges from one tenth to one full double-wall thickness of a wood cell. The

cutting edge does not impose the highly concentrated load on the fibers that an ideally sharp knife would. This causes the fibers to deflect greatly before they are severed by the cutting edge (Figure 8). This in turn influences the cutting behavior of wood. There are two stages to the cutting of wood: indentation and incision. During the indention stage, the force increases as the fibers bend from the pressure of the edge. Finally at the incision stage, the fibers fail which relieves the built-up forces. The cycle then begins again.

McKenzie defined two type of chips (Figure 9) which are distinctly different from those defined by Franz. The McKenzie Type I chip fails in the cutting plane. In addition vertical splits form along the fibers extending down into the wood. With the McKenzie Type II chip, the wood fibers fail below the cutting plane pulling chunks out of the wood. He postulated 5 zones of potential wood failure depending on wood properties which cause these types of chips (Figure 10). A clean-cut surface is the result of fibers failing in tension in zone 1. Shear failures in zone 2 cause the chips to break up into subchips. Failures in zone 3 cause the splits between the fibers. If the failure of the wood takes place in zone 4 due to excessive bending, a Type II chip is formed. Zone 5 is an alternate zone for zones 2 and 3.

McKenzie's cutting force results were compatible with those of Franz. Increasing chip thickness and specific gravity increase the cutting forces while increasing moisture content and rake angle decrease the cutting forces. He did note that for rake angles less

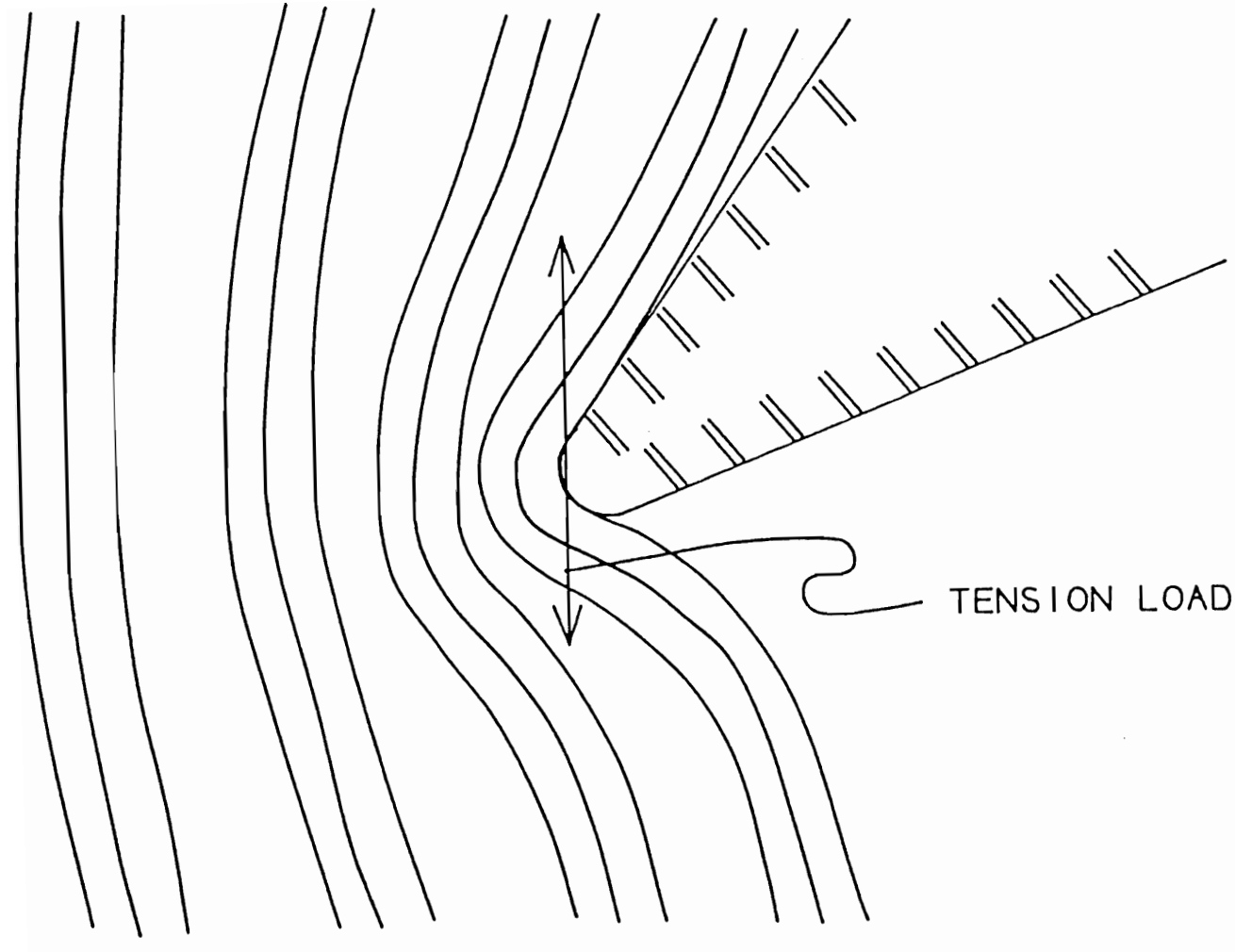

Figure 8. Fiber deflection during indentation phase of cutting

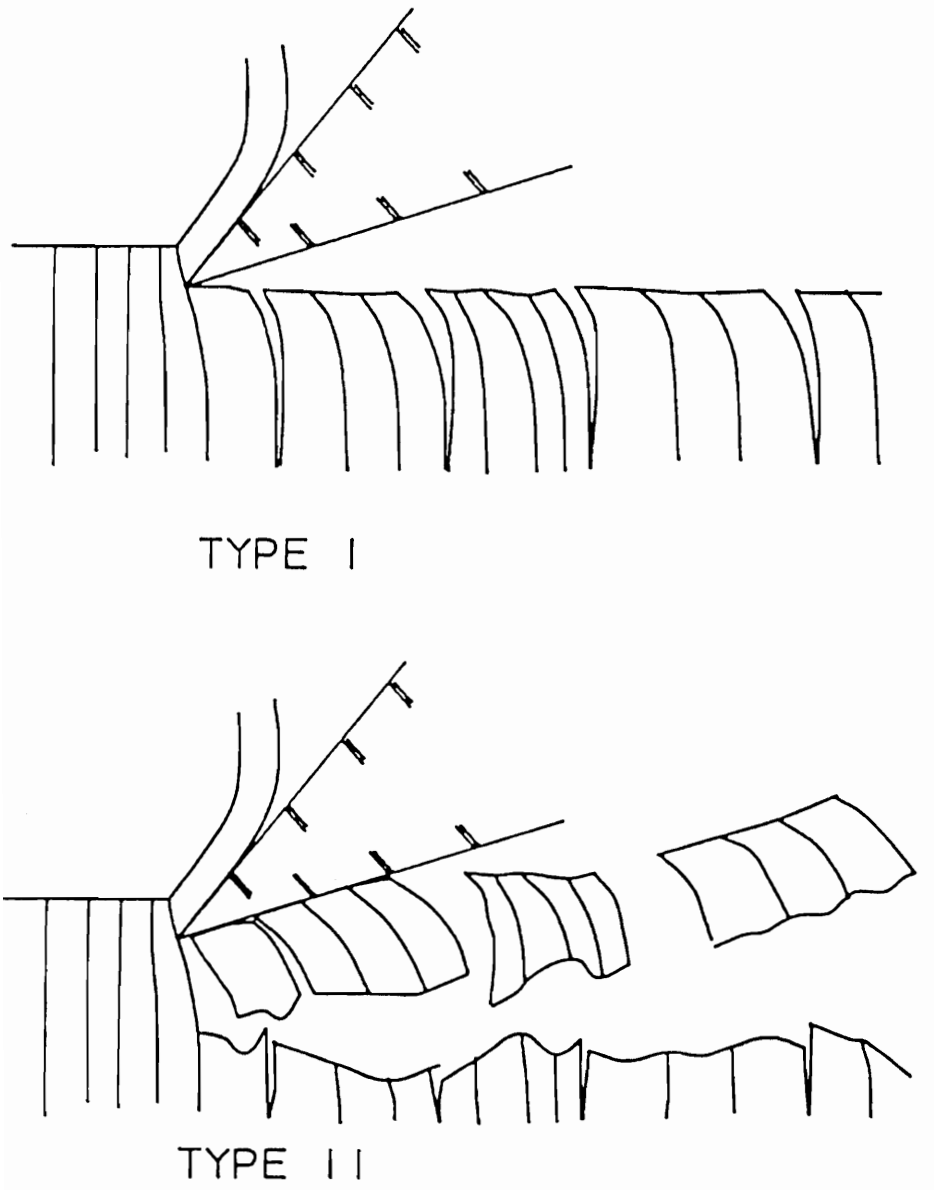

Figure 9. McKenzie Type I and Type II chips

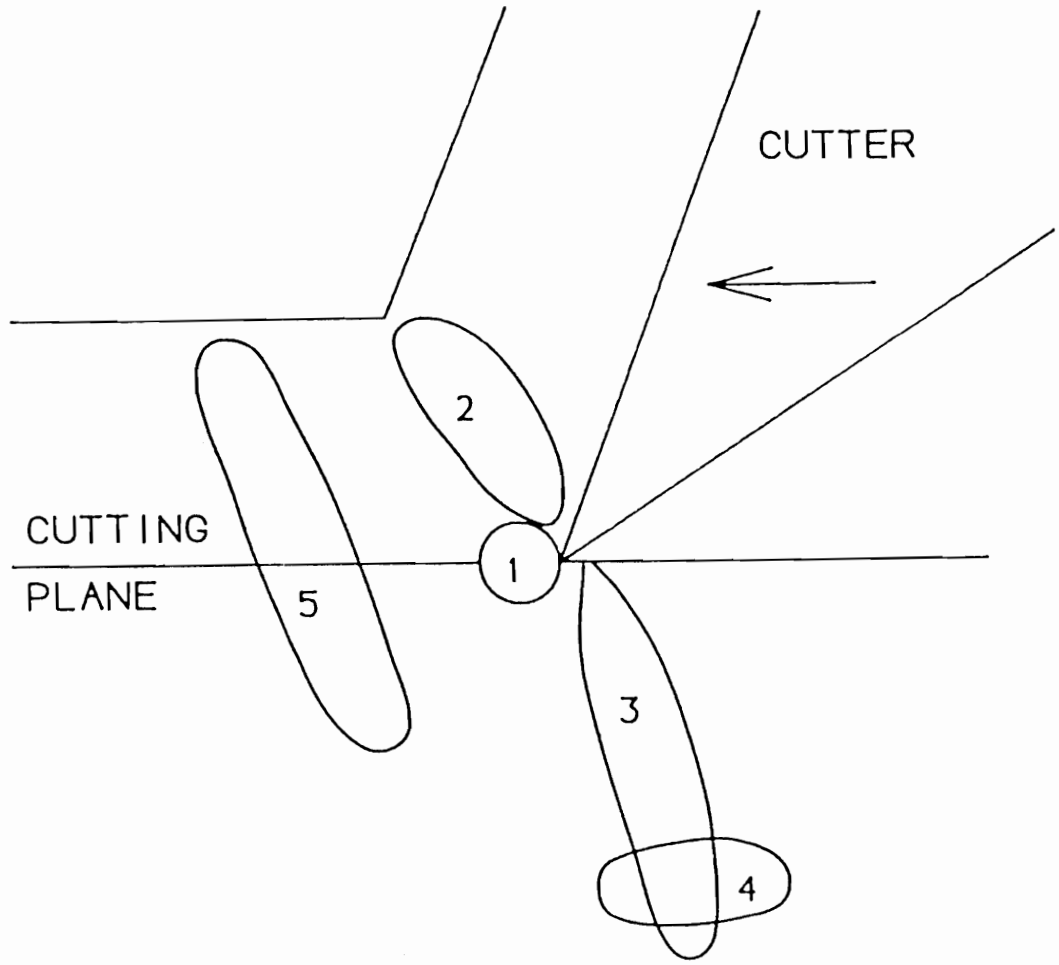

Figure 10. McKenzie's zones of potential failure: 1. tension failure at knife tip, 2. chip breaking into subchips, 3. cracks developing between fibers, 4. failure in bending causing Type II chip, 5. alternate location for failures at 2 and 3.

than 20 degrees, e.g. finger-joint cutters, the wood is removed by crumbling or scraping rather than clean cutting. He also noted that the most important variables involved are species properties, moisture content, rake angle, and chip thickness.

McKenzie used the results of the cutting force tests to model the cutting behavior of wood with a double beam theory. This model considers the way in which fibers deflect prior to severing in order to determine the parallel cutting forces. The wood fibers are modeled as a semi-infinite cantilever beam in an elastic foundation. Failure, i.e. cutting, is either at the knife tip caused by tension parallel to the fiber direction (McKenzie Type I) or down in the foundation caused by bending (McKenzie Type II). The model uses the moduli of elasticity, shear and tensile strength to define the wood properties. It uses an empirically derived cutting friction angle in its calculations.

McKenzie's double beam model uses the following machining variables and material properties:

w, the chip width,

t, the chip thickness,

σ, stress at failure in tension parallel to the fibers,

α, the rake angle,

β, the friction angle, empirically determined from

$Fn / Fp = \tan(\beta - \alpha)$ (typically 31.6 for sugar pine),

El, the modulus of elasticity in bending tangentially,

E1′, the E for an elastic foundation = 0.82 E longitudinal,

E2, the modulus of elasticity in bending longitudinally, and

E2′, the E for an elastic foundation, compression perpendicular to grain = 4.1 E tangential.

First, it evaluates the following constants

$$a = \frac{1440}{w E_2'} \left(\frac{E_2'}{E_2}\right) D^2$$

$$b = \sin(\beta - \alpha)$$

$$c = \frac{0.424 \; w \; t \; \sigma \cos(\beta - \alpha)}{\left(\frac{E_1'}{E_1}\right)^{1/2}}$$

where $D_{\lambda t} = e^{-\lambda t} \cos \lambda t$ and $\lambda = 10 \left(\frac{E_2'}{E_2}\right)^{1/3}$.

It then calculates the force parallel to the direction in which the knife is moving, Px, with

$$Px = \frac{b + \sqrt{b^2 + 4ac}}{2a}$$

(McKenzie, 1960, 1961, 1962).

The studies of Franz and McKenzie have been duplicated by other researchers (Woodson and Koch, 1970; Woodson, 1979) for southern pine

and some southern hardwoods. The relationships between the forces, surface quality, and cutting parameters were the same as those found by Franz and McKenzie, except for minor differences for each distinct species.

Inclined Cutting

Inclined cutting is similar to orthogonal cutting except the cutting edge is inclined at an angle other than 90 degrees to the direction of cutting (McKenzie and Franz, 1964; McKenzie and Hawkins, 1966). With inclined cutting a new lateral force component appears in addition to the normal and parallel cutting forces. A total force was resolved from a combination of the parallel, normal, and lateral forces. By increasing the inclination angle from 0 to 80 degrees they were able to reduce the resultant cutting forces by 50 % and more. They were also able to greatly improve surface quality. In cutting end grain, they were able to manufacture a surface without subsurface splits. They defined this as McKenzie Type 0 chip formation.

They concluded that angling the cutting edge had the effect of increasing the effective sharpness of the edge and the effective rake angle. Because of this the fibers were not deflected as much so stress stayed more concentrated and cutting was easier.

Inclined cutting of wood, either parallel or perpendicular to the fibers, increases the range of rake angles, chip thicknesses, and fiber angles over which a satisfactory surface can be machined.

Studies at Other Fiber Orientations

Of all the studies of wood machining orientations other than 90-0 and 90-90 (Stewart, 1968; Kollman, 1968; Mori, 1971), Harold Stewart carried out the most thoroughly documented investigations. The results of these studies show that cutting forces are slightly higher when cutting across the fibers, 90-90, than along the fibers, 90-0.

In the region from 90-0 to 90-20, Stewart (1968) observed chipped grain similar to that produced by a planer knife. This is a Franz Type I chip and is produced with fairly low cutting forces. As the fiber angle increases from 90-35 to 90-60, the cutting forces rise significantly. This is the area of maximum fiber deflection. The wood fibers are deflected farther before they are severed. This bending causes the angle between the tool and the fibers to approach 90 degrees when they are finally severed. At 90-70 and higher grain angles, the cutting forces drop off because the fibers seem to already be at some optimum angle for cutting. From 90-90 to 90-180, the knife moves with the grain and the parallel cutting forces gradually decrease.

Stewart derived a term which he called the "cutting friction coefficient" and defined it as

tan (arc tan Fn/Fp + rake angle).

This is the tangent of what McKenzie called the cutting friction angle. This quantity, although not actually a friction coefficient, does reflect the deflection of the fibers during cutting, which reached a maximum when cutting against fibers inclined at 40 degrees.

Other machining studies have been made with the wood oriented as in plywood lathe peeling. Kivimaa (1950 as cited in Koch, 1964) conducted some tests in this 0-90 cutting orientation. He found the same relationships as Franz and McKenzie between chip thickness, moisture content, specific gravity, rake angle, and cutting force. He also noted that the magnitudes of the forces were about one third to one half of those in the 90-0 configuration.

Finger-Joint Cutting Parameters

Finger-jointing is a complicated peripheral milling process because both the ends and sides of the bits are cutting wood. The tips of the bits are cutting end grain in a 90-90 orientation. They typically have a rake angle of 18 degrees and a clearance angle of 3 degrees (personal communication with industry personnel). The sides are cutting across the fibers similar to a veneer knife. Typically they have a 18-90

orientation. The sides of the cutters have a 0 degree rake angle, an inclination angle of 18 degrees, and a clearance angle of 5 degrees.

McKenzie (1961) noted for the 90-90 configuration at low rake angles failure may not occur in zone 1 at all. He compared the situation to the standard crush test in which fiber severance does not usually occur along the edge of the loading tool. In finger-jointing, the inclination angle which should improve cutting complicates the analysis and makes an extrapolation impractical.

A finger-joint cutting head consists of several stacks, or bolts, of individual finger-joint bits bolted into a circular head (Figure 11). There can be anywhere from two to ten of these bolts in a head. The most popular ones have ten. Typical cutting circle diameters for a finger-joint head are 9 and 10 1/2 inch. The individual cutters are made from high speed steel or carbide depending on the application.

Typical Operating Conditions

Finger-jointing machines typically operate with the following parameters (personal communication with industry personnel):

conveyor feed speed of 65 feet per minute,

3600 rpm spindle speed,

9 or 10.5 inch cutting diameter,

18 degrees rake angle,

10 knives per head,

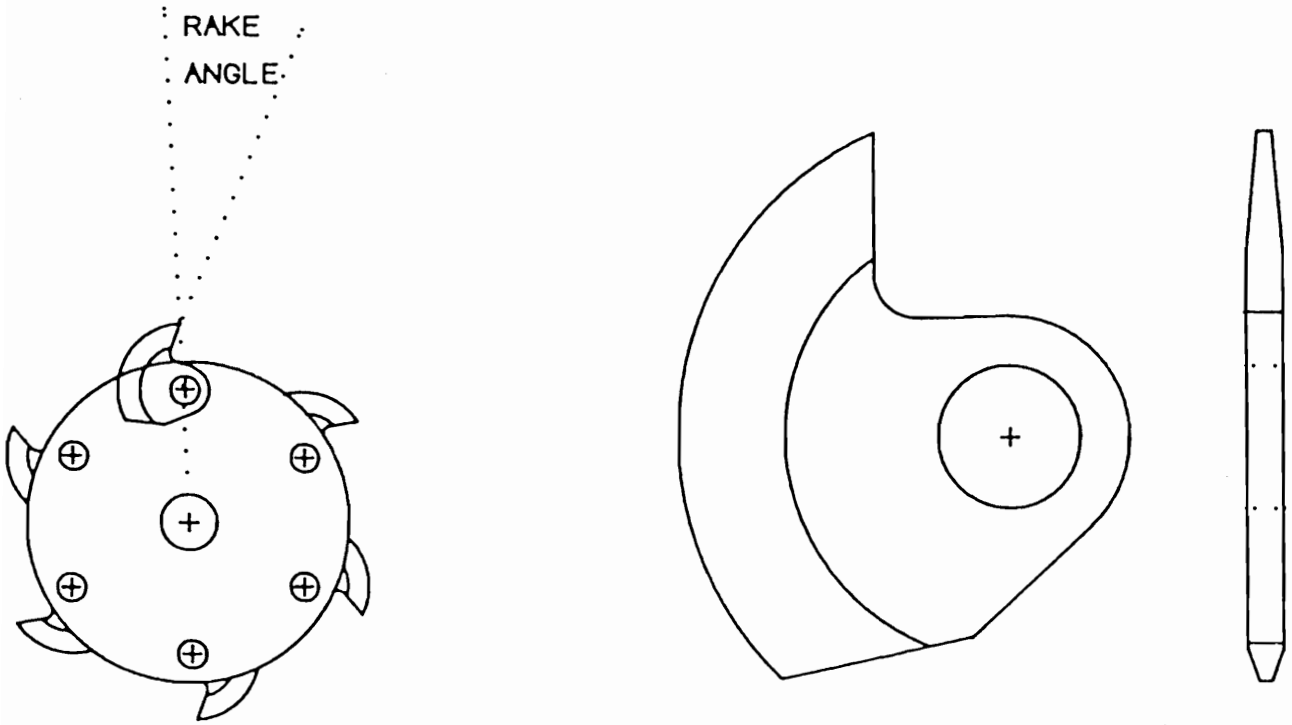

Figure 11. Finger-joint cutterhead and finger-joint bit

0.25 inch finger length,

feed per knife 0.030 inch,

maximum chip thickness of 0.010 inch, and

8 to 10 bits per bolt.

With a 1/4 inch finger on a typical cutting circle, the cutters rotate through approximately 12.5 degrees as they progress through the cut. This means that when the cutters exit the top of the board edge, they are cutting 12.5 degrees with the grain on straight grained wood. A smaller diameter cutting circle would have the effect of increasing this angle (Figure 12).

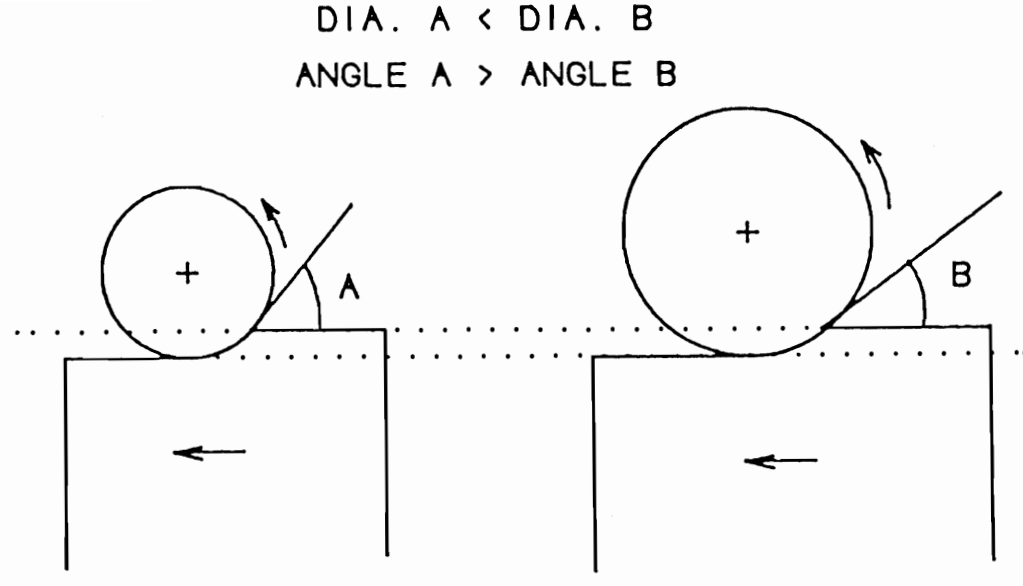

Figure 12. The angle at which the knife exits the edge of the board is increased by decreasing cutting circle diameter

METHODS AND MATERIALS

Tests Measuring Finger-Joint Cutting Forces

In order to develop a better understanding of what occurs during finger-joint machining, a series of laboratory tests were conducted measuring cutting forces and the occurrence of chip-out. These tests were patterned after the orthogonal cutting tests found in the literature.

A machine shop shaper was used for these tests because it was designed for orthogonal cutting with capabilities of positioning the cutting edge with precision (within 0.001 inch), smoothness and repeatability. The shaper was operated with a tool speed of one inch per second. This speed was convenient for data collection purposes and observation of chip formation.

The cutting tool consisted of three finger-joint bits bolted to a steel bar, which was held in the shaper's tool clamp. To keep results consistent with industry conditions, the bits were not ground or honed in any special manner and were set with a rake angle of 18 degrees. In addition to rake angle, chip thickness and chip width are known to influence cutting forces. Chip width, 0.0472 inch (width of the tip of a bit), was determined by the cutting tool. The following chip thicknesses were investigated: 0.005, 0.010, 0.015 and 0.020 inch.

A force-measuring dynamometer with a position sensor, as described below, was designed and built at the Oregon State University Forest Research Lab for these experiments. The data from the dynamometer were collected by a Campbell 21X Datalogger onto cassette tape and later transferred to a micro-computer. The datalogger reads the signals from the three load cells and the position sensor every one tenth of a second. For each pass of the cutter approximately ten force measurements were made while the tool was cutting.

Dynamometer Design

Clarke's dynamometer design (Clarke, 1963) was largely followed except the block of wood instead of the knife was clamped into the center of the dynamometer. This allowed the cutting to be visually monitored. The same dimensions for the dynamometer were used except for the sizing of the rings, which is done according to the expected load.

In an ideal cutting situation both the knife and the workpiece are perfectly rigid. Unfortunately dynamometers operate on the principal of deflection being proportional to load. A deflection of 0.001 inch was considered tolerable under the maximum expected load per cell of 25 pounds. The load cells were therefore designed to deflect 0.001 inch under a 25 pound load.

The load rings were sized by finding a suitable deflection, δ ,

$$\delta = P R^3 / (E I)$$

where P is the load, R is the radius of the ring, E is the modulus of elasticity, and I is the moment of inertia found with

$$I = 1 / (12 b t^3)$$

where b is the length of the ring, and t is the thickness.

Solving these for the expected load, P, of 25 pounds and deflection of 0.001 inch gives a length, b, of 1.25 inches and thickness, t, of 0.010 inch.

The readings from the individual load cells are mathematically combined to find the forces in the three primary directions. The functions which resolve the forces are derived from the physical dimensions of the dynamometer using statics, i.e. the sum of the forces equals zero and the sum of the moments equals zero (Figure 13).

In the actual design the knife is held above the block and moved into it to make the cut. Because the knife moves across the top of the block, the point of loading and dimension "a" are constantly changing.

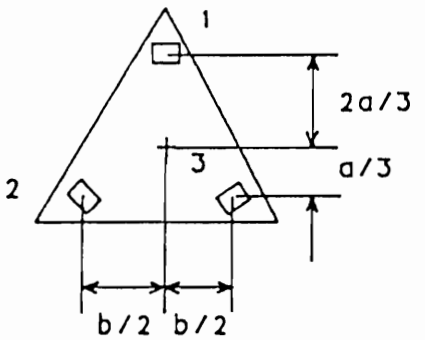

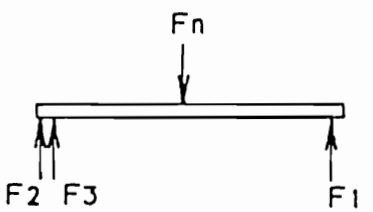

$$\sum_{FORCES} = 0$$

$$Fn = F1+F2+F3$$

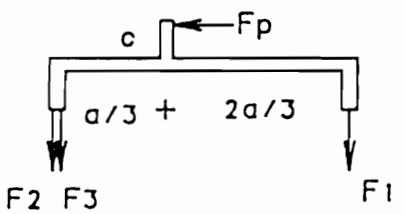

$$\sum_{MOMENTS} = 0$$

$$c\ Fp = a/3\ (F2+F3) - 2a/3\ F1$$

$$Fp = a/3c\ (F2+F3-2\ F1)$$

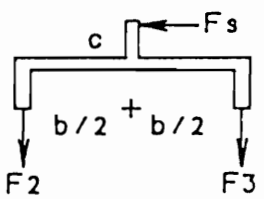

$$\sum_{MOMENTS} = 0$$

$$c\ Fs = b/2\ (F2-F3)$$

$$Fs = b/2c\ (F2-F3)$$

Figure 13. Force and moment diagram for dynamometer

The length "c", the vertical distance from the center of the load rings to the cutting plane, decreases with each pass of the head. In order to accurately derive the functions used to calculate the forces on the block, the position of the load point must be known at all times.

A potentiometer was used to detect the position of the knife relative to the block. A wire attached to the cutting head wraps around a pulley attached to a variable resistance potentiometer. A dead weight hangs on the other end of the wire. As the head moves, the pulley and potentiometer turn. Position, X, becomes a linear function of resistance and is easily calibrated. From this the load point and dimension "a" can be found. The value of "c" is found by subtracting the pass number times the chip thickness from the original block height plus 1.5 inches for the dynamometer. The moment functions are calculated in the same manner as before using the instantaneous position for finding "a" and "c".

Signal Noise Study

The no-load output of the dynamometer's strain gauges contained signal noise that could not be totally eliminated. The design of the tests allowed only very small deflections in the dynamometer's load cells even at maximum load. This in turn made the output voltage difference of the strain gauges very small from loaded to unloaded.

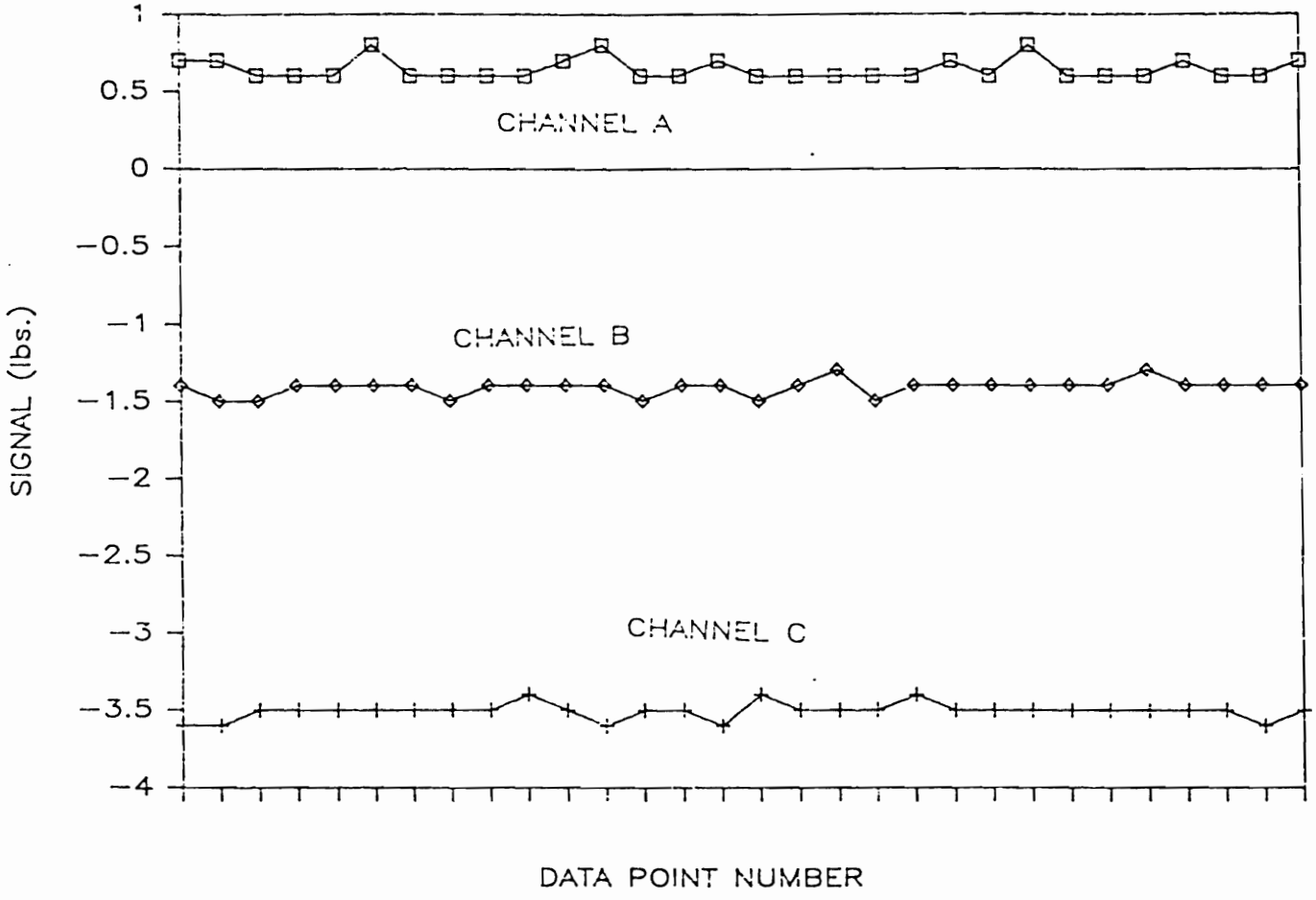

Figure 14. Signal noise from the three load cells

The noise is caused by minute, random fluctuations in this small signal voltage.

The noise from the three bridge circuits was collected under constant load and statistically analyzed. A correlation test showed that the three signals were not correlated with typical R squared of 0.1. A plot and regression of the signals showed that they varied about a mean value with no slope (Figure 14). The typical range of a signal was within +/- 0.15 lb. with a maximum variation on rare occasions of +/- 0.5 lb. For this reason, the noise is considered random. Using error estimating techniques (Rabinowicz, 1970) the signal noise was calculated to cause errors of 0.25 to 0.87 pounds per load cell or total errors 0.45 to 1.5 pounds for a force component. By repeating the tests under the same conditions for several blocks and averaging the results, the errors caused by signal noise can be further decreased.

Test Procedures

Before each block was machined, a calibration (no-load) pass was made with the shaper. These data were used to correct for the no-load offset of the dynamometer. The cutting tool depth was then zeroed by lowering the tool so that it just skimmed the surface of the block. The cutting tool was lowered, after each pass, a distance equal to the

chip thickness. The bits cut progressively deeper grooves into the blocks to form the wooden fingers. The length of the bit's sides which cut wood increased each time the cutter was lowered. The number of passes per block depended on the chip thickness. The machining was continued until the length of the fingers was at least one quarter of an inch.

Data Processing

The data collected during the cutting tests were transferred with the Campbell 21X software to an IBM AT micro-computer for processing. The data consisted of arrays of 120 elements of the three cutting forces and the knife position for each pass of the cutting head. A program was written in "C" to discard all data recorded when the knife was not cutting and calculate the three cutting forces: parallel force, normal force, and lateral force. The output of this program were arrays, grouped by cut and by block, seven elements wide, consisting of the position, the three load cell readings, and the three calculated forces.

These data were then processed with another "C" program which computed the average and standard deviation of the normal and parallel forces for each pass of the cutting tool. The four output values were grouped by cut and by block.

The data were then analyzed using Lotus 123 spreadsheet and Abstat. Abstat is a statistical software package by Anderson-Bell. Among its functions are standard deviation, mean, mode, median, and graphing. In addition it was used to calculate multiple linear regressions and Pierson's product moment correlation (r) matrix.

Material

Species, moisture content, specific gravity and fiber inclination are all known to influence cutting forces. Other wood characteristics also thought to possibly influence the machining of wood are growth rings per inch, and radius and angle of the growth rings (Booker, 1987). For each block all were measured and recorded. The standardized dimensions of the blocks were 0.65 x 1.6 x 2.3 inches.

The material used in these tests was kept as similar to that used in industry as was possible. Tests were confined to a single species, ponderosa pine. The samples were conditioned to the moisture content typical of the lumber being manufactured in industry, i.e. 8 to 12%. Specific gravity was determined by weighing each block with an analytical balance and measuring the block with calipers and then dividing their ratio by the weight per unit volume of water. The accuracy of this measurement is plus or minus 0.01. This specific

gravity was based on a 10% moisture content in the blocks, not on an oven dry basis. Fiber inclination was determined with a lumber scribe, hand lens, and protractor. Clear straight grain blocks were cut so that the fibers had the following angles: 0, 5, 10, 15, 20, 30 and 40 degrees. The accuracy of this measurement was estimated to be within 2 degrees, because of the method used and because fiber inclination varies within individual wood blocks. Tests were run both with and against the grain. The fiber angles were recorded as positive when cutting with the grain and negative when cutting against the grain. Growth rings per inch were measured by hand and recorded as inches per 10 growth rings. A template of arcs was used to estimate the radius of the growth ring in the center of each block. The angle of the radius with the edge of the block was measured with a protractor (Booker, 1987). A few test blocks containing local fiber deviation around knots were also machined.

As the test samples were being run it became apparent that certain fiber angles always experienced chip-out and others never did. Between these fiber angles lies a transition zone where chip-out occurs some of the time. A larger number of blocks were tested in these transition zones for each chip thickness in order to better define their boundaries (Table 2). This is the reason for the unequal number of observations for each chip thickness at each fiber angle. The total number of blocks tested was 457 with the number of individual force measurements exceeding 110,000.

Fiber Inclination	Chip Thickness 0.005	0.010	0.015	0.020
40	0	6	6	6
30	4	5	6	4
20	5	7	5	6
15	5	10 (6)	7	10
10	8	19 (6)	15 (10)	10
5	7 (1)	20 (10)	20 (10)	10
0	8	50 (10)	20 (10)	10
-5	8 (4)	22 (10)	6	6
-10	11	38 (13)	11	24
-15	5 (2)	5	5	0
-20	3	6	5	4
-30	4	5	0	0

Table 2. The total number of samples tested at each chip thickness and fiber inclination for chip-out and cutting forces (chip-out only)

RESULTS AND DISCUSSION

Orthogonal Finger-joint Chip-out Results

At a uniform moisture content, fiber inclination and chip thickness largely determine the occurrence of chip-out. It was found that when cutting against the grain chip-out occurred in all blocks. When cutting with the fibers, no blocks will chip-out if the fiber inclination is greater than some threshold angle. The chip-out threshold increases to higher fiber angles as the chip thickness increases.

Table 3 and Figure 15 show the frequency of chip-out in the orthogonal cutting tests.

Fiber Angle	Chip Thickness 0.050	0.010	0.015	0.020
15	0%	0%	0%	0%
10	0%	0%	27%	40%
5	0%	55%	75%	80%
0	50%	78%	90%	100%
-5	63%	82%	100%	100%
-10	64%	97%	100%	100%
-15	100%	100%	100%	100%

Table 3. The frequency of chip-out in the orthogonally cut test blocks

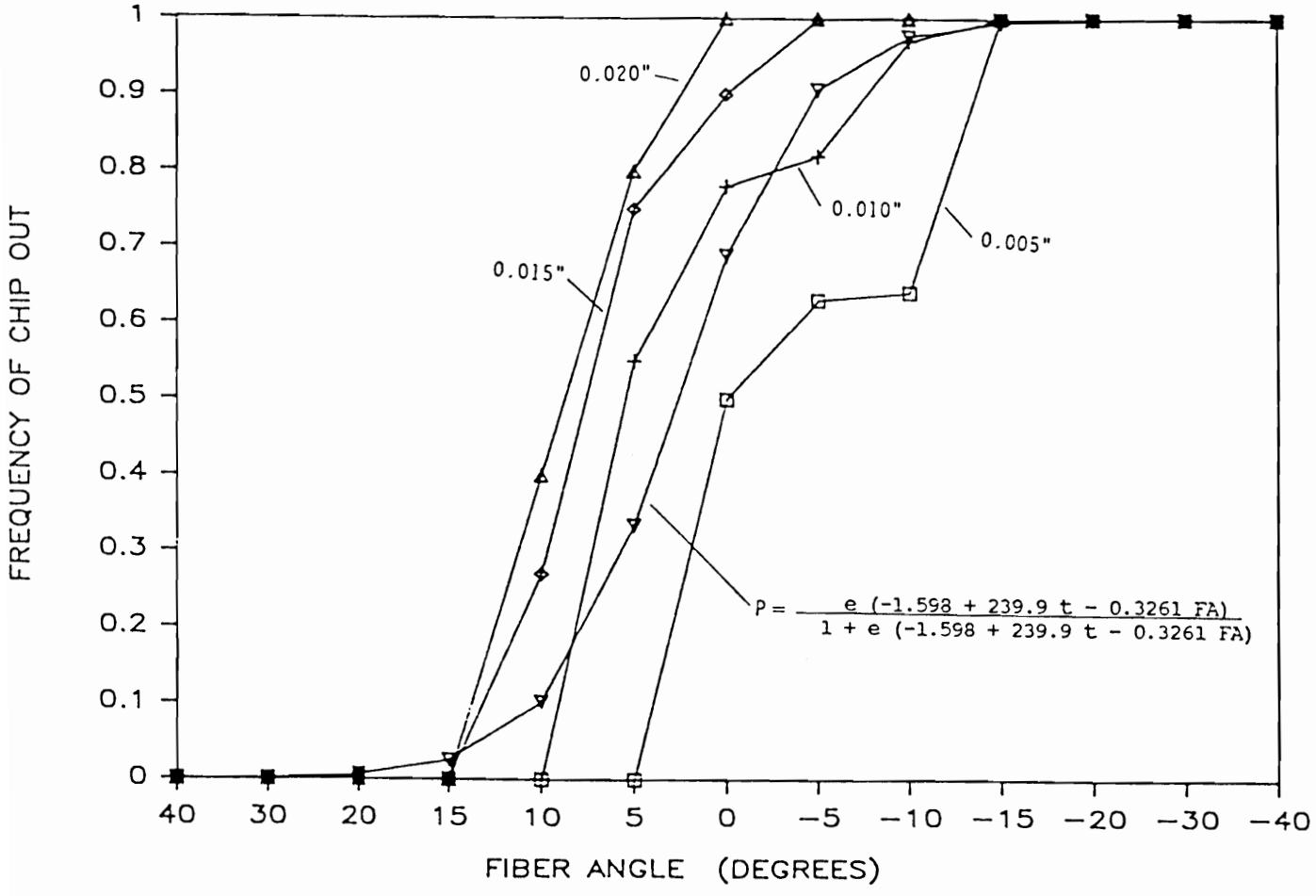

Figure 15. Frequency of chip-out of orthogonal blocks for different chip thicknesses

The standard deviation of these points (Table 4) can be estimated with

$$\text{standard deviation} = p\,q\,/\,n$$

where p is the probability of chip-out as a decimal, q is (1 - p) and n is the number of samples.

Chip Thickness	Estimated Maximum Standard Deviation
0.005	3.1%
0.010	1.2%
0.015	1.3%
0.020	2.4%

Table 4. Estimated standard deviations of the frequency of chip-out for different chip thicknesses in orthogonally machined blocks

A logistic regression software package called GLIM 3.77, copyright 1985 by the Royal Statistics Society of London, was used to derive the coefficients for an equation which predicts the probability of chip-out. The frequency of chip-out is

$$\text{frequency} = \frac{e^{(-1.598 + 239.9\,t - 0.3261\,FA)}}{1 + e^{(-1.598 + 239.9\,t - 0.3261\,FA)}}$$

where FA is the fiber angle (degrees), and t is the chip thickness (inches). GLIM also calculates the statistics for the logistic model (Table 5).

Statistic	Value
Scaled Deviance	52.07
Standard error of constant	0.506
Standard error of t coefficient	44.11
Standard error of FA coefficient	0.034

Table 5. Statistics for the logistic regression of the frequency of chip-out

A student's t-test was used to find the confidence limits for using the logistic regression equation to estimate the frequency of chip-out (Table 6).

Chip Thickness	Confidence Limits	
0.005	80%	* except at -10 degrees fiber angle which is rejected at all levels
0.010	99%	
0.015	95%	
0.020	90%	

Table 6. The confidence limits of the hypothesis that the GLIM equation can be used to estimate the frequency of chip-out. * The probability of an error at t = 0.005 and FA = -10 is 0.14%.

Further analysis showed that the angle between the cutting force and the wood fibers was the determining factor causing chip-out. Chip-out always occurred when the angle between the cutting force and the fibers was greater than 75 degrees and ceased when this angle dropped below 55 degrees. This is discussed in more detail in the section on Force Analysis.

Model of Peripheral Milling Finger-joint Chip-out

The model for predicting chip-out of finger-joints in the peripheral milling configuration (Table 7) consists of the GLIM logistic model with the following additional considerations. First the boards are not oriented as they enter the finger-jointer giving an equal probability to cutting with or against the fiber direction. The probability of chip-out becomes the average of the probability of the occurrence of chip-out with and against the fibers. The maximum probability of chip-out is 50%. The second consideration involves the knives in the cutterhead traveling in a circular pattern through an angle of 12.5 degrees. This changes the direction of the load on the fibers. Chip-out was observed to occur during the first few cuts in the orthogonal tests and probably takes place in the latter portion of the cut in peripheral milling. To account for this rotation of the cutting force, the exit angle was subtracted from the fiber inclination angle.

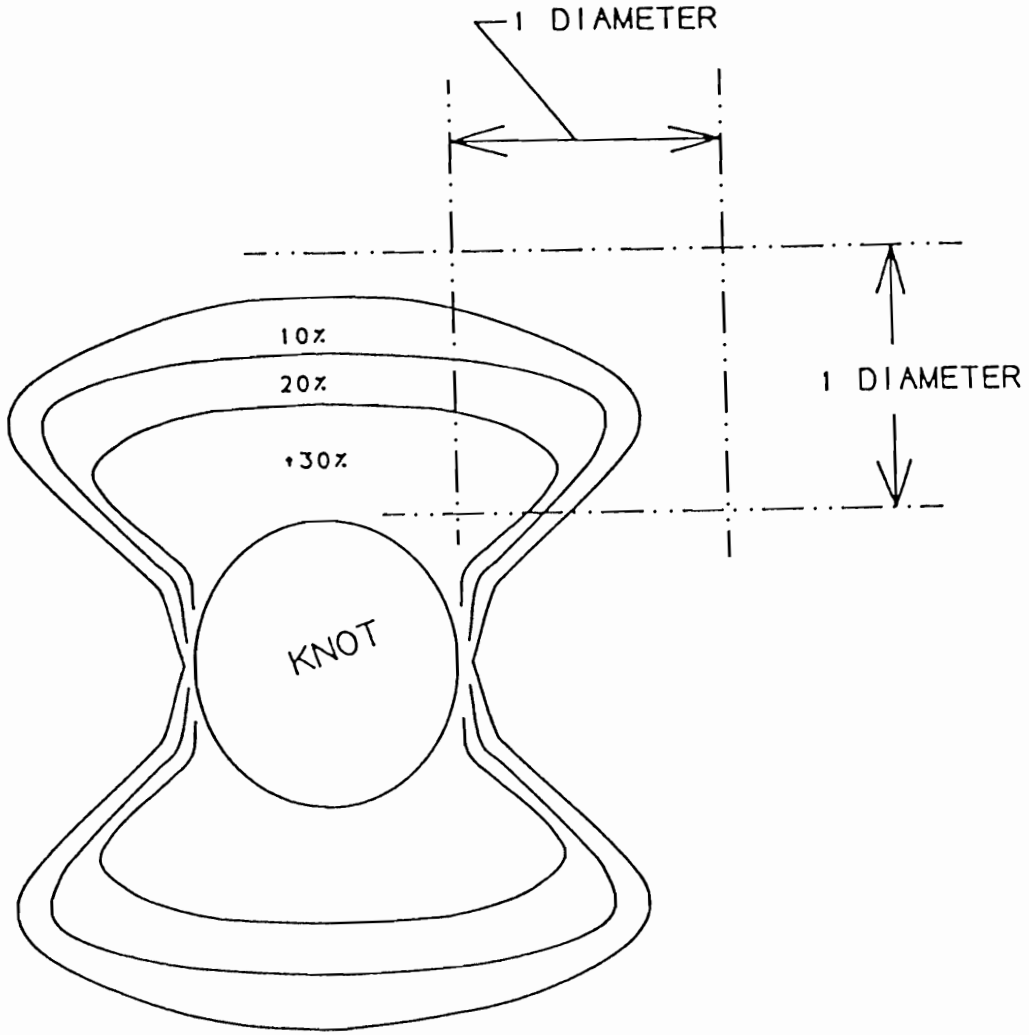

Figure 16. Zones of probable chip-out around a knot in a finger-jointing operation

Fiber Angle	Chip Thickness 0.005"	0.010"	0.015"	0.020"
0	1%	4%	13%	33%
5	5%	10%	23%	40%
10	13%	27%	40%	47%
15	32%	43%	47%	49%
20	45%	49%	50%	50%
25	49%	50%	50%	50%
30	50%	50%	50%	50%
40	50%	50%	50%	50%

Table 7. The orthogonal chip-out results extrapolated to model the probability of chip-out in peripheral milling

By combining the data from Table 7 with the results of the fiber mapping around knots conducted in Study II of this research project, zones of probable chip-out were developed (Figure 16). This diagram predicts the probability of chip-out when the trailing corner of a block falls within a particular zone. The fiber maps were developed in boards with no spiral grain. Spiral grain would have the effect of skewing the zones so that they are more in line with the fiber direction.

The probability of chip-out discussed above is based on the assumption that boards are not oriented before they enter the finger-jointer. If all of the other assumptions of the model are correct, simply orienting the boards before they enter the finger-jointer so that the knives cut with the fibers should nearly eliminate all chip-out regardless of the severity of the cross grain. Orienting the block

in this manner ensures that the cutting force applies a tensile load more parallel to the fibers.

Results of the Orthogonal Cutting Force Measurements

The cutting forces normal and parallel to the velocity vector of the cutting edge fluctuate as the knife moves across the block because of the way that wood cuts (Figure 17). Both of these forces can be characterized with a mean and a variation.

Statistic	Normal Force	Parallel Force
Mean	5.38	20.93
Variance	2.37	7.67
Standard Deviation	1.54	2.77
Coefficient of Variation	28.6%	13.2%

Table 8. Typical statistics of the parallel and normal cutting forces

Typical statistics of the parallel and normal cutting forces (Table 8) show that there is a substantial amount of variation in the cutting forces, both in relative and absolute magnitude.

The mean parallel and normal forces for the data collected for each block were calculated and plotted (Figure 18). The parallel cutting force increases linearly with each pass of the knife. This is because

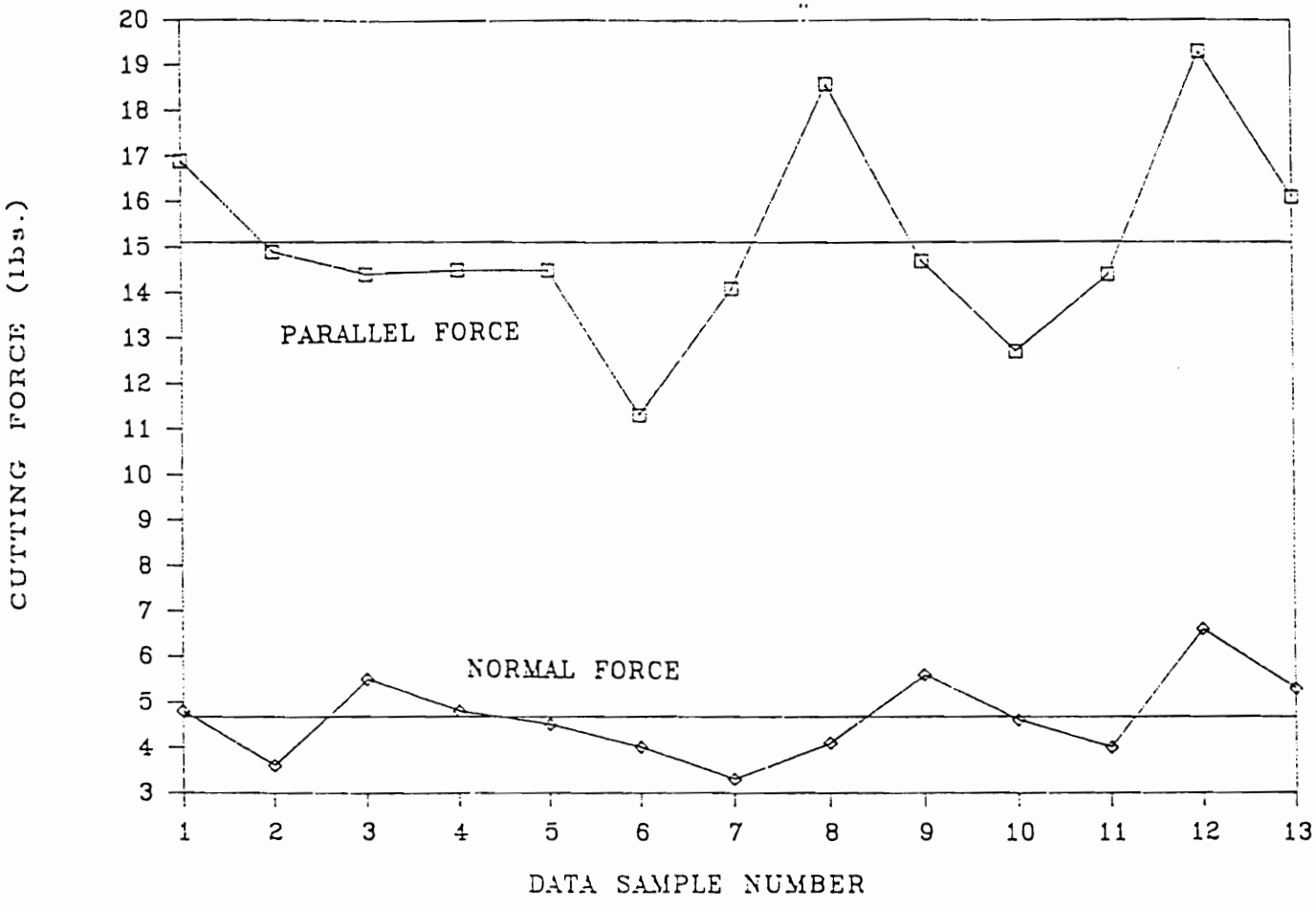

Figure 17. Typical orthogonal cutting force readings for a single pass of the cutting tool (block #29A cut #7)

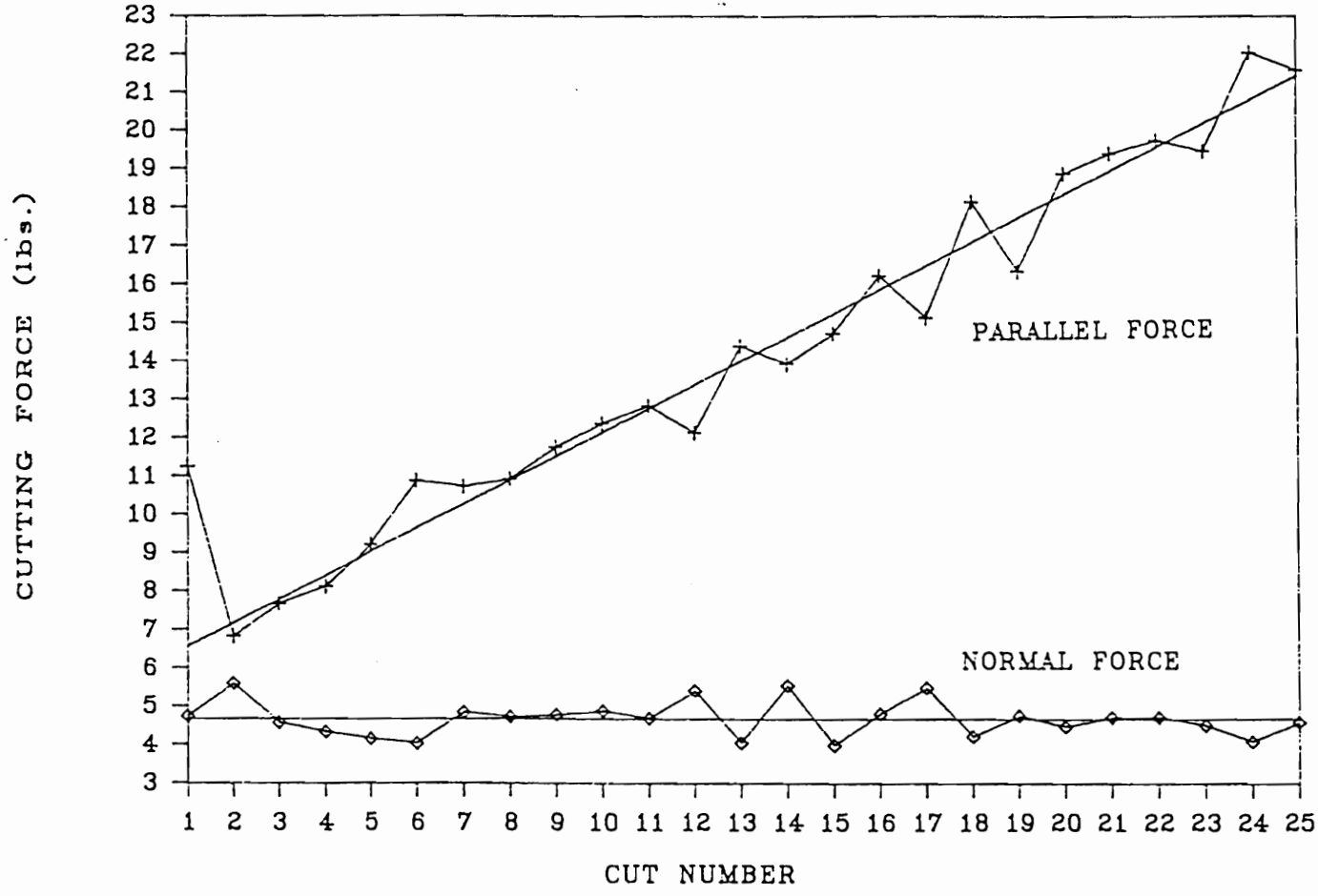

Figure 18. Typical average orthogonal cutting force readings for a block (block #65B)

the length of the bits' sides, which are cutting wood, increases with each pass. The parallel force is the sum of the parallel force caused by the tips and the parallel force distributed along the sides of the bits. The normal forces remain nearly constant from the first cut through the deepest cut. This indicates that the normal forces are due almost entirely to the cutting action of the tip of the bit. The normal force caused by the sides of the bits is below the sensitivity of the dynamometer. A linear regression was used to characterize these forces for each block. The standard error of these regressions was 1.5 pounds.

The parallel forces on the first pass seem to be unusually high. This is probably caused by the quality of the cutting surface. Initially it is a sanded, split-free surface. The first pass with the knives initiates small splits parallel to the fibers as in a McKenzie Type I chip. The second cut has lower cutting forces because the wood's strength and resistance to the knife have been decreased by these splits.

The forces in the second cut, the lowest in terms of parallel cutting forces, were attributed entirely to the tip of the cutter, since this was the only portion of the cutter in contact with the wood. With each succeeding pass, the length of the bit's side which was cutting increased. The increase in cutting force was entirely due to this increase in length of side.

For the following reasons, linear regressions were used to characterize the effects that specific gravity and chip thickness have on the cutting force. Plots of the data from this study indicated that both have a linear effect on cutting forces. Wood strength increases with specific gravity in an exponential manner (Bodig, 1982). However, over a narrow range as in this study, the effect is nearly linear. As for chip thickness, both Mckenzie (1961; 1962) and Lubkin (1957) found that chip thickness has a linear effect on cutting force.

Fiber angle had a very minor effect on cutting forces; this effect was barely within the sensitivity of the measuring equipment. Only the normal cutting forces were found to be measurably influenced by fiber angle. A linear regression was used to calculate this factor. The standard error of the equation with the fiber angle coefficient is 0.464 and is 0.674 without it. The error is significantly reduced by including the fiber angle in the cutting forces equation. In order to confirm the curvilinear shape seen by Stewart (1969) and Mori (1971), tests spanning larger fiber angles and using more sensitive instruments are needed.

The equations derived with these regressions for a single finger-joint bit allow one to calculate the parallel cutting force, Fp, the normal cutting force, Fn, and the resultant cutting force, Fr.

$$Fp = (64.6SG+893t-11)l+(1188t+8)SG+(-317t-2)$$

$$Fn = (-336.8t+7.1)SG+(-1.42t+0.0084)FA+(147.4t-1.35)$$

$$Fr = SQRT(Fn^2+Fp^2)$$

where t is the chip thickness (inches), l is the length of the side of the bit which is cutting (inches), FA is the fiber angle, and SG is the specific gravity. The graphs presented in the balance of this section show the average forces computed with the above regression equations.

Statistic	Value
correlation R squared	0.91
standard error of force	3.2 pounds
significance level of force	0.10 - accept model
standard error of resultant angle	2.5 degrees
significance level of angle	0.05 - accept model

Table 9. Statistics of the model of the orthogonal cutting force and angle of the resultant force (derived from 648 points from 27 blocks)

The statistics in Table 9 show that the regression equations can be used to predict the cutting force with an error of about 1 pound per bit and the orientation of that force within a few degrees. The t-tests show that the confidence limits of these estimates are at the 90% and 95% levels respectively.

Chip thickness was found to have the most pronounced effect on cutting forces. Increasing the chip thickness had the effect of increasing the cutting forces (Figure 19). The range due to chip thickness is 7 pounds per bit. Increasing the chip thickness also had the effect of increasing the variability of the cutting forces.

Specific gravity was found to be the next most important variable in determining the cutting forces. Increasing the specific gravity increased the cutting forces (Figure 20). Varying specific gravity from 0.35 to 0.50 caused the forces to vary over 5 pounds per bit.

The resultant force is defined as the vectorial combination of the normal and parallel forces and can typically range from 2 to 18 pounds (Figure 21). Cutting with the fiber direction has the effect of slightly reducing the resultant cutting force (Figures 22 and 23).

The other variables, rings per inch and the radius and angle of growth rings, were found to be statistically insignificant with regard to cutting forces because of their poor correlation to the residuals of the cutting forces (Table 10).

Variable	Correlation R squared
rings per inch	0.51
radius	0.48
angle	0.10

Table 10. Correlation between cutting forces and wood related variables

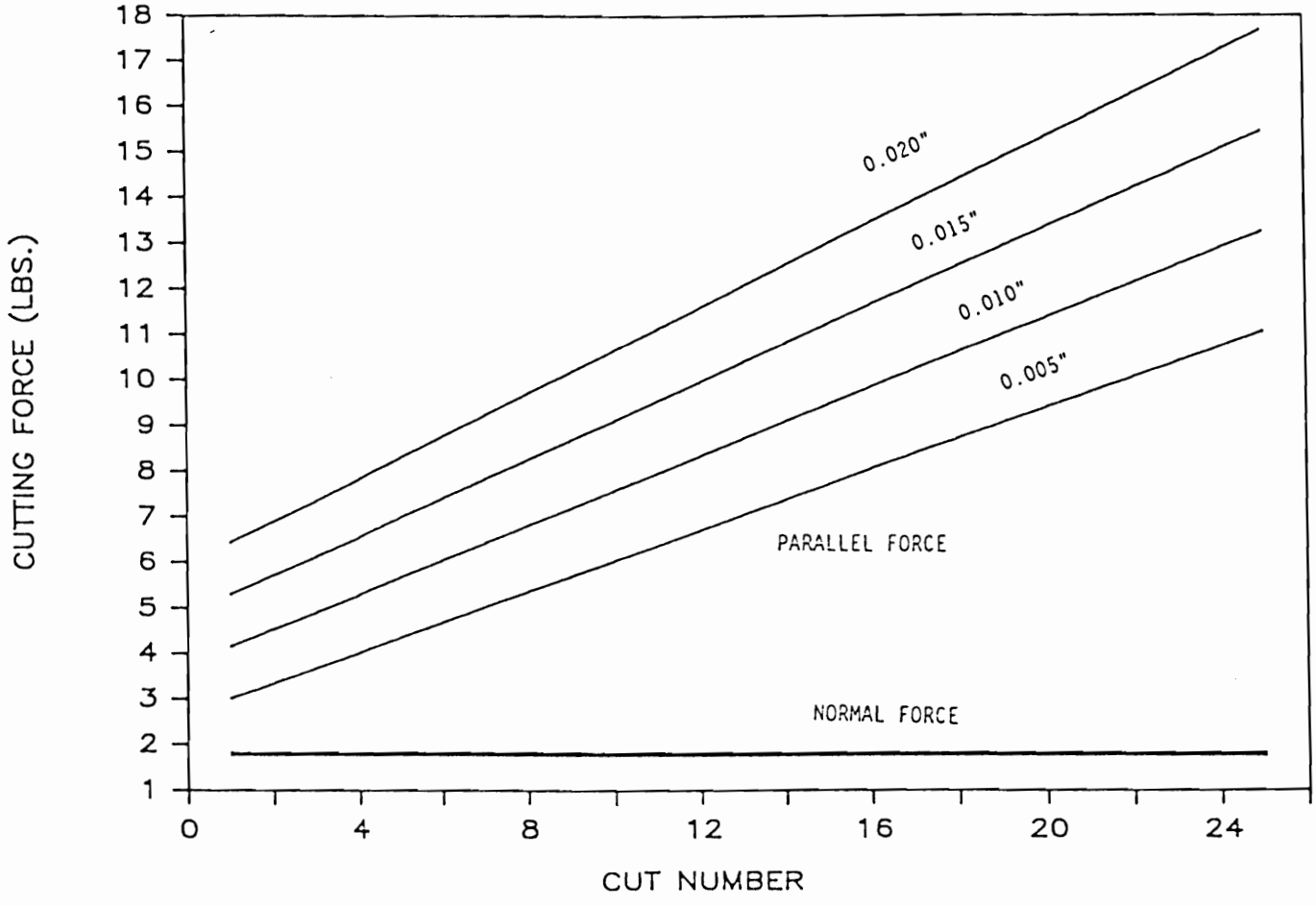

Figure 19. Average orthogonal cutting forces for different specific gravities, chip thickness = 0.010 inches

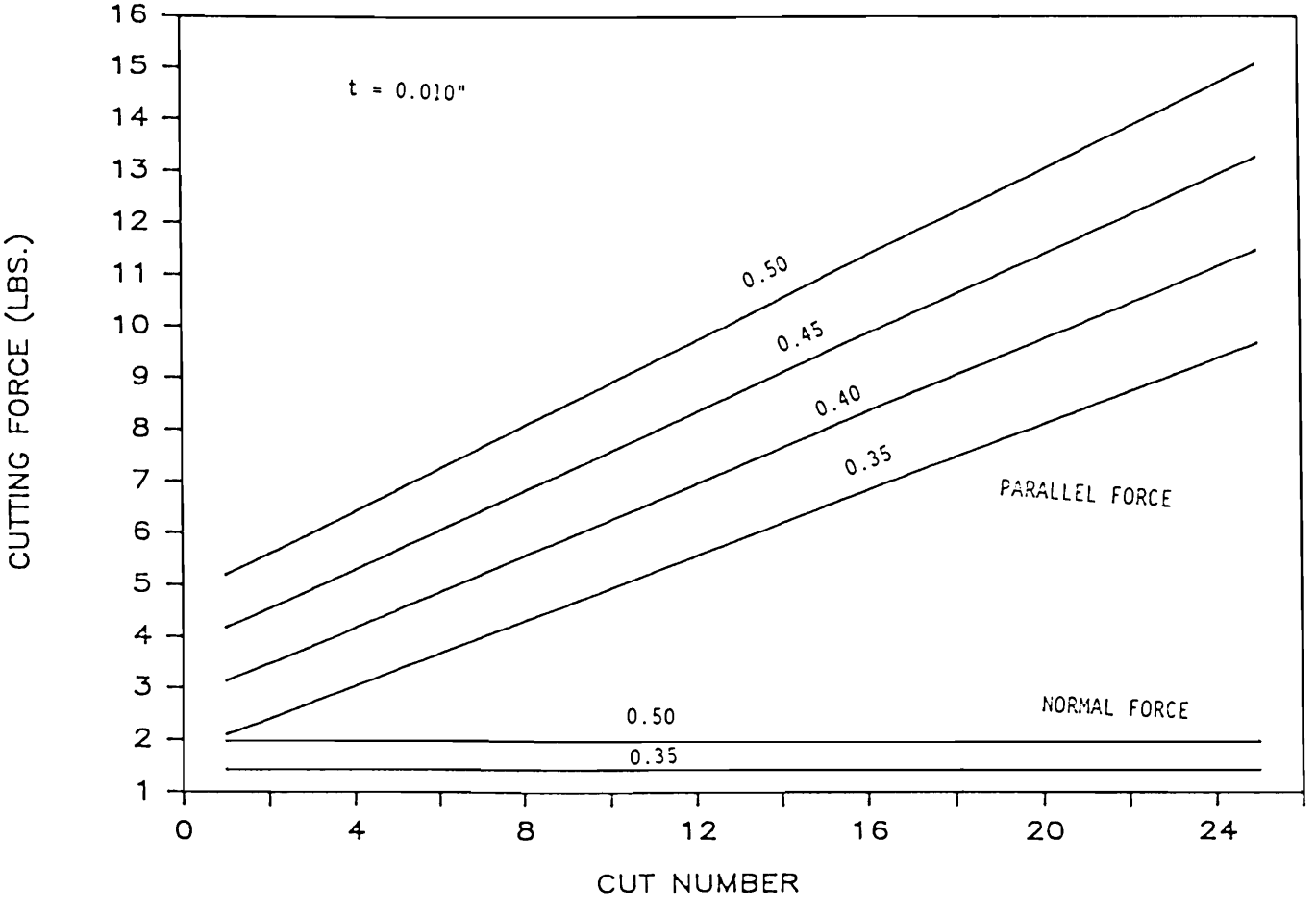

Figure 20. Average orthogonal cutting forces for different chip thicknesses, specific gravity = 0.45

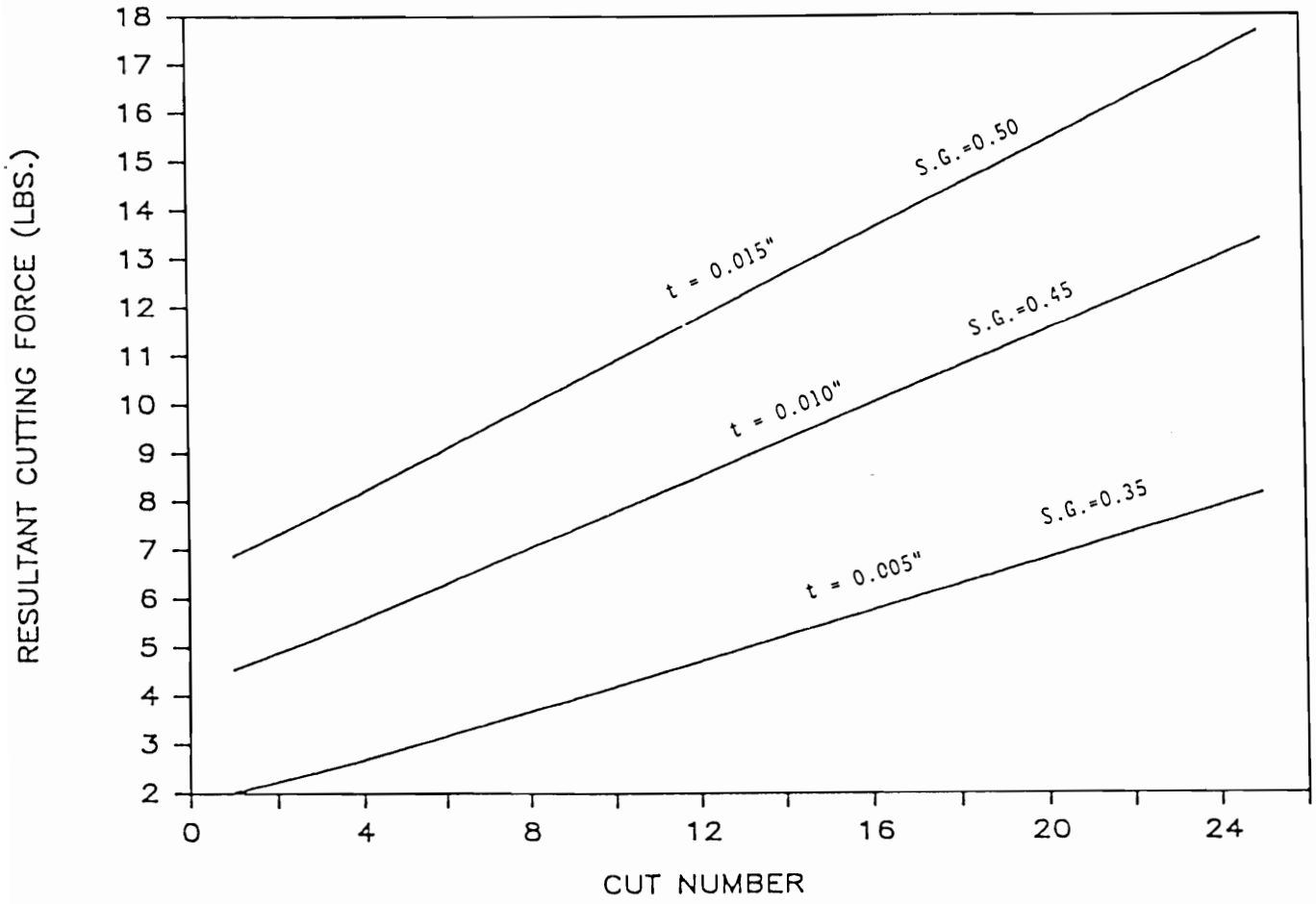

Figure 21. Range of resultant cutting force at various chip thicknesses and specific gravities

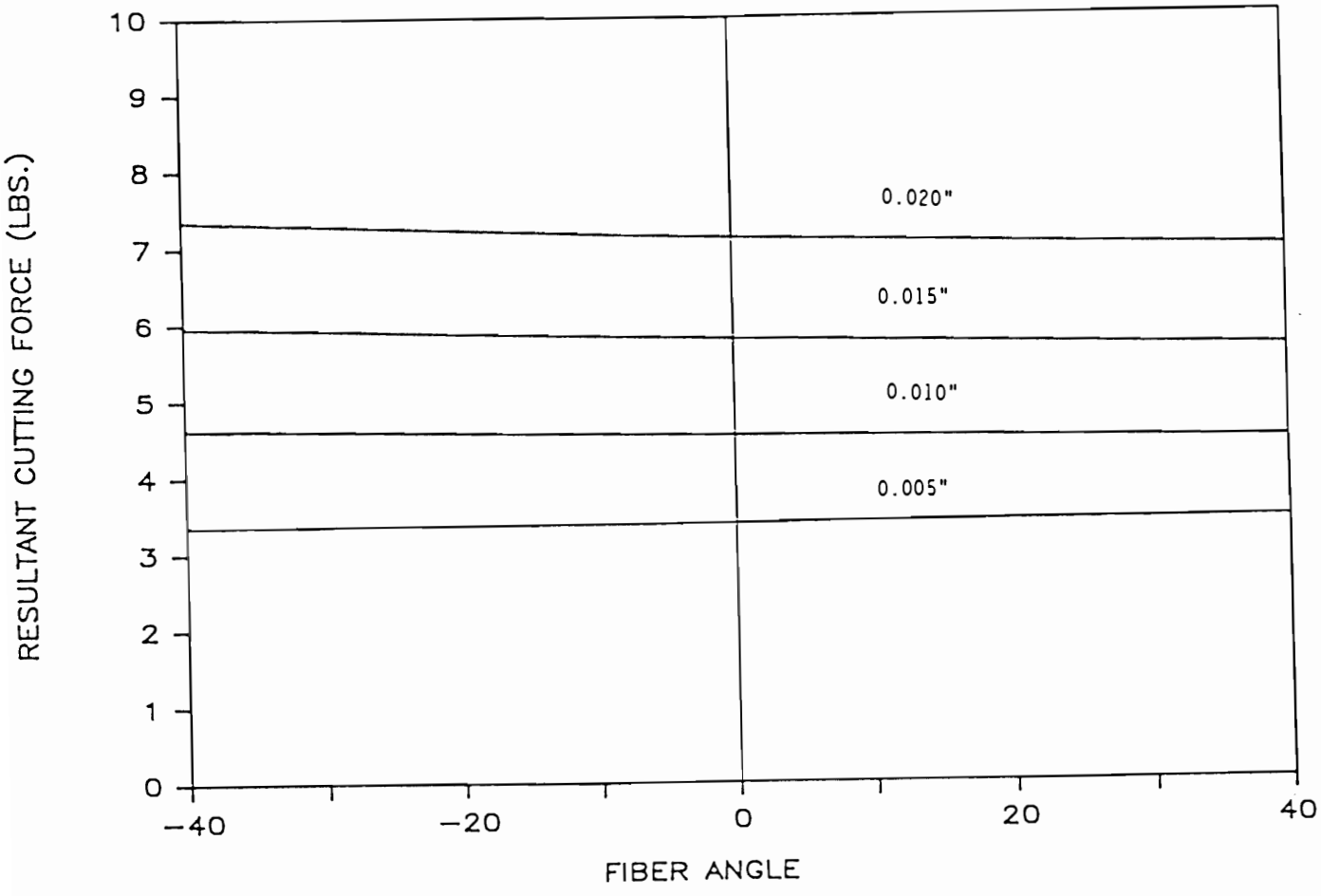

Figure 22. Average resultant cutting force versus test sample fiber angle for different specific gravities, chip thickness = 0.010 inches

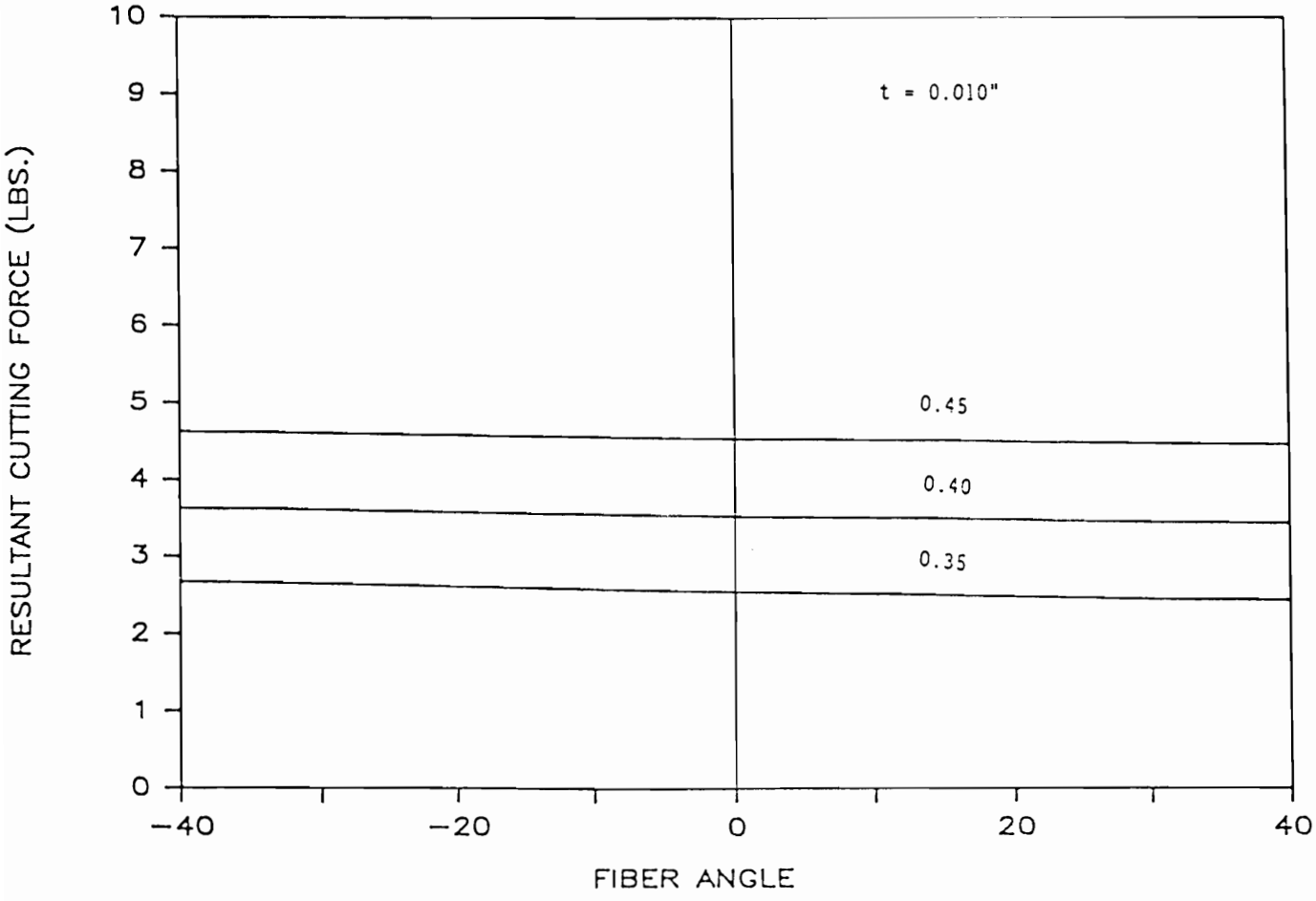

Figure 23. Average resultant cutting force versus test sample fiber angle for different chip thicknesses, specific gravity = 0.45

Force Analysis

The load applied by the cutting edge to the fibers during cutting can be analyzed in terms of its components which are parallel and perpendicular to the fiber direction (not to be confused with the normal and parallel cutting forces). A tensile load parallel to the fibers causes clean cutting, while a perpendicular load causes bending and chip-out. The magnitude and direction of these components can be calculated using the angle between the resultant force of the knife and the fiber orientation in the block of wood. The loading configuration of the fibers determines at what point and in what manner failure will occur.

The angle at which the resultant cutting force acts on the test block is the tangent of the normal force divided by the parallel force. This angle increases when cutting against the fibers of the test block (Figure 24). The angle between the cutting force and the fibers (Figure 25) determines how the fibers are loaded. This angle can be calculated by subtracting the sum of the fiber angle and the angle between the resultant force and the test block from 90 degrees (Figure 26).

The configuration of the cutting force relative to the fibers determines the force components parallel and perpendicular to fibers (Figure 27). When the knife is cutting against the fiber direction, the perpendicular force component is dominant. The force parallel to

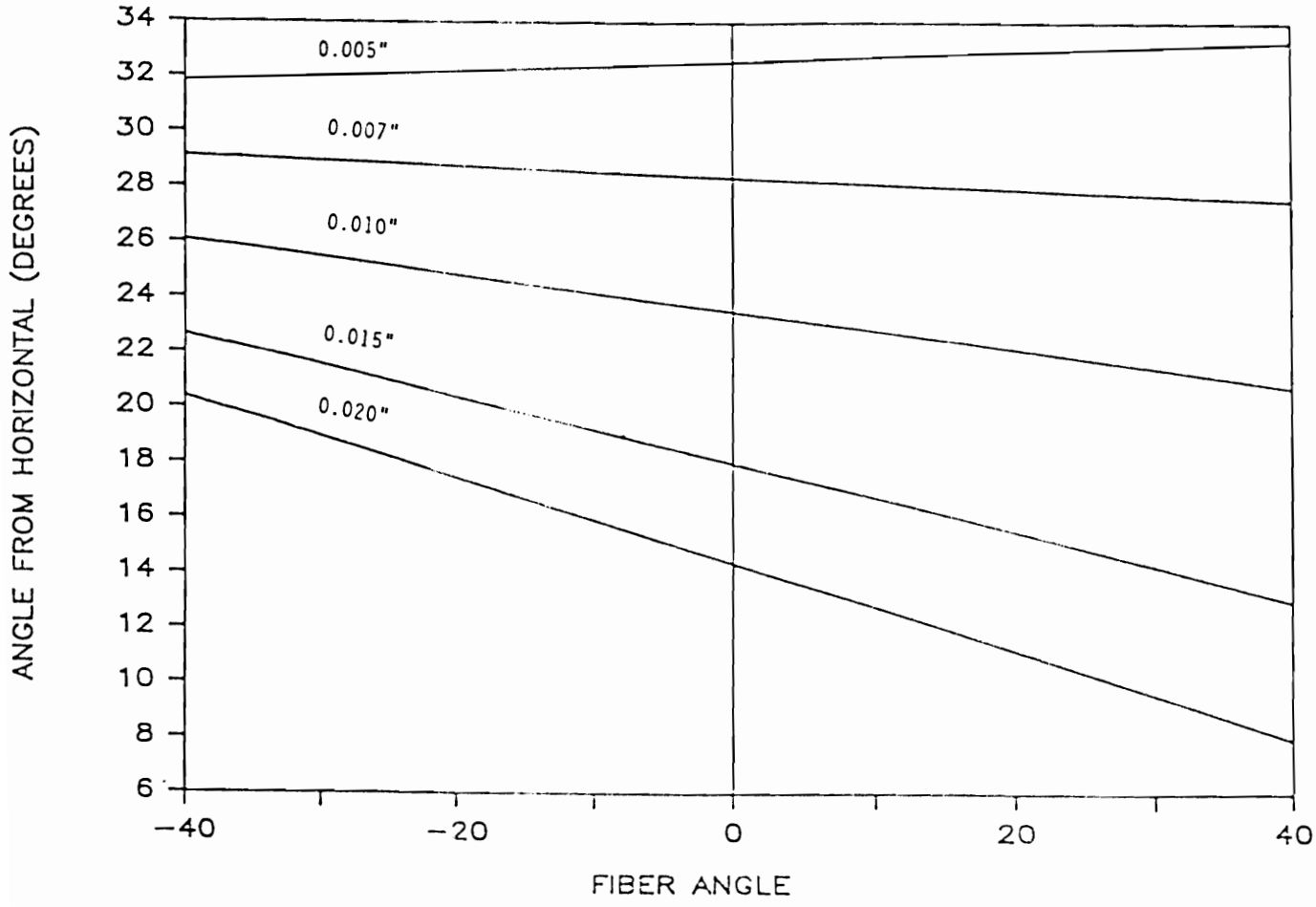

Figure 24. Angle between the resultant cutting force and the horizontal (block end) versus test sample fiber angle, specific gravity = 0.45

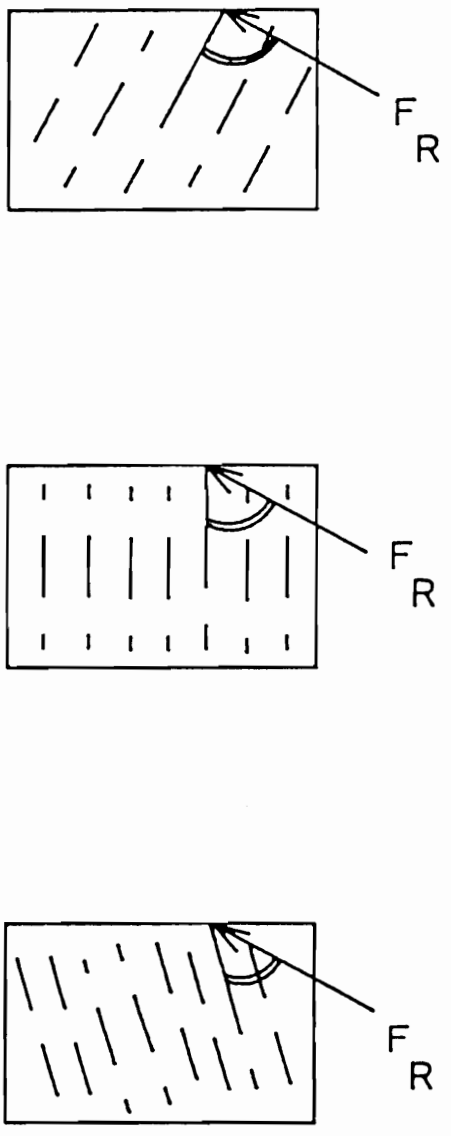

Figure 25. Angle between fibers and resultant cutting force

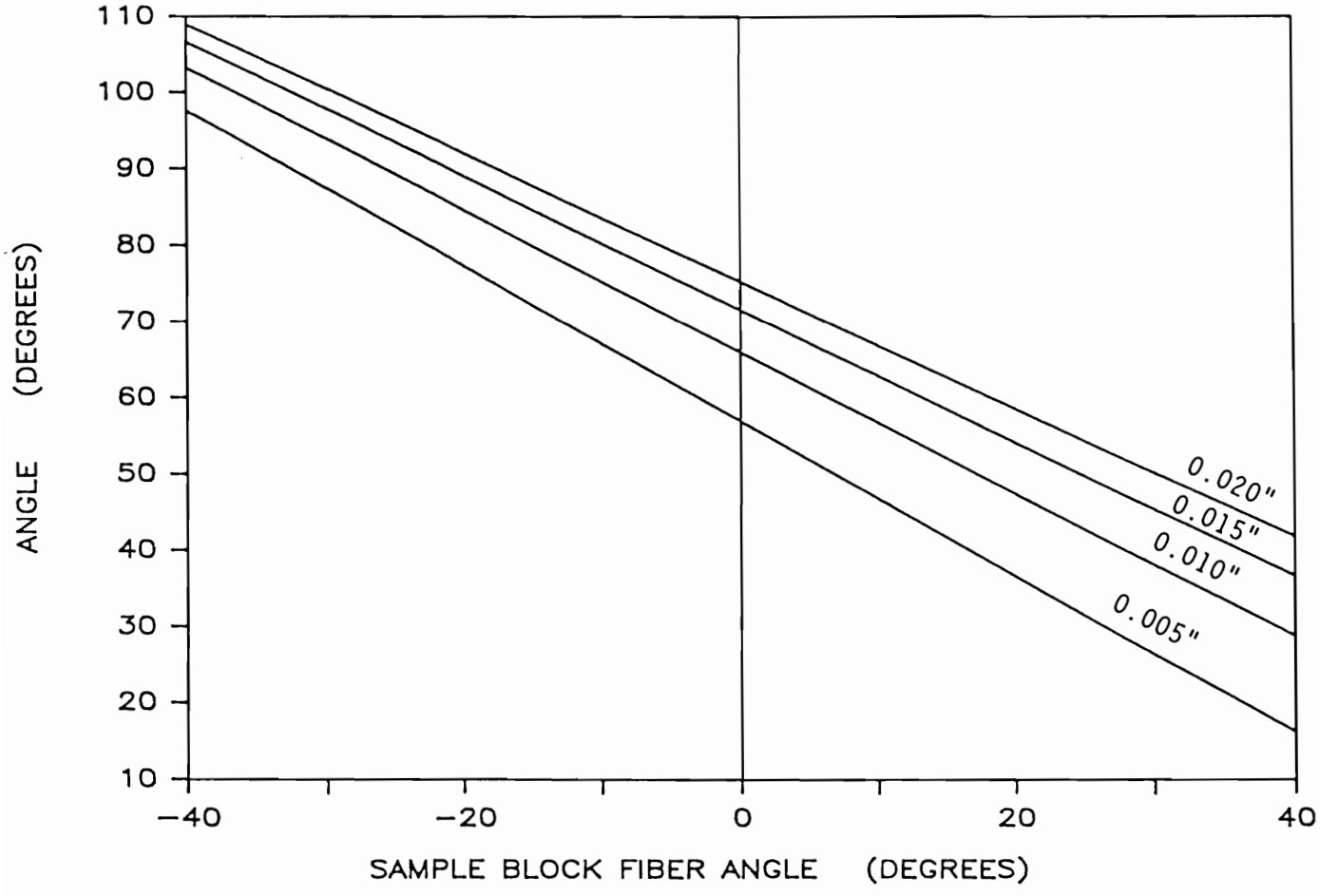

Figure 26. Angle between resultant force and the fibers in the test sample versus test sample fiber angle

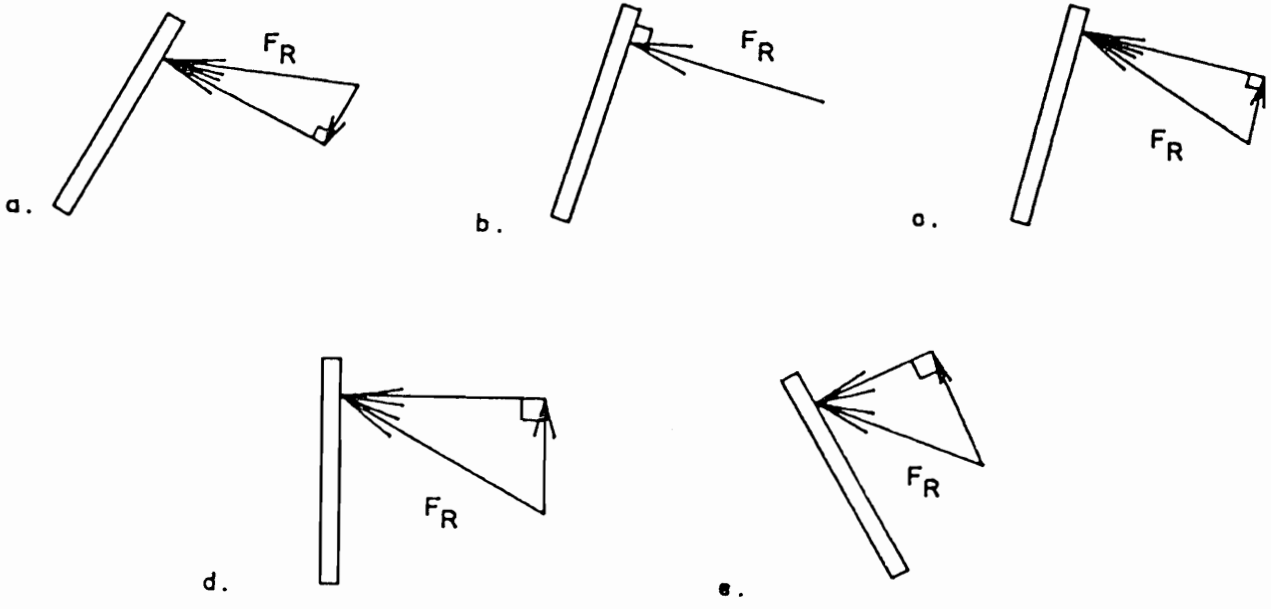

Figure 27. Resultant cutting force loading fibers at different orientations, force components parallel and perpendicular to the fibers

the fibers is small and changes from compression to tension as the fibers become more vertical. When cutting with the fibers, the parallel tensile force continues to increase while the perpendicular component decreases.

Quantitatively, the parallel and perpendicular force components are the resultant force multiplied by the sine and cosine, respectively, of the angle between the fibers and the resultant force, respectively. The magnitudes of the perpendicular and parallel forces change with the fiber orientation of the test block (Figure 28). It should be noted that these are average forces and that higher forces are expected due to the way in which wood cuts. However the relative proportions of the components will remain the same. (The intersection point of the two curves on the graph is not significant.)

Chip-out occurs when the angle between the cutting force and the fibers is greater than 75 degrees and ceases when this angle becomes less than 55 degrees with the fibers loaded in tension (Figure 29). This suggests that the perpendicular component causes chip-out before the fibers are severed. This perpendicular component loads the fibers in either tension across the grain or in cleavage.

As mentioned in the literature review, McKenzie (1962) found that the failure of wood fibers in front of a knife appears to be a tensile failure. When cutting with the fiber direction, the perpendicular component is small while the parallel forces have increased thus

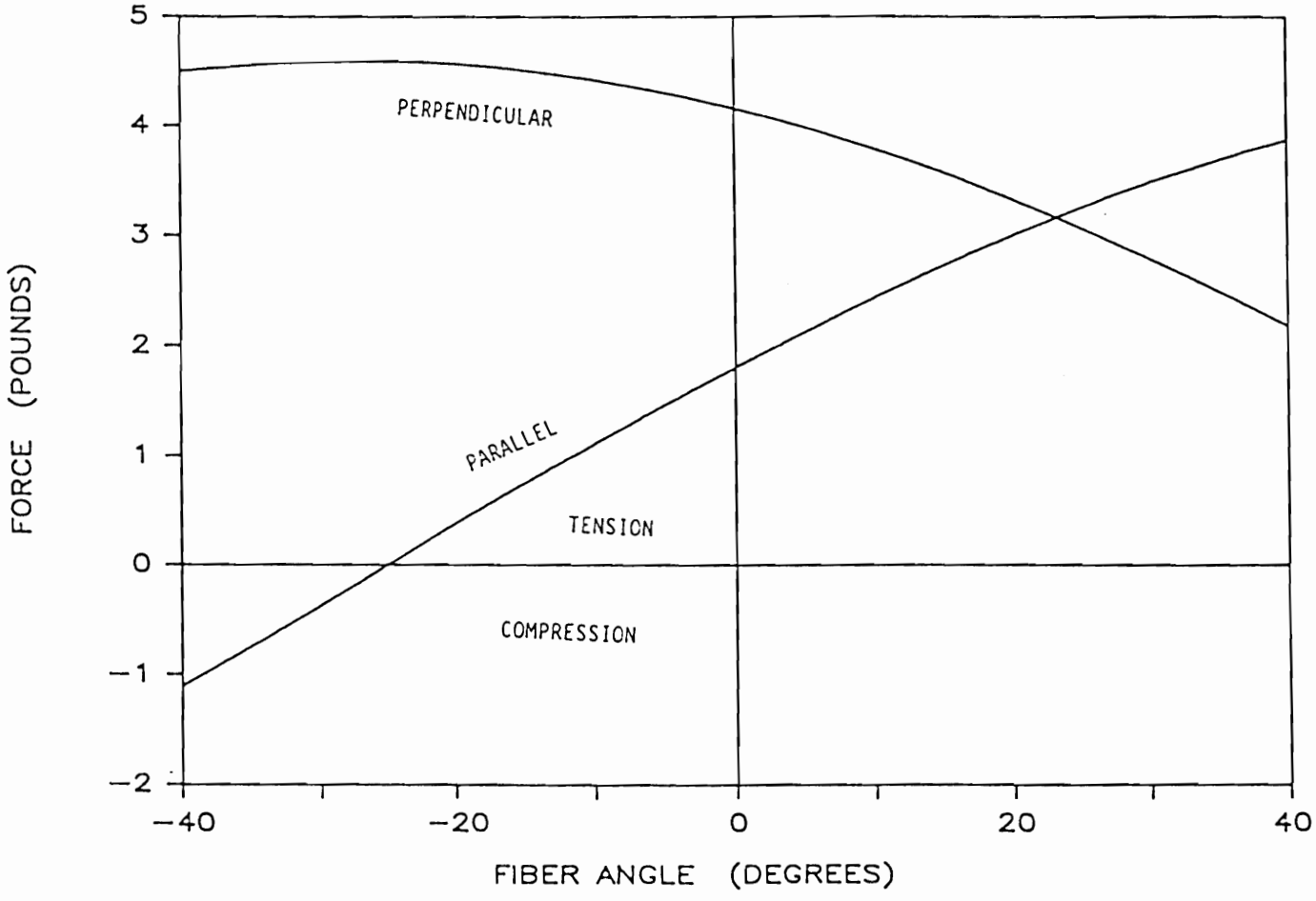

Figure 28. Magnitude of force components parallel and perpendicular to fibers versus test sample fiber angle

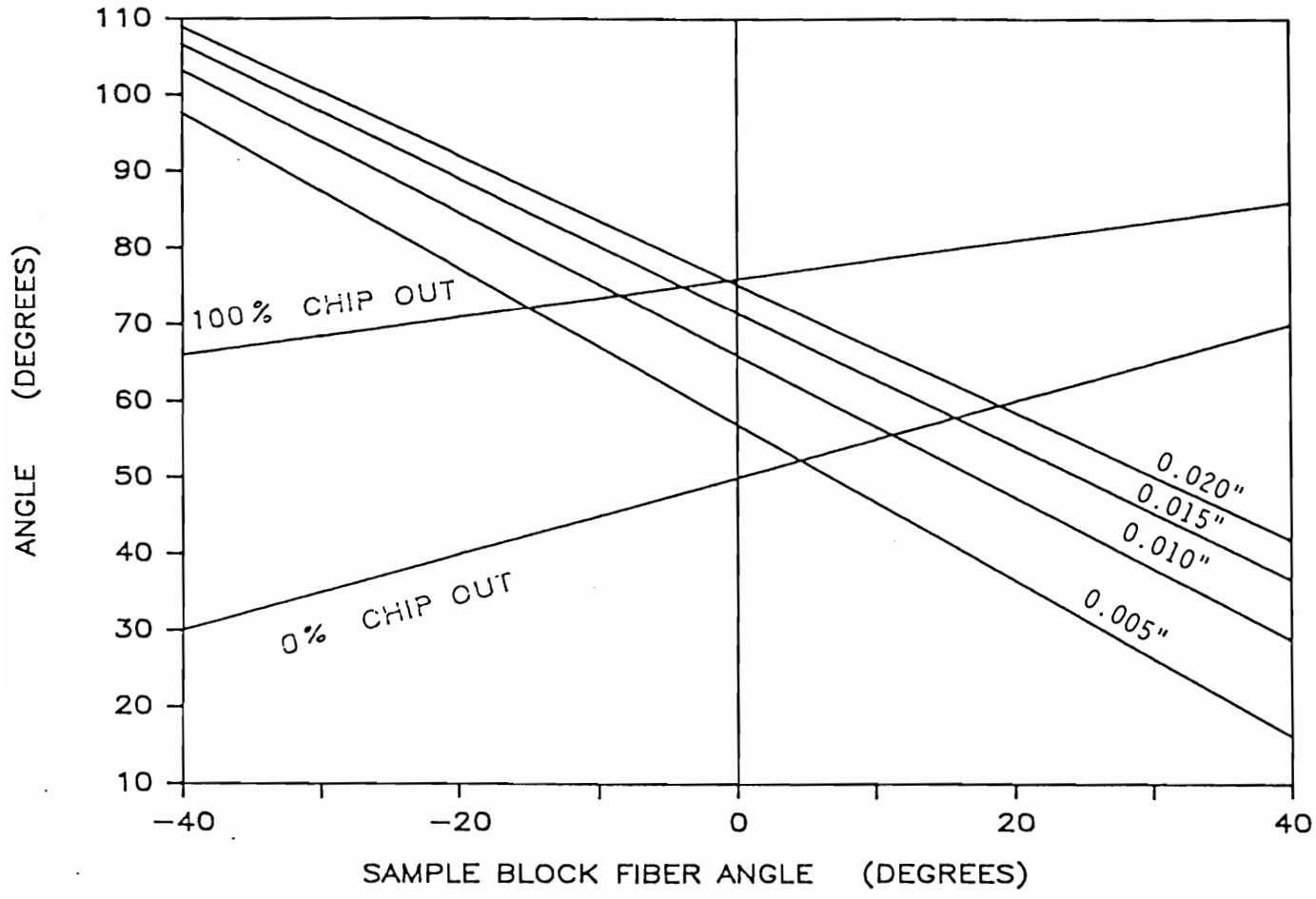

Figure 29. The occurrence of chip-out depends on the angle between resultant force and the fibers in the test sample

reducing the chance of chip-out and increasing the likelihood of clean cutting. When cutting against the fibers, the parallel component of force will be smaller or even in compression, and this will delay failure at the knife edge. The bending progresses until the deflection of the fibers causes either a sufficient tensile load for cutting or bending failure below the cutting plane.

Stress Analysis

Chip-out of the orthogonal test blocks is the result of the force applied perpendicular to the fibers in one of two types of loading: tension across the grain or cleavage. Some occurrences of chip-out were directly observed to be cleavage failures while most occurred at rates too quick to observe with the naked eye. Pine is noted as being weak in both cleavage and tension across the grain. The strength values for ponderosa pine are:

> 250 psi in tension across the grain and
> 150 lb/inch (width) in cleavage (Franz, 1958).

Wood failure occurs when the stress in the wood exceeds the strength of the wood. The stress caused by tension across the grain is dependent on the cutting force and the cross-sectional area. The load, i.e. cutting force, is fairly constant. The cross-sectional area,

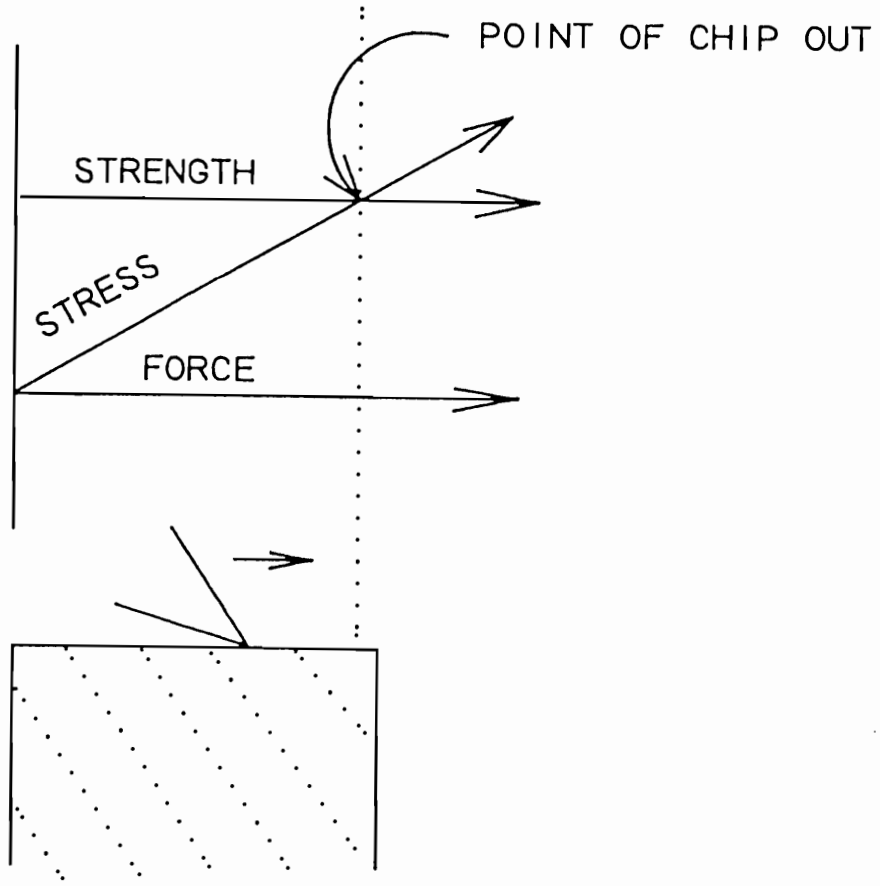

Figure 30. Chip-out results from the wood strength being exceeded by the stress caused by the cutting forces

however, decreases when cutting against the fibers as the trailing edge of the block is approached. This causes the stress to increase (Figure 30). Conversely, this area increases when cutting with the fibers which decreases the stress.

The area of chip-out was measured to be 0.02 to 0.10 square inch which would require a perpendicular force of 5 to 25 lbs. in tension across the grain to cause chip-out. From Figure 28, cutting against the fibers we get an average force (perpendicular) of almost 5 lbs. The peak forces will be higher than this average. This makes tension across the grain a possible candidate for causing the smaller chip-outs.

The force perpendicular to the fibers in conjunction with the splits along the fibers caused by previous passes of the knife are perfectly situated to cause cleavage. The same 5 pound load would cause cleavage of an untouched piece 0.03 inch wide. A load of 15 to 30 pounds would be required to split a chip 0.1 to 0.2 inch wide. The existing splits between the fibers caused by previous passes of the knife would reduce the strength of the wood and probably allow failure at a lower load. Thus both cleavage and tension across the grain could cause chip-out.

Surface Quality Results

By inspecting the blocks after they were machined, general conclusions were formed about the surface quality produced by each chip thickness. The smaller chip thicknesses produced the higher quality surfaces both on the sides and at the root of the fingers. Chip thicknesses of 0.005 and 0.010 inch produced satisfactory surfaces. Surfaces of chip thicknesses of 0.015 inch were marginal to poor and those of 0.020 were unacceptable because of extreme surface roughness. The roughness appeared to be caused by McKenzie Type II chips (torn grain). Fiber angle was also found to influence the surface quality. Smoother, higher quality surfaces were produced when cutting with the fiber direction.

Cutting Forces Near Knots

A set of sample blocks were cut from wood near knots (within 1/2 knot diameter) to see the effects of local fiber deviations and other irregular wood properties near knots. Tests were conducted at a single chip thickness of 0.010 inch. All of these blocks were machined without chip-out because cutting was done with the grain. The specific gravity of the machined wood was determined by the difference in weight and volume. This gave an average density of the wood being machined. The cutting forces had a low correlation to the model derived from the

orthogonal cutting (R squared = 0.4). The measured forces were higher than the model with a standard error of 13 pounds. This indicates that other undetermined wood properties near knots, perhaps interlocking grain, play a significant role in its machining. This set of blocks does show that with proper alignment the wood near knots is machineable.

Cutter Interaction Study

Another factor which might effect cutting forces is the interaction between finger-joint cutting bits. It seemed possible that because the bits are located closely together, the force applied to the wood by one bit might influence the forces felt by the adjacent bits. For this reason a set of blocks was run using only a single finger-joint bit in the tool holder and the results were compared to those obtained with three bits.

The results from this study indicate that there is no measurable interaction between the bits at least to the depth of standard finger-joints and to the sensitivity of the dynamometer. Forces from the single cutter were one third of those obtained from three cutters, within 0.003 pounds. The standard error of the orthogonal cutting regression equations for a single bit is 0.12 pounds. The plots of cutting force are parallel with a constant offset. If there was any

interaction between the bits, it was below the sensitivity of the instruments used in this experiment. It is therefore considered insignificant as far as affecting industrial finger-joint cutting forces.

Model of Finger-Joint Cutting Forces in Peripheral Milling

In order to better understand the cutting taking place in an industrial finger-joint machine, the results of the orthogonal cutting tests were extrapolated to the peripheral milling configuration. The logic upon which this model is based follows. Cutting force is determined by the specific gravity of the wood, the chip thickness, the length of the sides of the bit which are cutting, and the angle of the wood fibers. The forces will be the same for orthogonal cutting or peripheral milling as long as these parameters are the same.

This model estimates the cutting forces of a single finger-joint bit as it passes through a cut by first calculating the chip thickness, length of side of the bit which is cutting, and the fiber angle. Combining these with the specific gravity information, the forces are calculated.

The model is based on the following geometry. The cutterhead is rotating in an up-milling configuration. The knife first makes contact with the wood in the vertical position with zero chip thickness. The

chip thickness increases linearly until it reaches the maximum chip thickness just prior to the knife exiting the edge of the board. The angle between the cutting force and the fibers changes constantly as the cutting edge progresses through the cut. No attempt was made to estimate chip acceleration forces. This introduces a maximum error of 5% (McKenzie, 1961).

The data from the orthogonal tests were used as the basis for determining the cutting forces at different chip thicknesses and fiber angles. This extrapolation is not totally accurate because it ignores the additional support that orthogonally sliced material receives that peripherally milled material does not due to the cutter sweeping through the cut and exiting the edge of the board. It is thought that this effect is probably negligible because of the small angle through which the cutter sweeps.

The chip thickness, length of side cutting, and fiber angle are calculated from the following parameters: feed conveyor speed, cutterhead spindle speed, number of knives, cutting circle diameter, length of the fingers, specific gravity, and angular measure of any cross grain.

First the model finds the feed per tooth, F_t, with

$$F_t = 12\ F\ /\ (K\ n)$$

where F is the feed rate (feet/minute), K is the number of knives and n is the spindle speed (revolutions/minute).

Next the model finds the maximum chip thickness, Tmax, with

$$Tmax = 2\ F_t$$

where d is the depth of cut, i.e. length of fingers (inches), and D is the diameter of the cutting circle (inches).

The sweep angle from the knife's point of contact to its exit point, SA, is found next with

$$SA = \arccos (dia - FL) / dia$$

where dia is the cutting circle diameter and FL is the length of the fingers.

From these, the instantaneous chip thickness, t, the length of side of the bit which is cutting, l, and the fiber angle relative to the direction of cutter movement, RFA, are calculated for the angle of interest, a, with

$$t = Tmax \times (a / SA)$$

$$l = FL \times (1 - (a / SA))$$

$$RFA = \text{cross grain} - a\ .$$

Finally parallel, normal, and resultant cutting forces are calculated with the equations derived from the orthogonal data.

$$Fp = (64.6SG-11+893t)l+(1188t+8)SG+(-317t-2)$$

$$Fn = (-336.8t+7.1)SG+(-1.42t+0.0084)FA+(147.4t-1.35)$$

$$Fr = SQRT(Fn^2+Fp^2)$$

where Fp is parallel cutting force (pounds), Fn is the normal cutting force (pounds), Fr is the resultant cutting force (pounds), SG is specific gravity, FA is the fiber angle, t is chip thickness, and l is length of the side of the bit cutting wood.

Finally the angle between the resultant force and the edge of the board is found with

angle of Fr = arc tan (Fn/Fp).

The output of the model is a graph of force (from a single bit) versus the angle that the cutter sweeps through as it cuts (Figure 31). Verification of the peripheral milling model was not attempted. To do this would require testing equipment capable of measuring cutting forces and determining knife position and chip thickness at cutterhead spindle speeds of 3600 RPM's. The design and construction such equipment was considered beyond the scope of this project.

Output of Peripheral Milling Finger-joint Cutting Model

The peripheral milling model was run under a variety of conditions to investigate how changes in the machine parameters would effect cutting forces.

Under typical conditions the model predicts that the cutting force will reach its maximum near the start of its cut. This indicates that

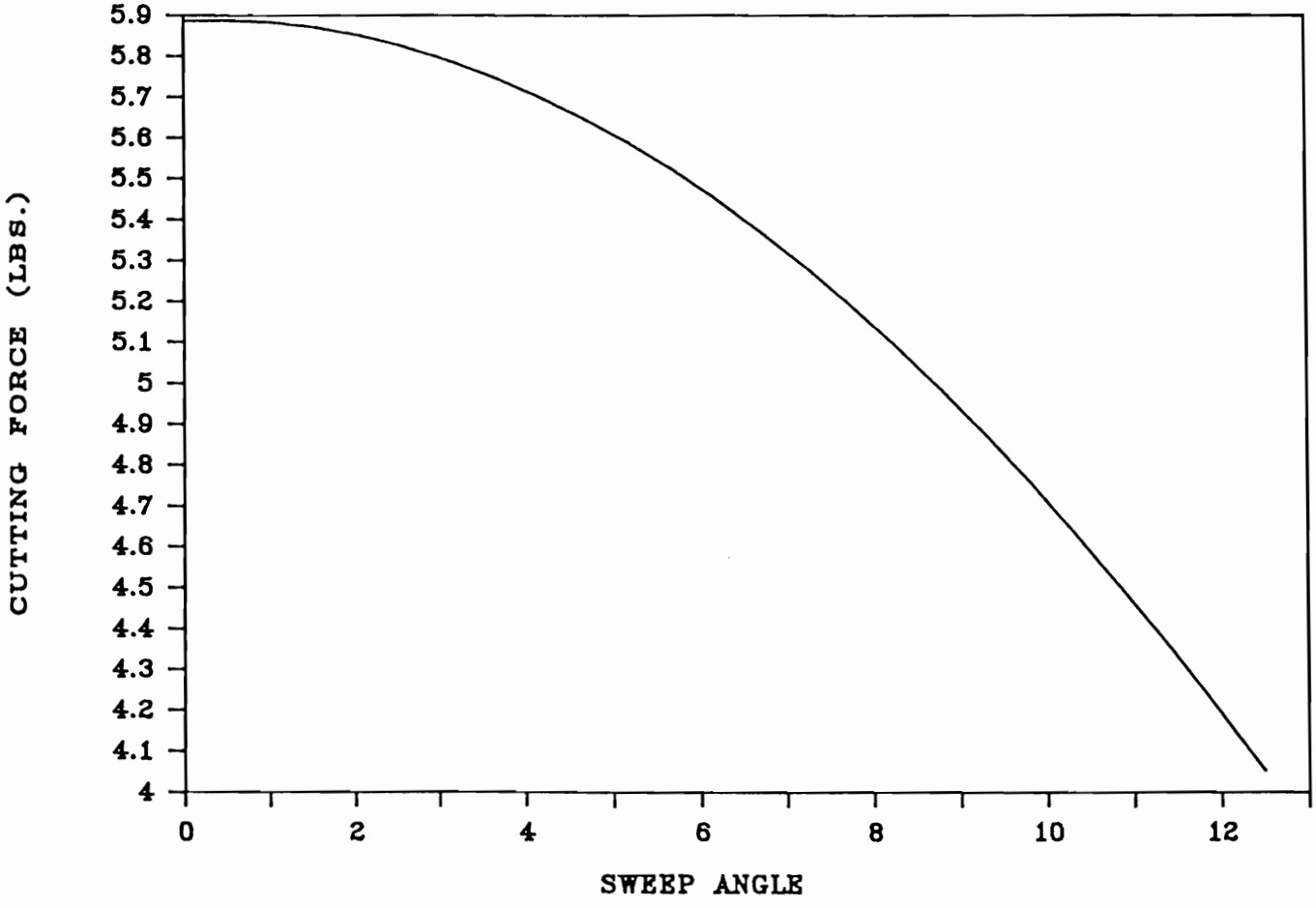

Figure 31. Typical output of the model of peripheral milling finger-joint resultant cutting force

the sides of the cutters are quite significant in determining the magnitude of the cutting force. At the zero chip thickness, cutting forces will be near zero because only the friction of the knives would be felt. Data at a zero depth of cut were not collected and therefore extrapolation error exists.

It was found that the specific gravity of the wood being cut and chip thickness have the most pronounced effect on the magnitude of the cutting forces and that increasing the specific gravity shifts the cutting force curve higher (Figure 32). The graphs are drawn for a chip thickness of 0.010 inch. The specific gravities plotted are those typically found in ponderosa pine and show the dramatic effect that density has on cutting forces.

Surface quality can be improved and chip-out can be reduced by using thinner chip thicknesses. Increasing the chip thickness shifts the peak in cutting forces as well as increasing their magnitude (Figure 33). The process variables, feed speed and cutterhead spindle speed, largely determine the chip thickness (Table 11).

Increasing the cutting circle diameter and increasing the number of knives will also decrease the chip thickness. These goals conflict in that increasing the number of knives forces the cutterhead to be larger. The net effect on cutting forces of one such compromise is to reduce the forces at most 3 pounds (Figure 34). Reducing the finger

length also reduces the chip thickness and cutting forces but the effects are minimal (Figure 35).

	FEED RATE (feet/min.)			
RPM	60	80	100	120
3000	0.007	0.010	0.012	0.015
3500	0.006	0.009	0.011	0.013
4000	0.006	0.007	0.009	0.011
4500	0.005	0.007	0.008	0.010
5000	0.004	0.006	0.007	0.009
5500	0.004	0.005	0.007	0.008
6000	0.004	0.005	0.006	0.007
6500	0.003	0.005	0.006	0.007
7000	0.003	0.004	0.005	0.006

Table 11. Chip Thickness as a Function of RPM's and Feed Rate
10 knife cutterhead
Cutting Circle Diameter = 10.5 inches

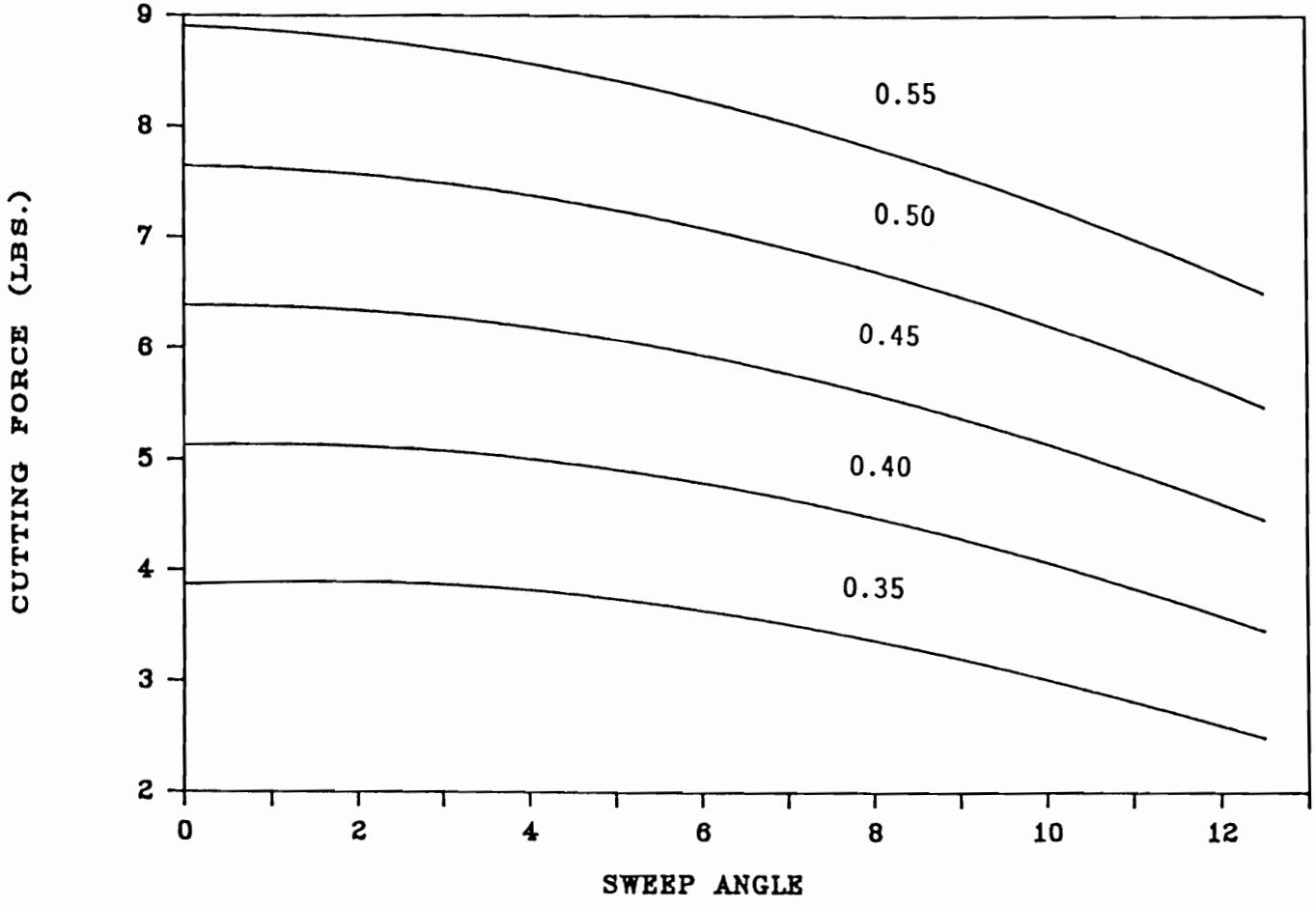

Figure 32. Peripheral milling finger-joint model output of resultant cutting force for different specific gravities, maximum chip thickness = 0.010 inch

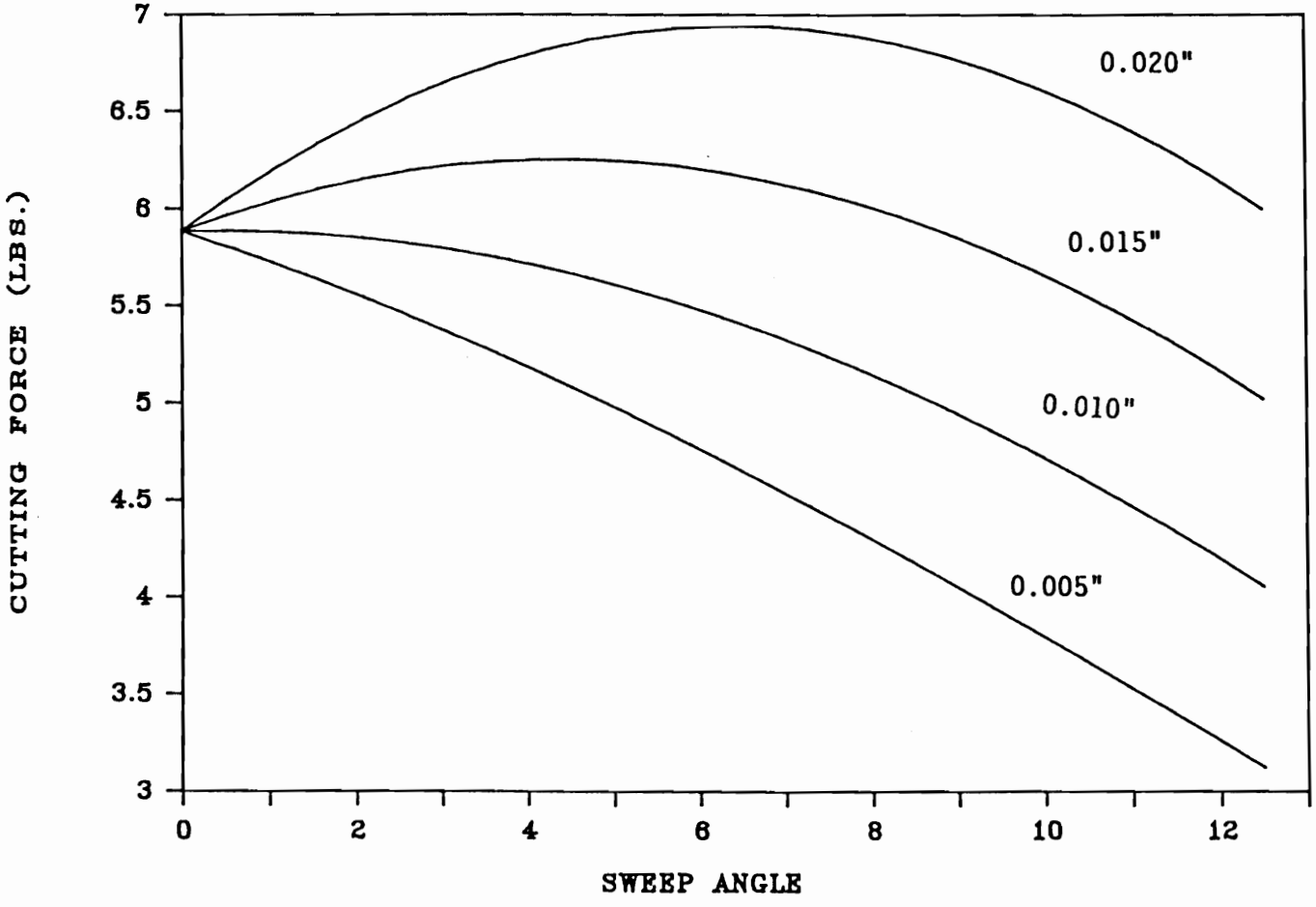

Figure 33. Peripheral milling finger-joint model output for different maximum chip thicknesses, Specific gravity = 0.43

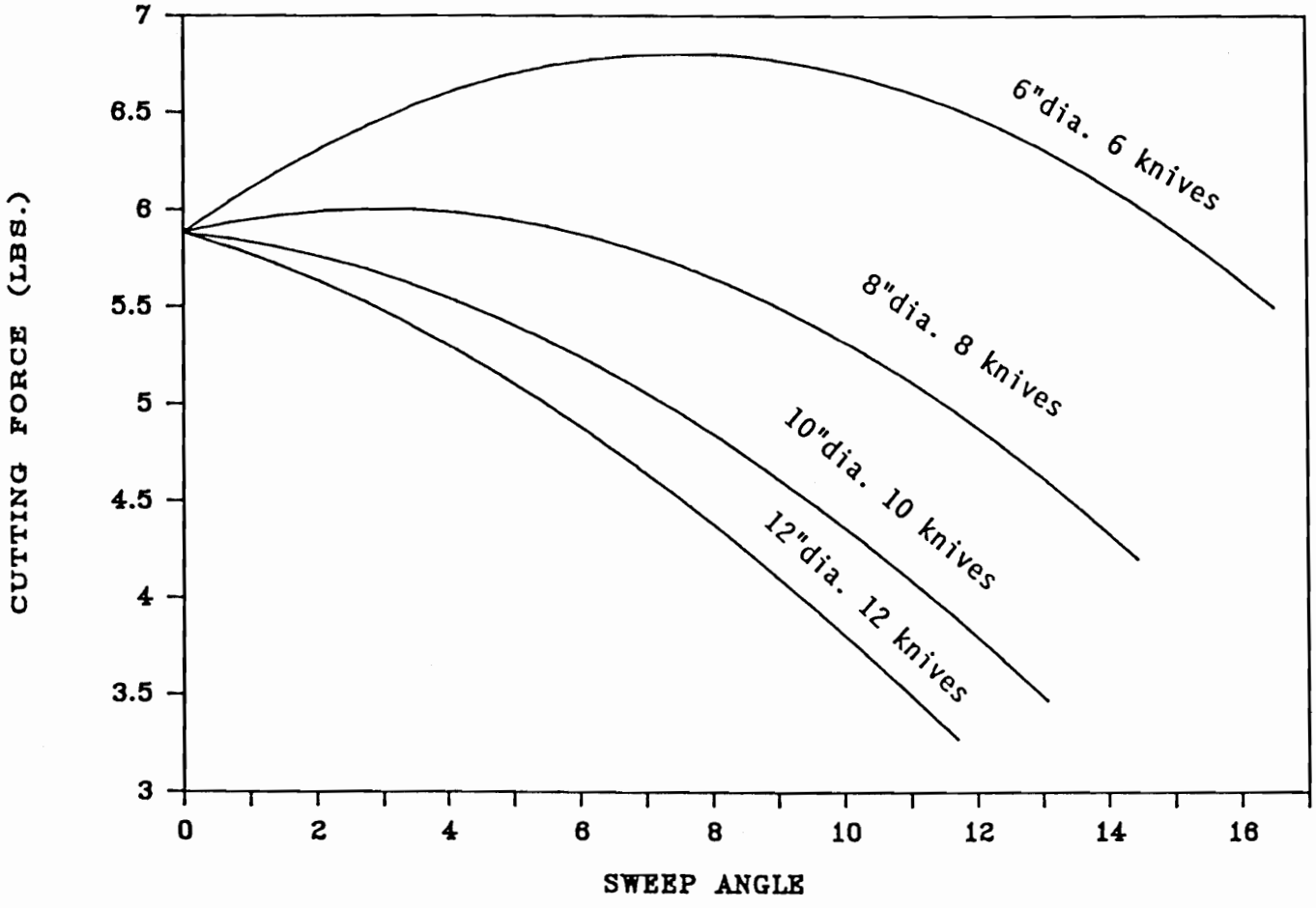

Figure 34. Peripheral milling finger-joint model resultant cutting force for cutterheads in which the number of knives is equal to the cutterhead diameter

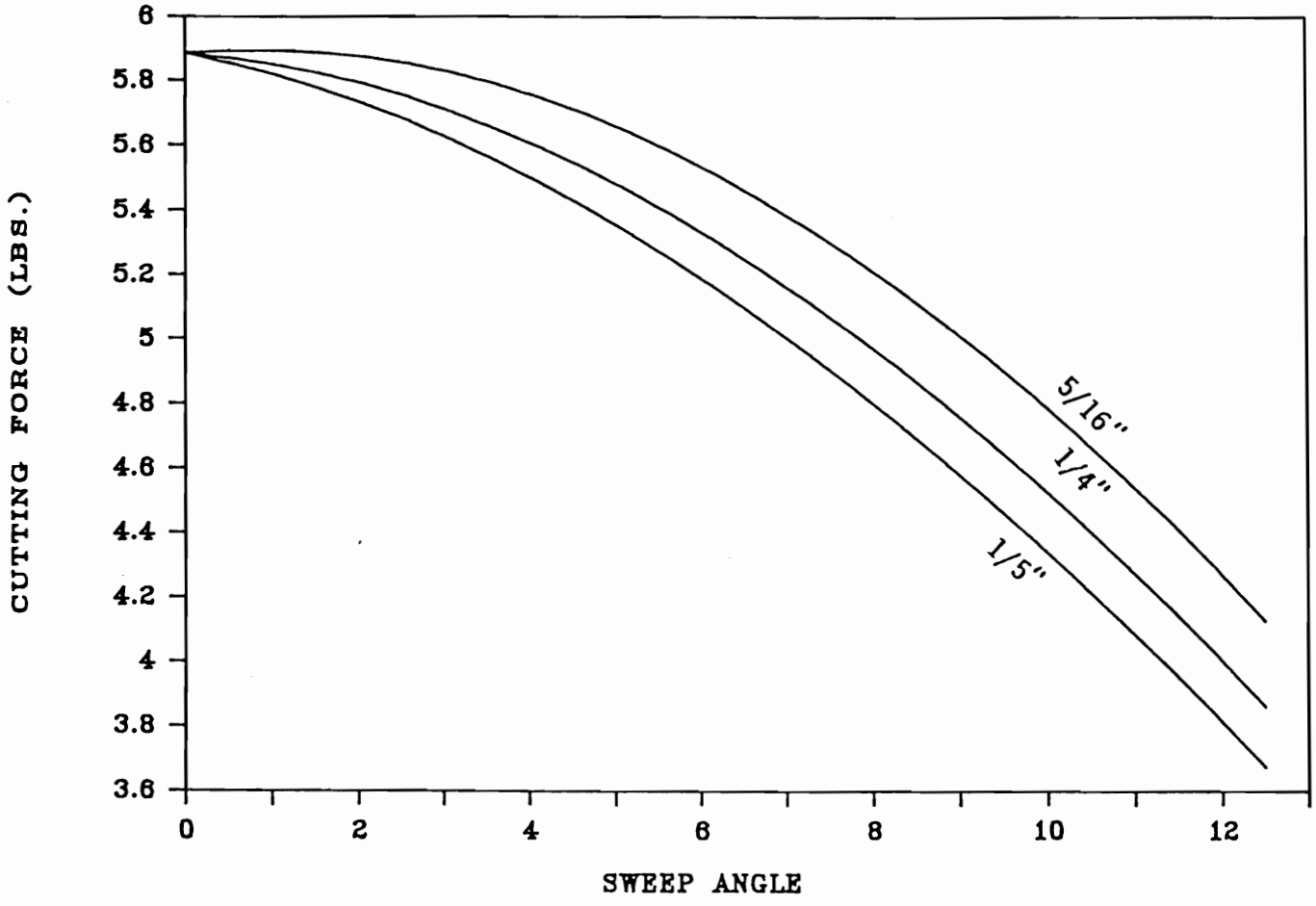

Figure 35. Peripheral milling finger-joint model, the effect of finger length on the resultant cutting force

CONCLUSIONS

1. Finger-joint cutting parameters can be modified to handle larger fiber angles. Chip-out can be practically eliminated by orienting the fibers so that the knives cut with them and not against them.

2. Cutting forces increase with specific gravity and chip thickness. Cutting forces increase slightly when cutting against the fibers.

3. Chip-out depends on chip thickness and fiber inclination. The chip-out threshold occurs at 0 to 5 degrees with the grain. Chip-out is tension perpendicular to the grain or a cleavage failure and is the result of loading geometry and increased stress rather than higher cutting forces.

4. Cutting forces are concentrated at the tip of the cutter. The sides of the cutters also make a significant contribution on the total cutting force and behavior.

5. A better quality surface results from thinner chip thicknesses and by cutting with the fiber direction.

6. No interaction of cutting forces between the bits was found.

7. Reducing feed speeds and increasing spindle speeds in a finger-joint machine appear to be the only means of significantly reducing chip thickness and the corresponding cutting forces. This should also produce a higher quality surface and less chip-out.

8. The angle between the cutting force and the fibers is significant in determining surface quality, chip formation and chip-out because a tensile load parallel to the fiber is needed for effective cutting.

Suggested Further Research

1. The past studies on measuring and modeling cutting forces have concentrated on the parallel force component. This project has pointed out the importance of considering the nature of the load on the fiber, i.e. tension, compression or bending. An appropriate study would use a simple straight knife and measure the normal force as well as the parallel force. The resultant force and its angle to the fibers could then be calculated and the chip type, mechanism of failure, and cutting forces could then be related to the loading configuration.

2. Rake angle is an important factor on both the cutting forces and chip formation. Another study would investigate the effects of a number of rake angles for finger-joint bits on cutting forces and chip formation.

3. The design of finger-joint bits might be changed so that the sides are cutting with a non-zero rake angle. The effects of such a design on cutting forces and chip formation would make another research project.

4. The effects of fiber angle on chip-out should be verified with a study conducted in a finger-joint plant. Sample blocks with clear straight grain as well as those containing fiber deviations around knots could be tested. The hypothesis of orienting the boards to prevent chip-out could be tested.

STUDY II - STUDY OF WOOD PROPERTIES ADJACENT TO KNOTS

Study I, machining of finger-joints, points out the importance of fiber angle and specific gravity on the cutting forces, chip formation and occurrence of chip-out. Knots are the most common defect which must be removed from cut-stock and are known to distort the wood adjacent to them. This study is an investigation of the fiber and specific gravity distortion adjacent to knots. The results of the machining study are combined with these results in an attempt to better define the defect boundary around knots. This could prove quite useful to industry by removing the uncertainty in locating cuts and thereby maximizing the recovery of raw material.

The current literature contains information on various techniques used to detect fiber orientation, both those commonly in practice and new scanning techniques just being perfected. A model of the fiber angle around knots was also located.

This study began by examining the current industry practice of using growth ring patterns to indicate cross grain. It then investigated the feasibility of applying a model of fiber angle around a knot to ponderosa pine. Finally the density of the wood surrounding intergrown knots was measured using an x-ray densitometer.

LITERATURE REVIEW

Definition

Cross grain is defined (Koehler, 1943; Wood Handbook, 1974) as wood fibers which are not parallel to the edge of a board. In the radial plane it is usually referred to as diagonal grain, and in the tangential plane it is called spiral grain.

In the radial plane the fibers are parallel to the growth rings. The easiest way to detect diagonal grain is to see if the growth rings are parallel to the major axis of the board. Diagonal grain is caused by sawing logs with crook, bulges, taper, pitch and bark pockets, curly grain, knots and healing-over injuries (Figure 36).

Spiral grain is much more difficult to detect. It occurs naturally in some trees. The fibers, rather than growing parallel to the stem, spiral around the tree. It can also be sawn into a piece of lumber by obliquely cutting a board from a straight-grained log. There are a number of different possible combinations of spiral and diagonal grain (Figure 37). Local fiber deviations, both spiral and diagonal grain, occur around knots (Figure 38).

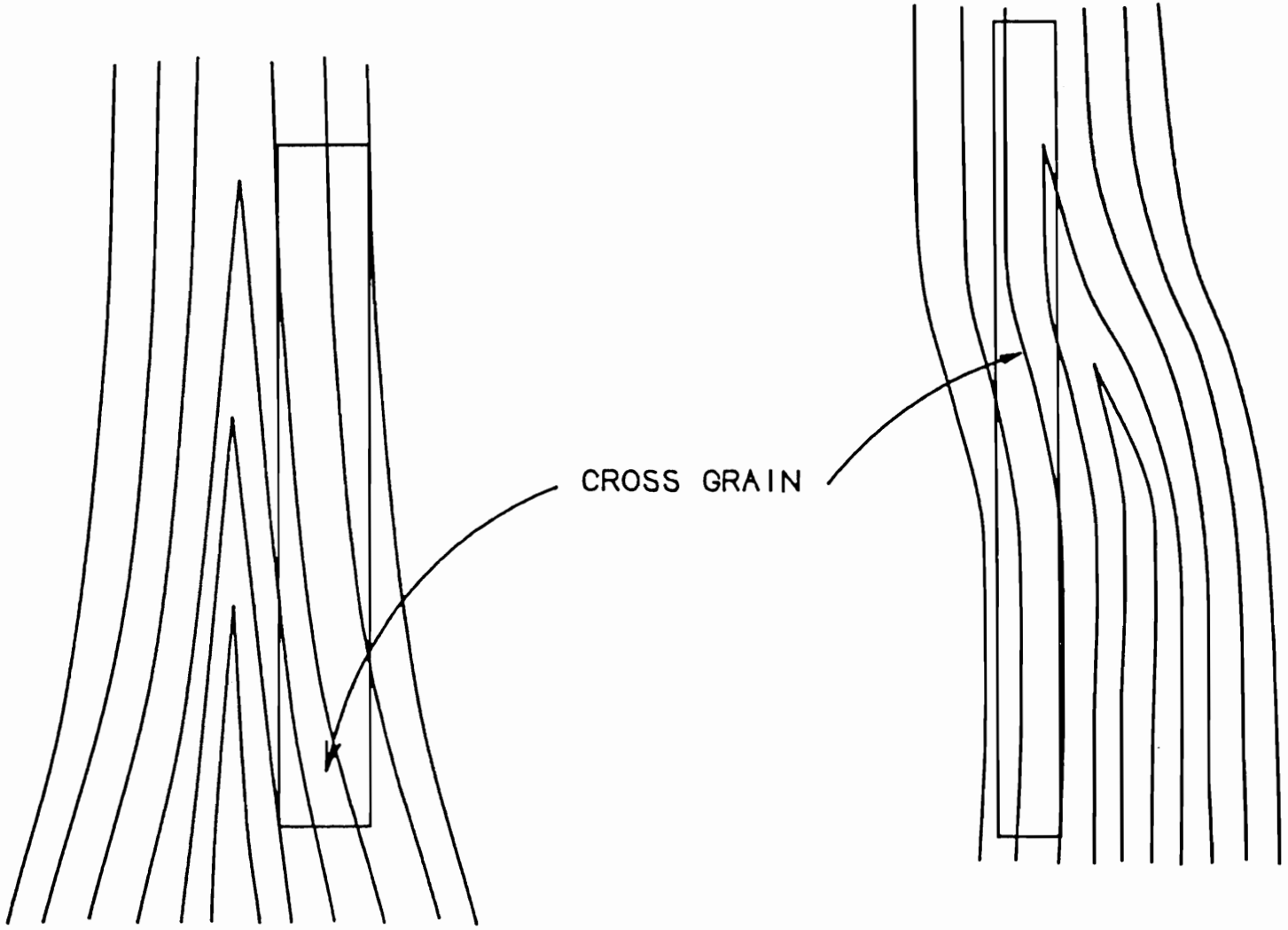

Figure 36. Cross grain caused by taper and crook in logs

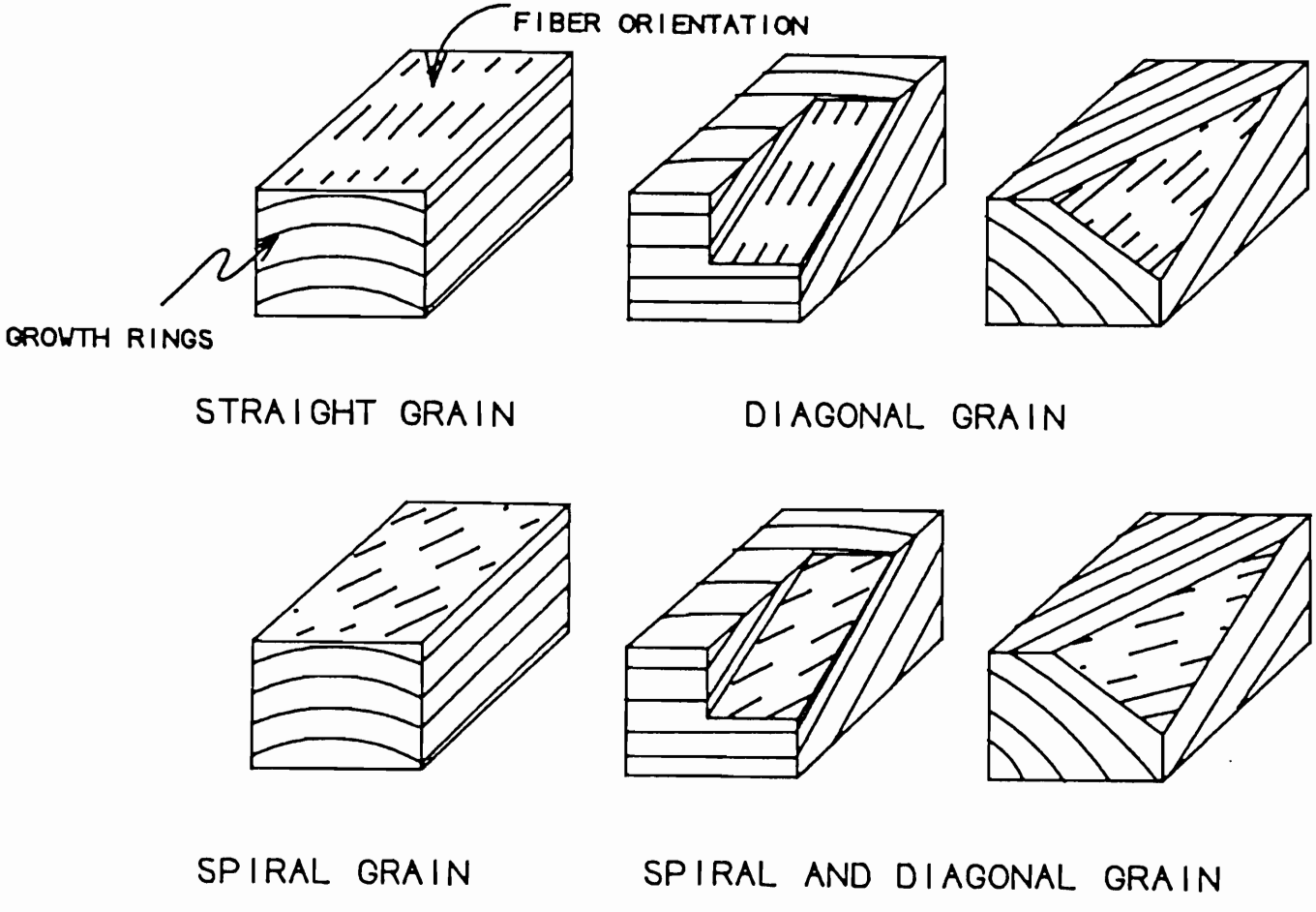

Figure 37. Blocks with straight, diagonal and spiral grain

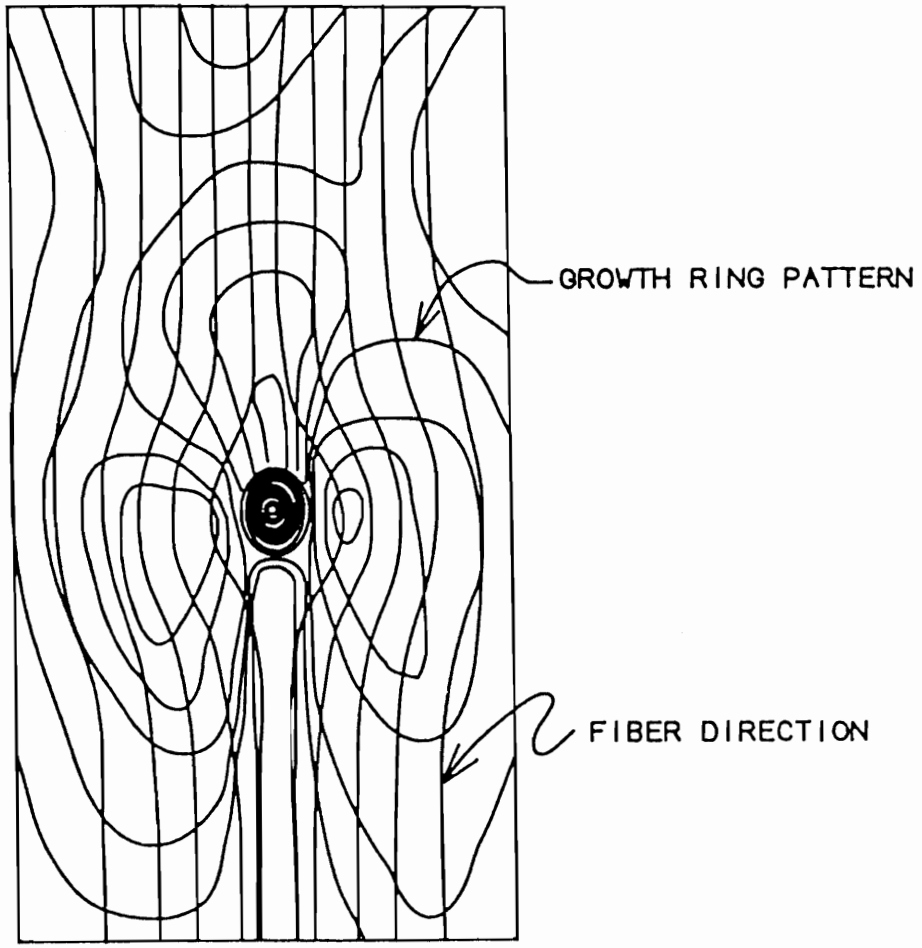

Figure 38. Typical growth ring patterns and fiber orientation around knot

Detection of Cross Grain

Lumber graders usually use a scribe, seasoning checks, and torn grain to detect spiral grain. Other tests used include the ink test, the pick test, and the splitting test. Inspecting fibers and resin ducts with a hand lens or microscope is another technique. All of these tests are either slow and/or destructive to the wood (Koehler, 1943; Anderson, 1955).

On the manufacturing floor at the present time, chop saw operators use growth ring patterns as indicators of localized areas of cross grain. Growth rings tend to make swirls in the areas containing cross grain; however, growth rings and fiber angle are different wood features. No literature was found on the relationship between cross grain and growth ring patterns.

Scanning for Fiber Orientation

Several scanning techniques are being developed which can detect cross grain. McLauchlan, Norton and Kusec (1972) have developed a technique which uses the dielectric properties of wood. The dielectric constant of wood is 50% greater when the magnetic field is parallel to the fiber direction.

Metriguard, of Pullman, Washington, is producing a commercial scanner which operates on this principal (McLauchlan and Kusec, 1978). Their non-contacting rotary transducer can measure fiber angle to within 1 degree, has a response time of 15 milliseconds, and can scan at 200 feet per minute. It is independent of species, density, moisture content, and surface roughness. It is, however, limited to scanning the surface.

McDonald (1986) successfully used one of these scanners to accurately map the local fiber angles around knots. The steep diving grain of the knot itself produced somewhat unusual results. This study is important because it proves this instrument's ability to measure local fiber angles.

Another scanning technique (Soest, 1984) uses the tracheid effect which causes light to scatter preferentially in the fiber direction unless it is disturbed by defects. Mathews and Beech (1976) have an apparatus for detecting defects which uses this principle.

Mathews (1987) and Soest (1987) have also developed a technique which uses the grain direction effect. Light has a higher reflected intensity when viewed across the fiber direction than along it. The higher intensity is attributed to specular reflectance bouncing directly from the sides of the cells. When viewing wood along the fibers, only diffusely reflected light is seen. Diving fibers can also

be detected by the shifting of the specular intensity peak to an angle equal to the inclination of the fibers.

Optical imaging techniques could also be developed to determine fiber orientation. Visual indicators include seasoning checks, rays, pores, resin ducts, long narrow pitch streaks, and growth ring patterns.

Model of Fiber Angle

Phillips, et al. (1980; 1981) developed a model of fiber angle around knots for a finite element analysis of the structural properties of wood. They found that the fiber orientation around a knot can be modeled as an elliptical object embedded in a two dimensional laminar fluid flow. The model inputs are the angle of spiral grain and the length of the major and minor axes of the knot. The model predicts the fiber orientation in the cells of the grid surrounding the knot. The grid consists of irregularly sized and shaped cells which are appropriate for finite element structural analysis.

This model makes the assumption that the fibers are symmetrical about two axes, above and below and to the sides of the knot. The assumption of symmetry about the horizontal axis is known to be slightly inaccurate. The model was found to have an error of 4 to 8 degrees around any individual knot. After applying an empirical

correction factor Phillips (1981) was able to predict grain angle to within 3 to 4 degrees. This correction factor was developed by mapping a number of knots.

Douglas-fir (Pseudotsuga menziesii) and lodgepole pine (Pinus contorta), the species used in this study, were found to have different fiber configurations representing two statistical populations.

Phillips used the stream function from fluid dynamics to model the fiber angle. From fluid dynamics (Plapp, 1968) the stream function of an elliptical cylinder embedded in a two dimensional fluid flow is

$$\Psi = V(a+b) \sinh(\epsilon - \epsilon_o) \sin(\eta - \alpha)$$

where Ψ is the stream function, analogous to fiber direction. In this case V, flow rate, equals 1 and α, the angle of attack (spiral grain), is zero. η and ϵ are elliptical coordinates. ϵ_o has a constant valve found by

$$\epsilon_o = 1/2 \ln\left(\frac{a+b}{a-b}\right).$$

The terms a and b are the semi-major and semi-minor axes of the embedded object.

The following equations can be used to transform the data to rectangular coordinates

$$X = c \cosh \epsilon \cos \eta$$

$$Y = c \sinh \epsilon \sin \eta$$

$$c = \sqrt{a^2 + b^2}.$$

Structure and Strength

Early in this study an examination of several finger-joint blocks with a hand lens revealed that chip-out in plain sawn lumber usually exposes a radial face. The reasons for this are that cross grain is more difficult to detect in plain sawn lumber and wood splits more easily in the radial direction exposing the radial face. Dinwoodie (1981) states that the strength of wood is about 20 % less in the radial plane than the tangential plane.

METHODS AND MATERIALS

Material

The ponderosa pine samples for this study were obtained from a moulding plant in Central Oregon. Both encased and intergrown knots in sizes ranging from 1/4 to 4 inches in diameter were examined. The associated fibers and growth ring patterns were exposed by sawing the blocks radially, tangentially and obliquely.

The samples were at 8 to 12 % moisture content, typical of the raw material in a manufacturing plant. Moisture content has no effect on fiber orientation or growth ring patterns and is easily accounted for when calculating specific gravity.

Growth Ring Patterns and Fiber Angles

Currently, industry uses growth ring patterns to locate cross grain for the purpose of removing it from the cut stock. This study began by looking at growth ring patterns around knots where local fiber deviations are known to exist. Several hours were spent in a plant with a chop saw operator learning to recognize the growth ring patterns used as indicators of cross grain.

Finally a laboratory examination of these patterns and the associated cross grain was made. The blocks for this study contained knots and several inches of wood containing growth ring patterns. They were sawn as closely as possible to the tangential and radial planes. They were then cut further into small blocks revealing tangential and radial surfaces around the knots. A hand lens and scribe were used to determine fiber angle. Some blocks were then sawn obliquely to see the influence that this had on the growth ring pattern.

Map and Model of Fiber Angle

The flow/grain model developed by Phillips et al. (1981) was used to model the fiber angle around a number of ponderosa pine knots. The predicted values were then compared with the actual fiber angle values.

A lumber scribe and hand lens were used to determine fiber orientation. A mylar grid was placed over the samples and a protractor was used to measure the dominant fiber angle in each grid cell. The grid pattern used was the same as that used by Phillips (Figure 42). The data were normalized for knot diameter by using a different-sized grid for different knot diameters.

A computer program was written to evaluate the stream function for each cell of the grid using 1.0 and 1.1 as the semi-minor and semi-major axes of the ellipse. These were estimated to be typical of

knots. The values of the stream function were plotted in cylindrical coordinates and equal values were connected to generate the stream lines. The dominant stream line angle for each cell was measured and mapped.

Local Specific Gravity Study

After machining a number of blocks in Study I of this thesis project, it became apparent that the specific gravity of the wood being machined is one of the most significant factors influencing the cutting forces. For this reason, an investigation was made of the specific gravity of the wood near knots. Samples of ponderosa pine containing intergrown knots were scanned with an x-ray densitometer and profiles of the density in the vicinity of knots were generated.

The x-ray densitometer used in this study has a Kevex x-ray tube with a tungsten target producing a polychromatic energy spectrum as a source. For a sensor it uses a Victoreen 500 cesium iodide, photo diode scintillation detector with a Victoreen 500 electrometer used as a picometer. The aperture, mounted on the sensor, is the primary collimating element of the system. Its dimensions are 0.1 by 1.0 by 2.0 millimeters, providing a 0.1 by 1.0 sample view. A translation table using a stepper motor positions the sample. The resolution of this instrument is 100 microns in the radial direction when scanning at two steps per second and 0.053 millimeter per step. The accuracy is

within 0.01 gram per cubic centimeter for a 1.5 millimeter thick specimen.

The densitometer was used to make measurements every 0.1 millimeter. The samples measured 4 millimeters thick by 25 millimeters wide. The samples were about 90 millimeters long, measured from the center of the knots to the end. All samples were sawn to expose the tangential surface. The output of the densitometer is an ASCII file which was plotted and statistically analyzed using the Lotus 123 spreadsheet software.

The data from the individual samples were normalized for knot diameter by converting the position of the specific gravity measurements from millimeters to position in terms of knot diameters. The specific gravity measurements were then plotted against position in terms of knot diameters and manually smoothed. An average curve was generated for each knot by averaging the specific gravity values of the smoothed curves for that knot. A curve was then fit by hand to these average curves.

RESULTS AND DISCUSSION

Growth Ring Study

Growth rings are bands of springwood and summerwood in a tree. These concentric layers of fibers make distinct patterns in lumber. The pattern on the lumber is the result of intersecting a plane with a curved surface; typically cylindrical, conical or convex (Figure 39). Looking at the radial surface, swelling can be seen because the growth rings, which are put down in layers, follow the shape of the protrusion. On the tangential surface the swelling pattern looks like a hill on a topographic map.

This study indicates that growth ring patterns indicate bumps and dents but do not indicate the presence of cross-grain. The area around knots is characterized by both a steep short swelling and local fiber deviations around the limb. The growth ring pattern is a result of the knot swelling and coincidentally occurs in the same area as the local fiber deviation around knots. By cutting out these swirls, the chop saw operators usually remove all of the cross grain but they also waste usable material.

This study then conducted a qualitative inspection of a number of knots of several softwood species: ponderosa pine, sugar pine (Pinus lambertiana), Douglas-fir, hemlock (Tsuga spp.) and incense cedar (Libocedrus decurrens). Observations indicate that the growth ring

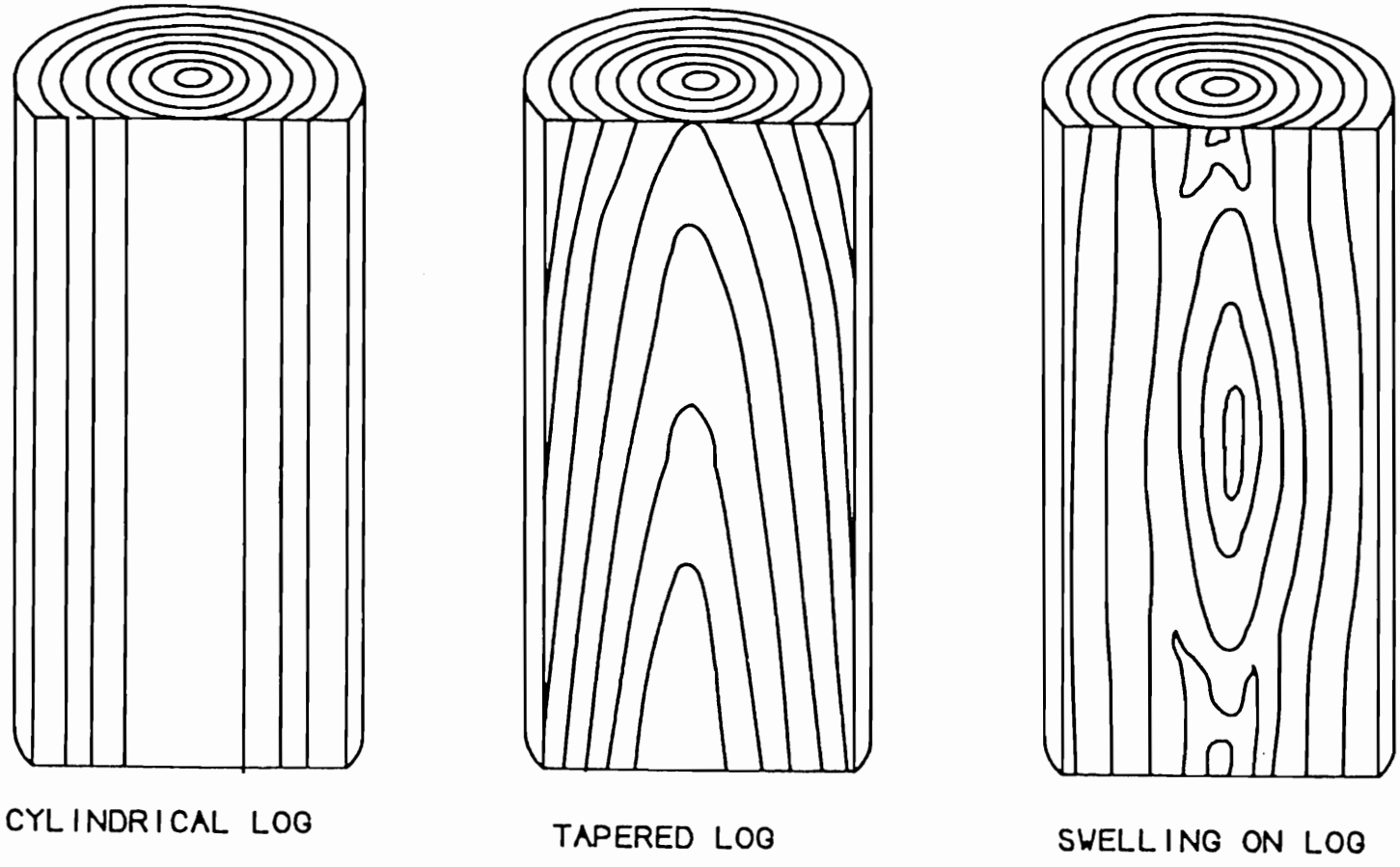

Figure 39. Growth ring patterns in logs caused by intersecting a plane with various convex surfaces

patterns around knots fall into two general categories, concentric swelling and symmetrical swelling to the sides of the knot (Figure 40).

The concentric pattern is fairly simple, like a hill with the knot at the center. This pattern is the most common. The second pattern, which was noted only in ponderosa pine, resembles two hills with the knot in the depression between them.

Boards are seldom perfectly tangentially or radially sawn, and as a result the growth ring patterns on most lumber are those described above except that they are skewed to one side. This asymmetrical pattern looks as if the swelling was entirely to one side of the knot (Figure 41).

Map and Model of Fiber Angle

The fiber angle for each cell of the grid was tabulated for each of the 36 knots measured. The mean and standard deviation for each cell was then calculated, and a high degree of variability between knots was found. These maps of individual knots show that values of individual cells vary up to 14 degrees. The flow/grain model was used to predict the average fiber angle, and this was compared to the average measured angle (Table 12). Typical differences between the predicted fiber angles and the average measured fiber angles are 5 degrees with a maximum error of 15 degrees. The accuracy of the model improves in cells farther from the knot edge.

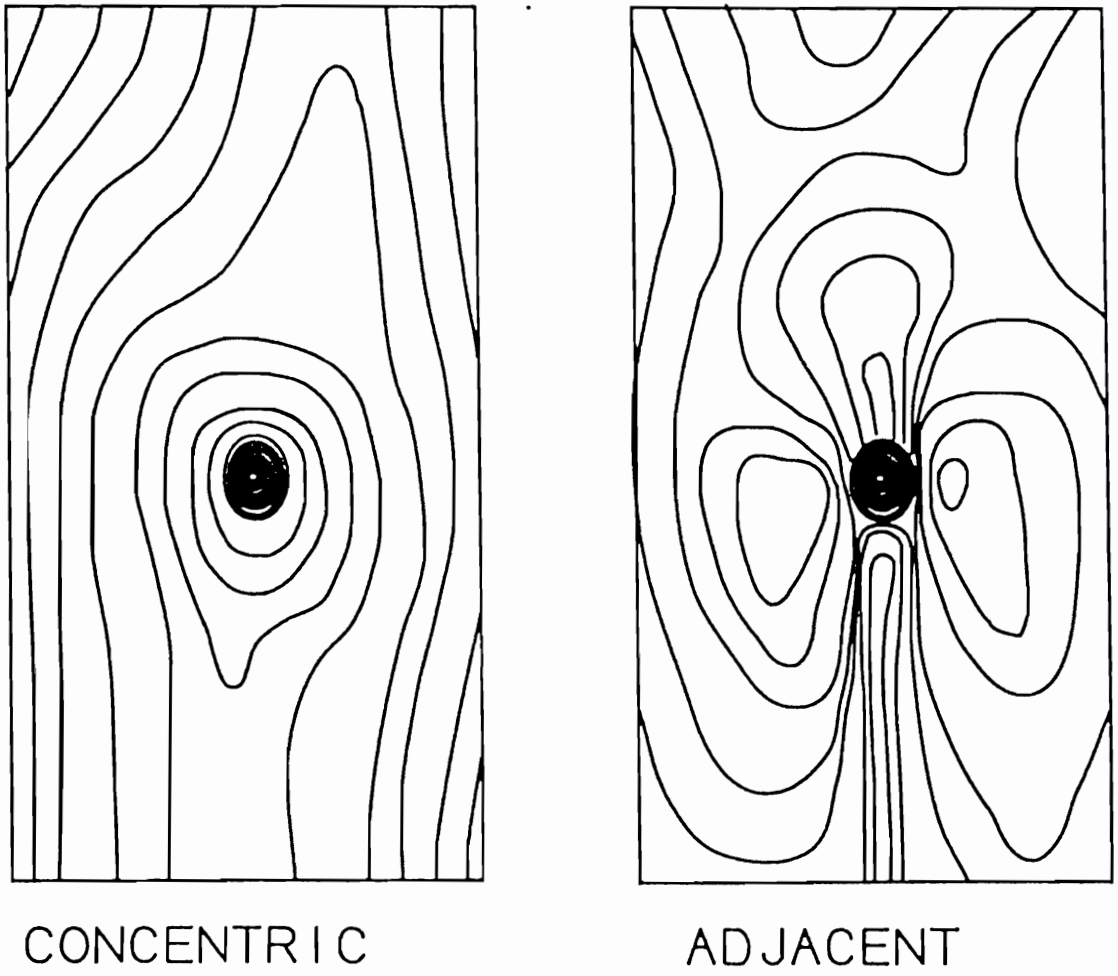

Figure 40. Two types of knot swelling and the associated growth ring patterns

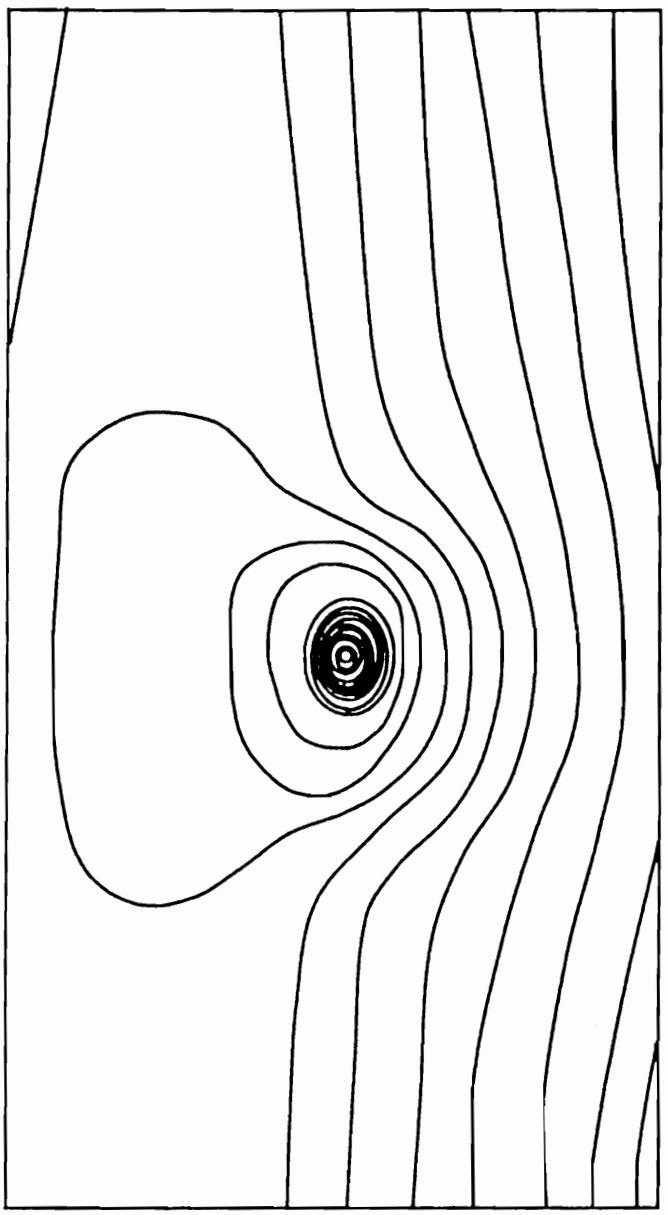

Figure 41. Concentric knot swelling sawn at an angle

Cell	Number of Samples	Mean	Standard Deviation	Flow/grain Model	Flow/grain with correction
A1	22	4.45	3.90	7 *	7 *
A2	13	4.69	2.73	6	6
A3	15	4.33	3.48	5	5
A4	5	3.40	2.15	3	3
B1	14	13.29	4.95	16	16
B2	18	10.17	4.55	9	9
B3	11	9.55	5.18	9	9
B4	4	6.75	5.12	4	4
C1	17	19.35	5.49	30 *	30 *
C2	26	14.73	5.17	13	13
C3	15	12.80	4.18	10	10
C4	2	6.50	2.50	7	7
D1	16	23.94	5.71	35 *	35 *
D2	25	17.36	5.97	20	20
D3	16	13.19	6.76	11	11
D4	7	11.86	5.89	8	8
E0	13	23.92	6.92	35 *	35 *
E1	24	25.00	8.31	40 *	40 *
E2	27	19.26	5.56	21	21
E3	20	15.25	3.99	12 *	14
E4	5	12.20	4.31	10	12
F1	28	22.86	6.42	15 *	21
F2	21	16.90	5.81	18	20
F3	12	13.92	6.05	11	13
F4	6	12.83	6.62	9	11
G1	33	15.79	6.78	7 *	13
G2	25	15.60	6.05	12 *	14
G3	18	12.33	5.50	10	12
G4	6	16.33	5.09	8 *	10
H1	23	13.78	6.57	6 *	12
H2	8	11.50	5.05	9	11
H3	9	9.56	5.27	8	10
I1	17	10.20	5.29	4 *	10
I2	10	10.30	5.00	6	8
I3	4	9.00	6.36	7	9

Table 12. The results of mapping the fiber angle around 36 Ponderosa pine knots and predicting the fiber angle with the flow/grain model. * Reject model at 0.01 significance level.

Cell location is shown in Figure 42.

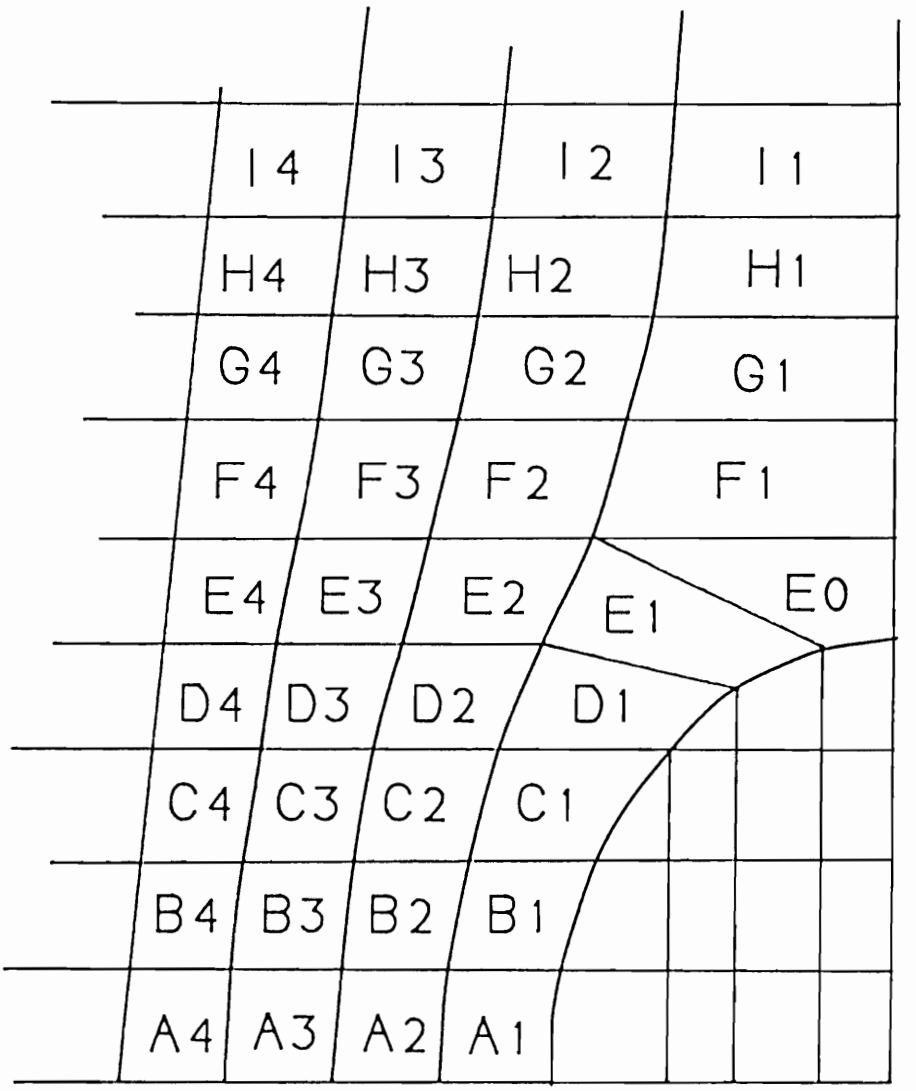

Figure 42. Fiber angle map grid and cell numbers

At the 99% confidence limits, the hypothesis that the flow grain model can be used to predict the average fiber angle must be rejected for a number of cells. In the cells immediately adjacent to the knot, the fiber angle was extremely difficult to measure, impossible in some cases. For that reason it is not surprising that the model fails for these cells. For the other cells it can be seen that the model is consistently low and could be improved with an empirical correction factor. Adding 2 degrees to the model for all cells greater that E2, except cells along the vertical axis (F1, G1, H1 and I1) to which 6 degrees are added, makes the model statistically acceptable at the 99% confidence limits for all the cells except those immediately adjacent to the knot.

This investigation indicates that the flow/grain model which incorporates a correction factor could be used as a predictor of fiber angle in ponderosa pine. A larger sample of knots should be mapped using a more accurate method of determining fiber angle. This would better define the variability between knots and the best correction factor to be used.

Local Specific Gravity Study

The specific gravity of an intergrown knot in ponderosa pine was measured to be about 1.0, roughly twice the density of the wood in an area of the board away from any defects, 0.45. The density of the band

of wood surrounding a knot decreases from the density of the knot to the density of the regular wood in an exponential fashion. The change in density seems to be linked more to the diameter of the knot than simply to the distance from the knot edge. At one half of a knot diameter from the edge of the knot, the density is 45% above the density of the board, and at one full diameter from the edge of the knot, it is 17% above its normal value (Figure 43). A curve was fit to these data in an attempt to model the specific gravity change between 0 and 2 knot diameters away from the edge of the knot (Figure 44). The equation for this curve is

$$\text{Specific Gravity} = 0.98 - (\arctan(0.1 + 2.6\,X) / 2.45)$$

where X is the distance from the edge of the knot in terms of knot diameters.

Statistic	Value
Correlation R^2	0.98
Standard error	0.043
Confidence limits	99%

Table 13. Statistics for the curve which predicts the specific gravity adjacent to knots

Statistically the results of this study are quite good (Table 13); however, a larger sample size of knots spanning a greater range of diameters is required for a better estimate of the variability of

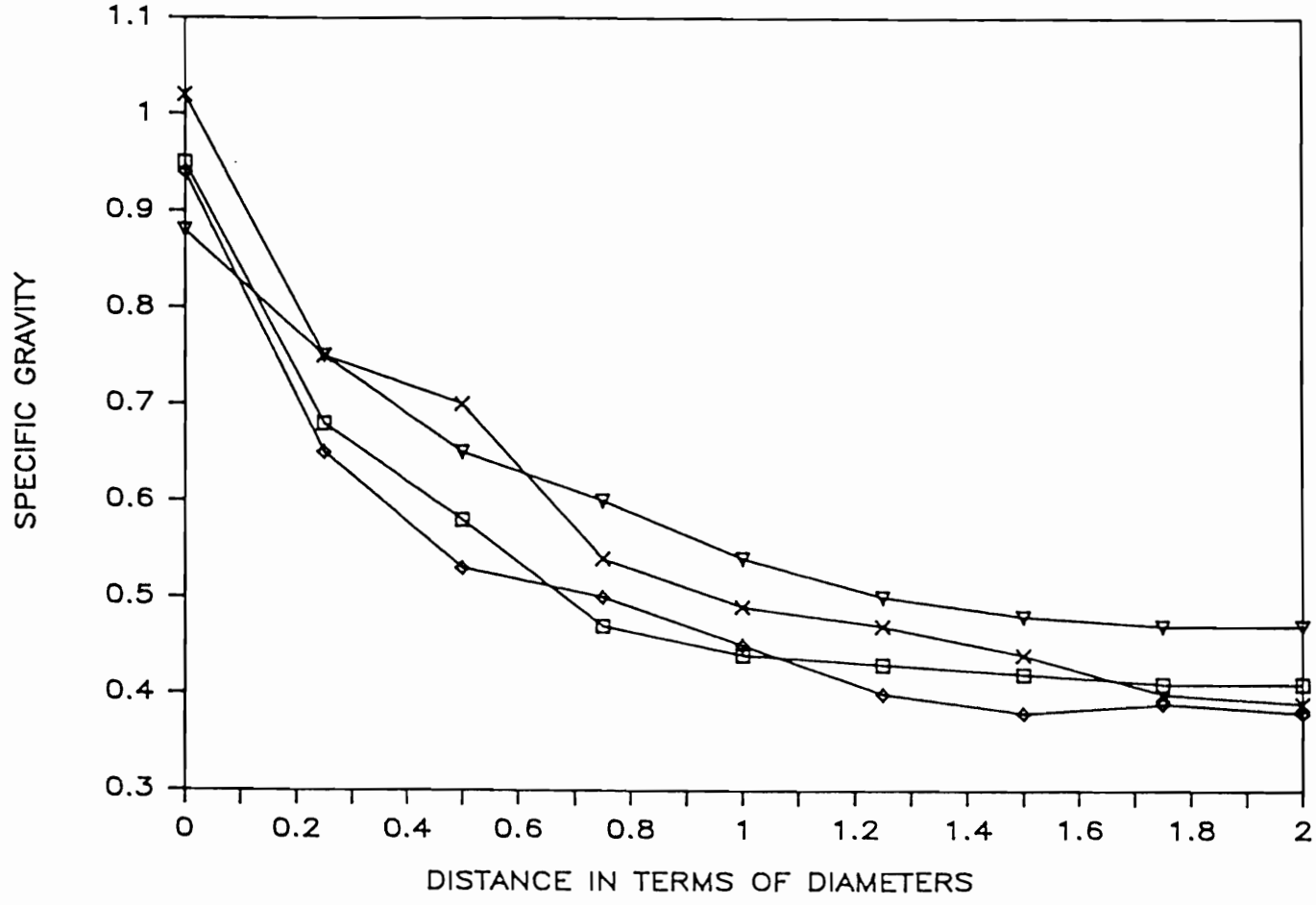

Figure 43. Local specific gravity of wood around knots versus distance from edge of knot for four knots, curves have been smoothed and averaged

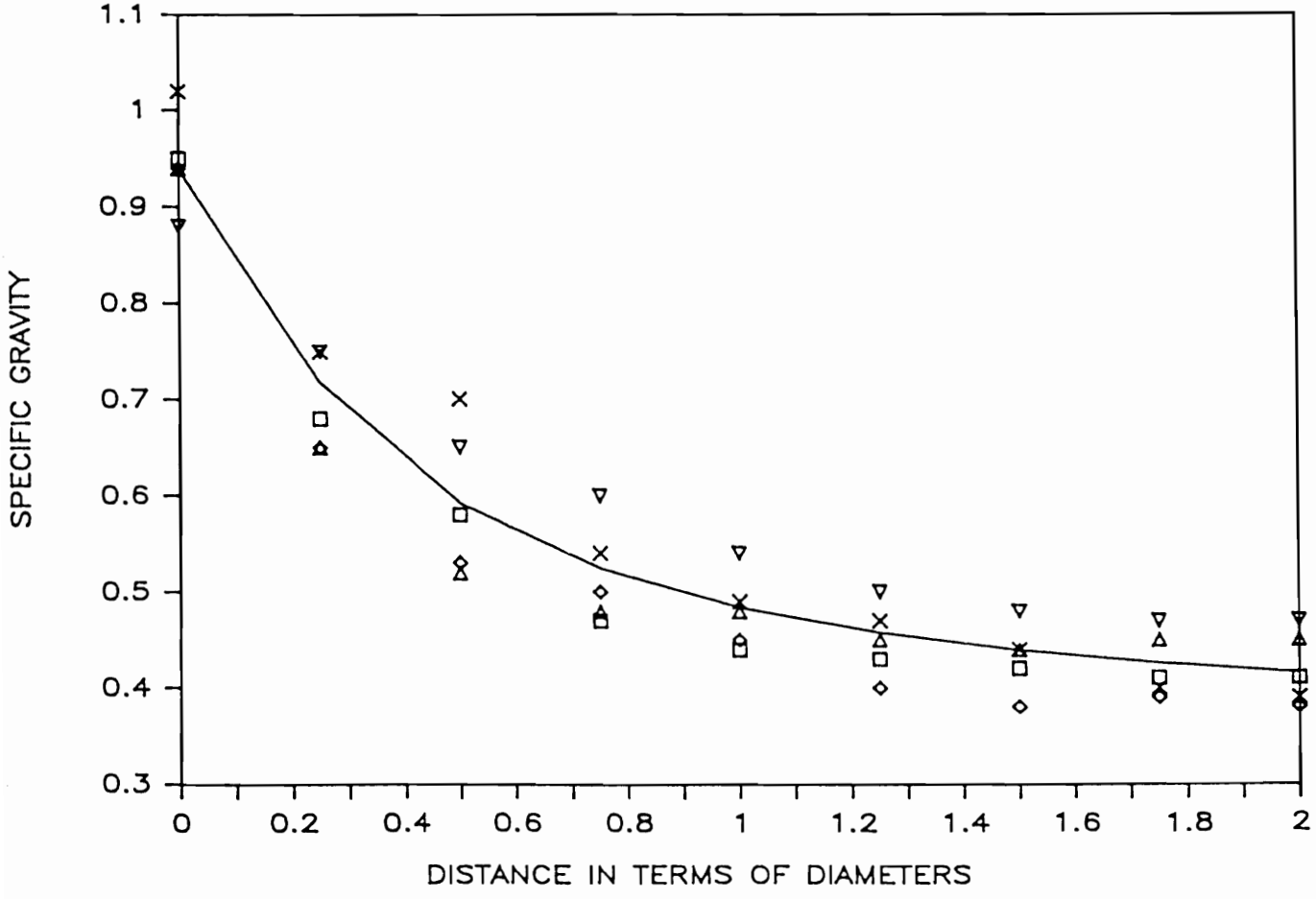

Figure 44. Local specific gravity of wood around knots versus the distance from edge of the knot, data and curve derived from data

knots. The results are, however, thought to be representative of typical knots.

Knot Defect Boundary Definition

The boundaries of knots and the defects associated with knots are often difficult to locate. This presents problems to manufacturers who wish to remove these defects. In industry over-trimming means throwing away usable wood while under-trimming results in defective products.

Clearly locating the boundary of the knot becomes important, because the size of the defects surrounding a knot tend to be proportional to the knot's size. A knot is defined by the Wood Handbook (1974) as what was at one time a limb which has been grown over by the trunk of the tree. Encased or black knots have a boundary indicated by the branch's bark. The branch which caused an encased knot has died and is being grown over by the trunk of the tree. The boundary or edge of an intergrown knot, where the limb is still alive and growing, is not always easily recognizable because of the transition from the knot to the normal wood in the tree. Often these knots have pitch or heartwood in their centers, which can be mistaken for the edge of the knot. In this study, I have defined the edge of an intergrown knot as the location where the bands of springwood become approximately equal in width to the bands of summerwood.

The defects which often surround knots that manufacturers remove for cosmetic reasons are bark pockets, pitch streak and stain. The other defects surrounding knots, local specific gravity and fiber distortions, help define the boundary between the machineable and non-machineable wood (Figure 45). This boundary is perhaps the most difficult to determine and obviously the most important.

First of all, the location of this boundary depends on the machining process. In processes where the entire knot and cross grain around it are left in the board, all of the wood can usually be machined without any problems, as this is common practice in industry. The surrounding wood gives the knot and distorted wood around the knot enough support that it can be machined. Problems usually arise when the knot has been removed from the adjacent wood and the weak cross grain wood is left unsupported on the edge or end of a board.

In processes such as finger-jointing, the knot itself is removed but as much of the wood around the knot as is possible is left in order to maximize recovery. Combining the results of the specific gravity study, the flow/grain model, and the machining study provides the basis for locating the boundary of machineable wood. The wood outside of one knot diameter from the edge of a knot should be considered machineable for almost all processes. It may be considered defective for other reasons, such as stain or pitch, but it should be machineable. The wood from one half to one knot diameter from the edge of a knot should be machineable in most processes. There is some cross grain (knot

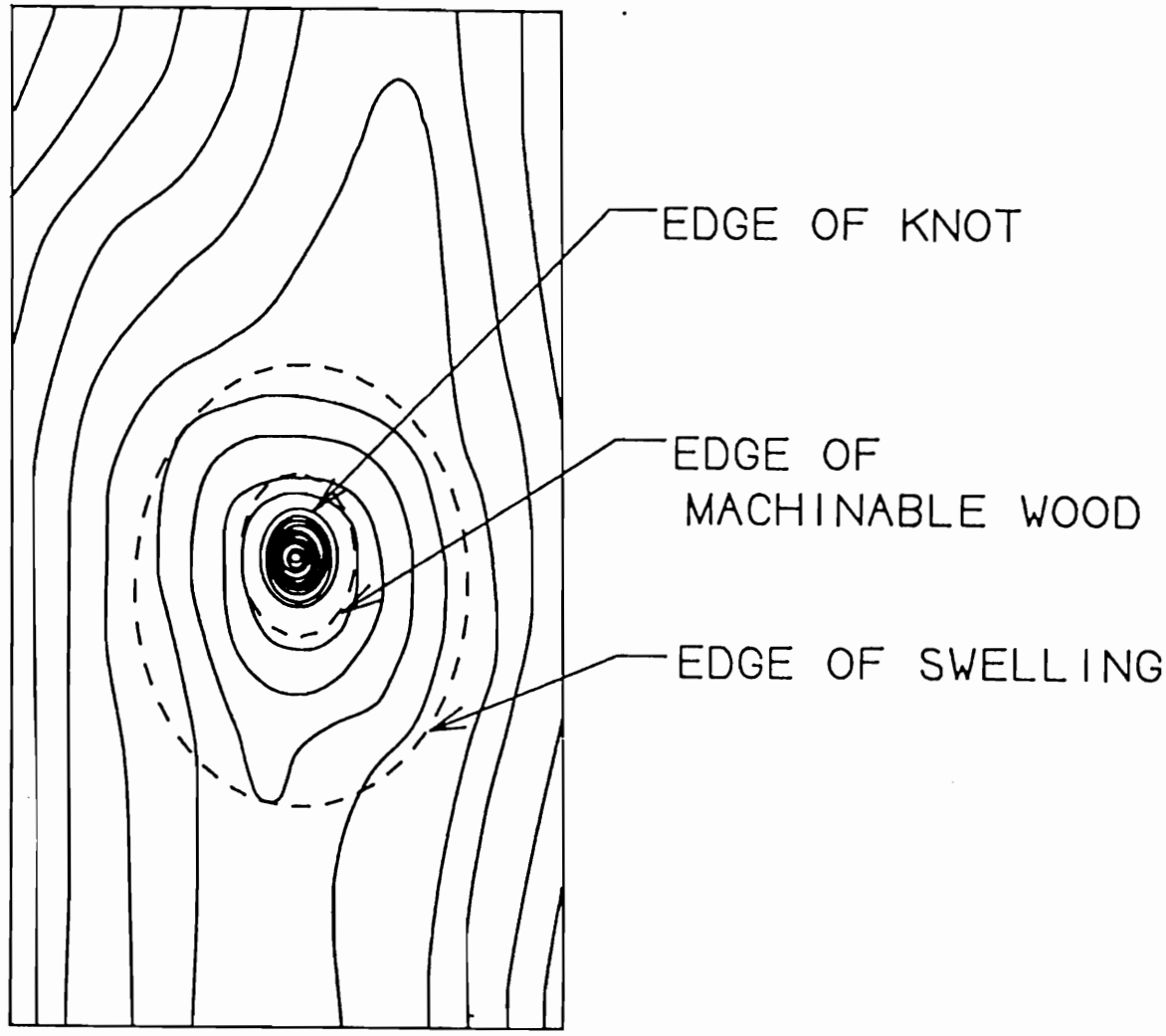

Figure 45. Location of various boundaries around a knot

swirl) but usually not enough to cause problems. The wood inside of one half of one knot diameter of the edge of the knot will begin to contain wood with a higher density and severe fiber distortion as well as some other unusual properties. Some of this wood may be machineable if special care is taken, such as orienting the board so that the cutting force loads the fibers in tension. There is a narrow band of wood immediately next to the knot which does not appear to be machineable. The width of this band is about 1/8 inch. The wood to the sides of a knot tends to be machineable closer to the knot than that above and below the knot.

CONCLUSIONS

1. Growth ring patterns can be used to predict cross grain because of knot swelling. This technique would be more useful to machine operators if they understood the relationship between growth ring patterns and fiber angle.

2. Several methods of accurately determining fiber angle will be ready for production applications which could replace the growth ring pattern technique. Among these is a machine vision system which uses a laminar flow-fiber angle model to estimate fiber angles around knots.

3. The edge of a knot is readily located. The edge of machineable wood, however, is more critical and more difficult to define because it is process dependent. The higher specific gravity and fiber distortion in the wood around knots makes cutting forces higher and machining more difficult in this area.

4. The wood near knots (less than 1/2 knot diameter) is machineable if the cutting forces and fibers are oriented properly.

Strategies for Reducing Chip-Out

The first strategy is to better recognize cross grain so that it can be removed before it gets to the finger-jointer. This can best be achieved with an educational program for mill personnel. They need a better understanding of growth ring patterns and cross grain and how they both relate to knots.

The second strategy is to modify the process so that it can handle larger fiber angles. Some of these strategies conflict and design compromises must be worked out.

1. Orient the fibers so that the knives always cut with them.
2. Reduce the diameter of the cutting head.
3. Reduce the chip thickness by increasing the number of knives, reducing the feed speed and increasing the cutterhead spindle speed.
4. Center all knots in the boards so that the knives will always cut with the fiber direction.
5. Increase the support to the back side of the board at the fingers.

Suggested Further Research

1. A full study is needed to fully develop the flow/grain model around knots for ponderosa pine.

2. Another study should be done on the growth ring patterns around knots. This would investigate knot swelling, its relationship to tree species, age, size and growth rate. It may be possible to be categorize the patterns mathematically.

3. A study of the specific gravity profile of the wood around knots would provide important information to manufacturers which machine this material.

BIBLIOGRAPHY

Anderson, E., A. Koehler and R. Krone. 1955. Instruments for rapidly measuring slope of grain in lumber. U.S.D.A. Forest Products Lab. Report no. 1592. Madison, WI.

Armarego, E.J. and R.H. Brown. 1969. The machining of metals. Prentice-Hall. Englewood Cliffs, NJ.

Bodig, J. and B. A. Jayne. 1982. Mechanics of wood and wood composites. Van Nostrand Reinhold Company. New York, NY.

Booker, R. 1987. A method for recording annual ring orientation in boards. Forest Products Journal. 37(6):31-33.

Clarke, L. N. 1963. A new dynamometer for measuring cutting forces in three dimensions. Division of Forest Products, CSIRO, Melbourne, Australia.

Dinwoodie, J. M. 1981. Timber, its nature and behavior. McMillan Press. London, England.

Franz, N. C. 1958. An analysis of the woodcutting process. University of Michigan Press. Ann Arbor, MI.

Kivimaa, E. 1950. Cutting forces in woodworking. Pub. 18. State Institute of Technical Research. Helsinki, Finland.

Koch, P. 1964. Wood machining processes. Ronald Press. New York, NY.

Koehler, A. 1943. Guide to determining slope of grain in lumber and veneer. U.S.D.A. Forest Service Report no. 1585, Madison, WI.

Kollman, F. P. and W. A. Cote. 1968. Principals of wood science. Springer-Verlag. New York, NY.

Loewen, E. G., E. R. Marshall and M. C. Shaw. 1951. Electric strain gauge tool dynamometers. Proceedings of the Society for Experimental Stress Analysis. 8(2):1-16.

Lubkin, J. 1957. A status report on research in the circular sawing of wood, volume 1. Central Research Lab, American Machine and Foundry. Greenwich, CT.

Mathews, P. C. and B. H. Beech. 1976. Method and apparatus for detecting defects in timber. U.S. Patent No. 3,976,384.

Mathews, P. C. 1987. Wood, light and objective scanning. Second International Conference on Scanning Technology in Sawmilling. Miller Freeman. San Francisco, CA.

McDonald, K. and B. A. Bendtsen. 1986. Measuring localized slope of grain by electrical capacitance. Forest Products Journal. 36(10):75-78.

McKenzie, W. M. 1960. Fundamental aspects of the wood cutting process. Forest Products Journal. 10(9):447-456.

McKenzie, W. M. 1961. Fundamental analysis of the wood-cutting process. Dept. Wood Technology. Ann Arbor, MI.

McKenzie, W. M. 1962. The relationship between the cutting properties of wood and its physical and mechanical properties. Forest Products Journal. 12(6):287-294.

McKenzie, W. M. and N. C. Franz. 1964. Basic aspects of inclined or oblique wood cutting. Forest Products Journal. 14(12):555-566.

McKenzie, W. M. and B. T. Hawkins. 1966. Quality of near longitudinal wood surfaces formed by inclined cutting. Forest Products Journal. 16(7):35-38.

McLauchlan, T. A., J. A. Norton and D. J. Kusec. 1972. Slope-of-grain indicator. Forest Products Journal. 23(5):50-55.

McLauchlan, T. A. and D. J. Kusec. 1978. Continuous non-contact slope-of-grain detection. Fourth Nondestructive Testing of Wood Symposium Proceedings. Engineering Extension Service. Washington State University. Pullman, WA.

Mori, M. 1971. An analysis of cutting work in peripheral milling of wood. II. The cutting force, power and energy requirements in up-milling parallel to the grain. Journal of the Japan Wood Research Society. 16(1):1-9.

Plapp, J. E. 1968. Engineering fluid mechanics. Prentice-Hall. Englewood Cliffs, NJ.

Phillips, G. E. 1980. Grain deviation around knots in conifers. Unpublished Masters thesis. Colorado State University. Fort Collins, CO.

Phillips, G. E., J. Bodig and J. R. Goodman. 1981. Flow grain analogy. Wood Science. 14(2):55-64.

Rabinowicz, E. 1970. An introduction to experimentation. Addison-Wesley. Menlo Park, CA.

Soest, J. 1984. Optical scanning technique for defect detection. Scanning For The Eighties. Forintek Canada Corp. Vancouver, BC.

Soest, J. 1987. Applications of optical measurement of slope of grain. Second International Conference on Scanning Technology in Sawmilling. Miller Freeman Publications. San Francisco, CA.

Stewart, H. A. 1969. Effect of cutting direction with respect to grain angle on quality of machined surface, tool force components, and cutting friction coefficient. Forest Products Journal. 19(3):43-46.

Stewart, H. A. 1971. Chip formation when orthogonally cutting wood against the grain. Wood Science. 3(4):193-203.

U. S. Forest Products Lab. 1974. Wood handbook: wood as an engineering material. U.S.D.A. Agriculture Handbook no. 72, rev. Madison, WI.

Woodson, G. E. 1979. Tool forces and chip types in orthogonal cutting of southern hardwoods. U.S.D.A. Forest Service Research Paper SO-146. Southern Forest Experiment Station. Pineville, LA.

Woodson, G. E. and P. Koch. 1970. Tool forces and chip formation in orthogonal cutting of loblolly pine. U.S.D.A. Forest Service Research Paper SO-52. Southern Forest Experiment Station. Pineville, LA.